UNIVERSITY OF CAPE TOWN

Faculty of Engineering and the Built Environment

Department of Civil Engineering

MSc. Dissertation

Steven Ivan Gregan

The Fatigue Performance Assessment of Corrosion Damaged RC Beams, Patch Repaired and Externally Strengthened Using CFRP

Supervisors

Prof. Pilate Moyo and Dr. Hans Beushausen

21st August 2012

The Fatigue Performance Assessment of Corrosion Damaged RC Beams, Patch Repaired and Externally Strengthened Using CFRP

Steven Ivan Gregan

Thesis submitted to the faculty of Engineering and the Built Environment, University of Cape Town, South Africa, in partial fulfilment of the requirements for the degree of Masters of Science in Engineering

Cape Town, 2012

Declaration

I declare that this thesis is essentially my own, unaided work. It is being submitted for the degree of Masters of Science in Engineering in the University of Cape Town, Cape Town, South Africa. It has not been submitted before for any degree or examination in any other University.

……

Steve Gregan

(31st August 2012)

Abstract

The focus of the dissertation was to provide an in depth investigation towards the fatigue performance of Carbon Fiber Reinforced Polymers (CFRP) which were externally bonded onto concrete beams as a repair and strengthening technique for internally corrosion damaged RC beams.

It was identified that more research concerning the fatigue performance of externally bonded CFRP laminates used as a composite material for originally damaged concrete structures was required. Therefore, there was a need to study the failure mechanisms between the externally bonded CFRP, corrosion damaged internal steel, and patch repaired section and the original substrate concrete with respect to the long term performance, whilst treating the system (CFRP, substrate concrete, patch repair and bonding agents) as a composite material.

The methodology of the dissertation included the introduction of accelerated corrosion techniques to degrade the internal steel reinforcement. The damaged RC beams were repaired by removing the damaged concrete, treating the corroded internal steel reinforcement, replacing the damaged concrete section removed with a rapid-hardening high strength patch repair mortar, and finally externally bonding CFRP laminates along the patch repaired section and entire tensile face to restore the bending capacity lost due to the reduction of internal steel and subsequent patch repair.

Two of the six RC beams which were patch repaired and CFRP strengthened, were subjected to a monotonic load in order to establish the ultimate static load at failure for the RC beams. The ultimate static load at failure was then used to derive the maximum imposed cyclic fatigue loading that was applied. The remaining four RC beams were then subjected to constant sinusoidal cyclic loads at varying amplitudes, the range of amplitude dependent on the corresponding static load at failure for the identical RC beam. The aim of the cyclic load tests was to determine the long term behaviour of the repaired and strengthened RC beams at different degrees of loadings. The test specimens were tested until fatigue failure was reached. At ultimate fatigue failure, the RC beams exhibited excessive concrete cracking, but eventual fatigue failure was determined when the CFRP finally delaminated along a portion or the entire length of the tensile face. It was evident that once fatigue failure

occurred due to concrete cracking, the fully laminated CFRP would then withstand a large majority of the tensile stresses still being applied. The CFRP momentarily restored the overall strength of the repaired and strengthened RC beam until ultimate failure occurred at the point of CFRP delamination.

The outcome of the dissertation observes and describes the failure mechanisms during RC beam and CFRP fatigue failure. The results obtained from the extensive testing plot a failure curve for each RC beam which had been corroded, patch repaired and finally CFRP strengthened. The cumulative results captured display a predicted failure curve graph. This graph indicates the percentage of ultimate cyclic load applied which was a function of the corresponding ultimate static load applied for an identical RC beam versus the number of cycles applied until failure. This curve can be used as a guideline to predict the number of cycles until failure for a repaired and CFRP strengthened RC beam of similar dimensions for a specific percentage of static loading, this loading being dependent on the increased ultimate static load at failure for a patch repaired and externally strengthened CFRP reinforced concrete beam.

The predicted failure curve clearly indicates that for repaired and CFRP strengthened RC beams experiencing low fatigue cyclic amplitudes equaling 45% of the corresponding total static loading at failure, the fatigue performance is significantly increased versus the identical test specimens with increased loading of approximately 55% and 67% of the corresponding ultimate static loads, these beams exhibit considerably decreased long term performance.

The static load tests also indicated that the influence of the accelerated corrosion on the ultimate capacity of the RC beam is minimal since the addition of the externally bonded CFRP doubled the ultimate static capacity of the identical RC damaged beams.

The experimentation was also able to capture the failure mechanisms for each tested beam throughout the cyclic loading phase. Identifying the failure mechanisms was useful when conducting on site investigations which focused on the long term performance of either the reinforced concrete beams that were patch repaired and strengthened or not.

As expected, the combination of combining a high strength patch repair mortar and external CFRP strengthening scheme significantly increased the long term performance of the RC structure. Finally, due to the investigations performed in this dissertation, the increased long term performance of a patch repaired and CFRP strengthened RC beam can now be empirically quantified and the failure mechanisms physically observed.

Keywords: CFRP strengthening, cyclic loading, fatigue performance, patch repair, accelerated corrosion.

Acknowledgements

The author would like to thank the following people for their support and assistance during the dissertation period:

- My supervisor, Professor Pilate Moyo, for all the time he dedicated towards my study and the manner in which he always challenged me to test the boundaries of CFRP investigations during my undergraduate and post graduate dissertations.
- A special thank you must go to Dr Billy Boshof, Mr Adriaan Fouche and all the lab staff at Stellenbosch University. This dissertation would not be possible without the use of their laboratory and equipment and all the time dedicated ensuring that my experimental program was completed on time and succeeded.
- A personal thank you must go to the Concrete Structures Materials Integrity Research Unit (CoMSIRU) for providing the financial assistance needed in order undertake a dissertation of this nature.
- Appreciation must also be given to the University of Cape Town laboratory and workshop staff. Mr Noor Hassen and his staff, Mr Charles May and Mr Elvino Witbooi, for all their assistance when needed to help out at Stellenbosch University.
- Anthony Webster from Sika for the donations of all the CFRP, bonding agents and patch repair mortar needed throughout the experimental program.
- Finally a special thank you to my parents, Derek and Sally, for all the encouragement and support throughout the dissertation period, and to my friends for their continued support.

Table of Contents

Declaration ii

Abstract iii

Acknowledgements vi

List of Tables x

List of Figures xi

List of Abbreviations xiii

List of Symbols xvi

1 *Chapter 1:* INTRODUCTION 1

1.1 Background to Study 1
1.2 Statement of the Problem 2
1.3 Dissertation Objectives 2
1.4 Outline of the thesis document 3

2 *Chapter 2:* LITERATURE REVIEW 5

2.1 Introduction 5
2.2 Reinforced Concrete Damage 6
2.2.1 Introduction 6
2.2.2 Corrosion Damage 6
2.2.3 Bond Deterioration due to Corroded Steel 8
2.2.4 Corrosion Initiation 9
2.2.5 Corrosion monitoring techniques 10
2.2.6 Behaviour of Corroded RC Beams under Loading 12
2.3 Localised Corrosion Repair of RC Beams 17
2.3.1 Repair Techniques 17
2.3.2 Patch Repair 18
2.3.3 Behaviour of corroded RC Beams after Patch Repairs 20
2.4 Fibre Reinforced Polymers (FRP) 22
2.4.1 Introduction 22
2.4.2 Uses of FRP in Civil Infrastructure 22
2.4.3 Types of Fibres 23
2.4.4 Types and Production of Fibre Reinforced Polymers (FRP) 24
2.4.5 Properties of Fibre Reinforced Polymers 28
2.4.6 CFRP Installation 30
2.5 CFRP Strengthening 31
2.5.1 Introduction 31
2.5.2 CFRP Application 33
2.5.3 Behaviour of FRP Strengthened RC Beams under Fatigue loading 44

2.5.4 Influence of External CFRP Strengthening of Corrosion Damaged RC Beams 53
2.6 State of Practice of FRP Application 56
2.6.1 The Use of Advanced Composites in Civil Infrastructure 57
2.7 Codes of Practice 60
2.7.1 British and European Codes 60
2.7.2 USA 61
2.7.3 Canada 61
2.7.4 Japan 62
2.8 Summary 62
3 *Chapter 3:* EXPERIMENTAL INVESTIGATION 64
3.1 Introduction 64
3.1.1 Specimen Details 64
3.1.2 Material Properties 65
3.1.3 Test Specimen Notation 66
3.1.4 Accelerated Corrosion 69
3.2 Repair Process 73
3.2.1 Repair preparation 73
3.2.2 Patch Repair 74
3.2.3 CFRP Strengthening 76
3.3 Testing 78
3.3.1 Sustained Load during preparation 78
3.3.2 Data Acquisition 79
3.3.3 Dynamic Testing 80
3.4 Summary 82
4 Chapter 4: RESULTS 83
4.1 Introduction 83
4.2 Accelerated Corrosion and Patch Repair 83
4.3 Static Loading 85
4.3.1 Introduction 85
4.3.2 Results 86
4.4 Fatigue Loading 90
4.4.1 Introduction 90
4.4.2 Results 90
4.5 Summary 106
***5 Chapter 5: CONCLUSIONS* 111**
5.1 Accelerated Corrosion 111
5.2 Patch Repair 112
5.3 Static Loading 113
5.4 Dynamic Loading 114

5.4.1 The objectives of the fatigue load tests 114
5.4.2 General Fatigue Behaviour 115
5.4.3 Locations of Fatigue Failure 115
5.4.4 Representation of Captured Data 116
5.4.5 Results Conclusions 116
5.4.6 Failure Prediction Curve 117
5.4.7 Summary 117
5.5 Recommendations for future study 118
5.6 Limitations to current study 119
References 120
Appendices 123

List of Tables

Table 1: Mechanical Properties of common FRP's (Keller 2003) 28
Table 2: Fatigue Test Program 45
Table 3: Load Parameters and Failure Modes 49
Table 4: Mix Quantities/1m3 for beams S40 and F401 64
Table 5: Reinforcement Requirements per RC beam 65
Table 6: Summary of Concrete compressive strengths per batch 66
Table 7: Compressive Cube Strengths 68
Table 8: Accelerated Corrosion Program 72
Table 9: SikaCrete 214 Patch Repair mortar compressive strength 76
Table 10: Fatigue Test Program 81
Table 11: Static Load Program 81
Table 12: Summary of Load versus Number of cycles 108

List of Figures

Figure 1: Progression of steel corrosion and concrete damage (www.corrosion-club.com) 8
Figure 2: Longitudinal corrosion cracking (www.nachi.org) 8
Figure 3: Bond Strength with Corrosion level (FIB 2002) 9
Figure 4: Schematic set-up for electrochemical measurements on reinforced concrete structures (fhwa.dot.gov) 11
Figure 5: El Maaddawy - loading frame 13
Figure 6: Measured versus predicted mass loss of steel using Faraday's Law 16
Figure 7: Glass fibre (www.glassfiber-fabric.cn) 25
Figure 8: Carbon fibre (www.alibab.com) 27
Figure 9: Aramid fibres (www.nauticexpo.com) 28
Figure 10: Possible failure modes for a RC beam strengthened for bending using CFRP 31
Figure 11: Different failure mode in shear (Taljsten 2006) 35
Figure 12: CFRP Side Laminate Strips 36
Figure 13: CFRP U-Jacketing 38
Figure 14: CFRP Fully Wrapped 39
Figure 15: Near Surface Mounting of CFRP 40
Figure 16: Principles for strengthening in bending (Taljsten 2006) 40
Figure 17: Principle for torsion capacity for FRP (Taljsten 2006) 43
Figure 18: Details of specimen and test set up 45
Figure 19: Gussenhoven and Brena (2005) - Test set up and CFRP Strengthening Configuration 48
Figure 20: Fatigue life as a function of CFRP laminate force on first cycle 52
Figure 21: Fatigue life as a function of CFRP laminate force/width in first cycle 53
Figure 22: The development of the fibre matrix composite from early 1970 into the 21st century (Hollaway 2010). 56
Figure 23: Test specimen reinforcement arrangement 65
Figure 24: Moulds with internal reinforcement 66
Figure 25: Cast Test specimens 67
Figure 26: Concrete Compressive Strengths 69
Figure 27: Accelerated corrosion preparation 70
Figure 28: Accelerated Corrosion series layout 70
Figure 29: Accelerated corrosion under sustained load 71
Figure 30: Constant current of 480 mA/cm^2 supplied. 71
Figure 31: Internal corrosion of the RC beams 73
Figure 32: Damaged Concrete removed and internal steel treated 74
Figure 33: Internal steel pitting and treatment technique 75
Figure 34: Treatment of surface and internal reinforcement with the Sikatop Armatec 110 EpoCem 75
Figure 35: Patch repair casting and moulds under sustained loading 75

Figure 36: Cured Patch repair under sustained loading 76
Figure 37: CFRP laminate application along the tensile face 77
Figure 38: CFRP Wrap applied at support ends for anchorage 78
Figure 39: Set up for accelerated corrosion stage 78
Figure 40: Static load set up and accelerated corrosion phase 79
Figure 41: Data acquisition and Instron set up 79
Figure 42: Dynamic test set up 80
Figure 43: Internal steel fracture 82
Figure 44: Loss of Ultimate Capacity due to long term corrosion 84
Figure 45: Patch repair crack propagation 85
Figure 46: S-40 Bending Failure 87
Figure 47: S-40 Crack failure pattern 87
Figure 48: S-50 Shear Failure 89
Figure 49: S-50 Crack failure pattern 89
Figure 50: F-50-1 CFRP debonding at failure 92
Figure 51: F-50-1 Crack distribution 93
Figure 52: Internal Steel fractured after approximately 2,400,000 cycles 94
Figure 53: F-50-1 - Number of Cycles versus Displacement 94
Figure 54: F-50-2 Cracking and debonding at failure 96
Figure 55: F-50-2 Crack Distribution 97
Figure 56: Internal steel fractured 97
Figure 57: F-50-2 - Number of Cycles versus Displacement 98
Figure 58: F-50-3 Cracking, debonding and spalling 99
Figure 59: F-50-3 internal steel fracture 100
Figure 60: F-50-3 Crack distribution 101
Figure 61: F-50-3 - Number of Cycles versus Displacement 101
Figure 62: F-40-2 Combined shear-bending failure 103
Figure 63: F-40-2 Shear failure 103
Figure 64: F-40-2 Crack Distribution 104
Figure 65: Internal steel fracturing (1) 105
Figure 66: Internal steel fracturing (2) 105
Figure 67: F-40-2 - Displacement versus Number of cycles 106
Figure 68: F-50-2, F-50-3, and F-40-2 - Displacement versus Number of Cycles comparison 109
Figure 69: Predicted failure curve for F-50 and F-40 RC repaired and CFRP strengthened beams 110

List of Abbreviations

Accelerated steel corrosion – Steel corrosion at a faster-than-normal rate by subjecting steel to anodic current.

Amplitude – The maximum value of a function as it varies with time.

Anode - The electrode in electrolysis where steel corrosion occurs.

Bar spacing - The distance between parallel reinforcing bars, measured centre- to- centre of the bars perpendicular to their longitudinal axes.

Bond strength - Resistance to separation of a repair or CFRP from substrate concrete.

Bonding agent - A material applied to a suitable substrate to enhance bond between it and a new repair layer or CFRP laminate.

CFRP – Carbon Fibre Reinforced Polymer

Cathode - The electrode at which chemical reduction occurs.

Composite - A combination of two or more constituent materials such as a substrate concrete and a repair.

Concrete substrate – The original concrete. However, when FRP repair follows patch repair then it is a combination of existing concrete and patch repair.

Concrete Cracking – When the structure has visible cracking on the surface, dismemberment of the concrete as a whole.

Corrosion - Destruction of metal by a chemical, electrochemical, or electrolytic reaction within its environment.

Corrosion agents – Compounds such as water and oxygen that promote corrosion.

Corrosion cracks – Cracks on concrete due to steel corrosion.

Corrosion rate – The rate of loss of steel.

Cracked section - A section with a crack.

Cyclic Load – A repetitive load at a constant frequency and amplitude

Debonding – A separation at the interface between the substrate and adherent material.

Deformation – A change in shape or size.

Delamination/Debonding – When the CFRP laminate detaches from the original substrate or patch repair material, caused by excessive loading

Depth of the neutral axis – A distance from the outer surface of concrete to the neutral axis (in this thesis it is often measured from the compression face).

Deterioration - Physical manifestation of failure of a material (e.g., cracking, delamination, flaking, pitting, scaling, spalling, staining) caused by service conditions or internal autogenous influences.

Drying shrinkage – Shrinkage of the structure as a result from the loss of moisture.

Durability - The ability of a structure or its components to maintain serviceability in a given environment over a specified time.

End-of-service life – When the structure severs no more purpose.

Fatigue Failure – When the structure no longer is able to withstand a load

Fibre reinforced polymer (FRP) – A general term for a composite material that consists of a polymer matrix reinforced with cloth, strands, or any other fibre form.

Interface – The interfacial boundary between two materials, e.g., an existing concrete substrate and a bonded patch repair material or CFRP laminate.

Interfacial bond – The bond between two different substances e.g. patch repair and CFRP

Laminate – One or more layers of fibre bound together in a cured resin matrix.

Level of steel corrosion – Degree of steel lost due to corrosion measured here as percentage mass loss of steel or as percentage loss in the area of steel.

Load-bearing capacity - The maximum load that a structure or structural element can withstand before it ultimately fails.

Neutral axis - A line in the plane of a structural member subject to bending where the longitudinal stress is zero.

Oxidise - To combine with oxygen.

Partial surface steel corrosion – Steel corrosion where loss in steel is localised on one surface of steel.

Patch Repair – A material used to substitute a portion of removed damaged concrete

Pit depth – The depth of steel loss after accelerated corrosion has completed.

Pitting - Development of relatively small surface cavities in corrosion of steel.

Poisson's ratio - The absolute value of the ratio of transverse strain to the corresponding longitudinal strain or vertical strain resulting from uniformly distributed axial stress below the proportional limit of the material.

Ponding - A shallow pond situated at the region of intended accelerated corrosion, consists of a salt solution on the surface of a concrete.

Propagate – When a crack increases in length and size over time whilst under loading

Repair - To replace or correct deteriorated, damaged, or faulty materials, components, or elements of a structure.

Service life - An estimate of the remaining useful life of a structure based on the current rate of deterioration or distress, assuming continued exposure to given service conditions without repairs.

Service load – The load specified by general building codes that will not cause loss of serviceability of the structures.

Serviceability – A state of a structure where specified service requirements are met. In this thesis it is mainly associated with cracks and deflections that do not affect appearance.

Spall – A fragment of the cover concrete that is detached from the parent concrete.

Stagnate – To delay or stall.

Static load – A single applied load at a constant rate or time

Stiffness - Resistance to deformation.

Stirrup - Reinforcement used to resist shear and torsion stresses in a structural member.

Strain - The change in length, per unit of length, in a linear dimension of a body; measured here in micro strains.

Stress - Intensity of force per unit area.

Wetting cycle – A period during corrosion where concrete surface was wetted with NaCl solution.

List of Symbols

Δ	=	Measured deflection
Δm	=	Mass of steel consumed
A	=	Amps
a	=	A distance from centre of corroding bar to a point of consideration on the cover concrete
a_1	=	Inner radius of a thick concrete cylinder (bar diameter + thickness of the porous zone)
a_2	=	Outer radius of the thick concrete cylinder (bar diameter + thickness of the porous zone + cover depth)
A_{sc}	=	Area of compression reinforcing steel
A_{st}	=	Residual area of tensile reinforcement after corrosion
B	=	System constant
b	=	Width of concrete section
c	=	Concrete cover depth
d	=	Bar diameter
d'	=	Distance from the extreme compression fibre to the centroid of compression reinforcing steel
E_c	=	Elastic modulus of concrete
E_{eff}	=	Effective modulus of elasticity of concrete
E_f	=	Modulus of elasticity of FRPs
E_s	=	Young's modulus of steel before yielding
E_{sp}	=	Young's modulus of steel reinforcement after yielding
F	=	Faradays constant (96 500 A/s)
f'_c	=	Characteristic compressive strength of concrete
f_{cr}	=	Concrete cracking force
F_c	=	Internal compression force carried by the concrete in compression

f_{ct}	=	Tensile strength of concrete
F_{st}	=	Internal tensile force carried by the tensile steel reinforcement
F_{uls}	=	Ultimate tensile strength of tensile steel reinforcement
f_y	=	Yield stress of tensile steel reinforcement
h	=	Height of the beam
i	=	Corrosion current density
i_{corr}	=	Corrosion current density
I_g	=	Gross second moment of area of a beam
l	=	beam span
I	=	Current (A)
M	=	External applied moment
M_{cr}	=	Cracking moment of a beam
M_{uls}	=	Ultimate capacity of the beam
r	=	Radius of uncorroded steel bars
t	=	Time of testing
V_{steel}	=	Volume of steel
w_f	=	Width of FRP plate
x	=	Depth of the neutral axis of the beam as measured from the extreme compression fibre
z	=	Ionic charge
y_g	=	Gross depth of the neutral axis of a beam
π	=	Pi (3.14)
ε_f	=	Strain in the FRP plate
ε_{fu}	=	Rupture strain of FRP plate
ε_{sc}	=	Strain in the compression steel reinforcement
ε_{st}	=	Strain in the tensile steel reinforcement

ε_{su}	=	Ultimate strain of tensile steel reinforcement
ε_{tt}	=	Transverse strains on the surface of concrete
ε_{u}	=	Ultimate strain of concrete in compression
ε_{y}	=	Yield strain of tensile steel reinforcement
υ	=	Poisson's ratio of concrete

1 *Chapter 1:* INTRODUCTION

1.1 Background to Study

The durability of a RC structure is defined as the capability of maintaining the serviceability of the structure over a specific period of time. Reinforced concrete structures are designed with a specific design service life, often 50 or 100 years. This is often reduced due to the premature deterioration of the concrete structure as a result of external factors. The most common form of deterioration in RC structures, near marine environments, is the corrosion of the reinforcing steel. Steel corrosion starts when the alkaline boundary that protects the steel is broken down in the presence of water and oxygen. Corrosion products increase the volume around corroding steel resulting in tensile forces being generated along the entire length of the corroded reinforcement, leading to cracks on the concrete surface. The steel corrosion results in a reduced area of internal steel reinforcing within the RC beam, this has a significant influence in the load-bearing capability of the structure.

In order to restore the original durability and service life of a corrosion damaged RC structure, a concrete repair technique needs to be implemented. After the damaged concrete and internal steel has been treated and repaired, additional strengthening of the affected area is required to restore the lost load-carrying capacity due to the reduction of reinforced steel area. The most common method used to repair a corrosion damaged section of RC structural elements is patch repair. This involves removing all damaged concrete, treating the internal affected steel appropriately and replacing the corrosion affected section of concrete with a cementitious patch repair mortar. This technique of repair adequately addresses the problem of further corrosion damage, however external strengthening is required to restore the load carrying capacity lost. The use of fibre reinforced polymers as an external strengthening scheme is not a new method of strengthening but is among the most easy to implement on existing structures. CFRP laminates are often externally bonded onto existing structures to provide additional load bearing capacity.

While sustained work has been carried out on the short term improvements in the strength of RC elements strengthened using CFRP, little is reported on the fatigue performance of the

resulting composite system. The primary focus of this study is to investigate the long term performance of corrosion damaged RC beams which have been repaired using a cementitious patch repair and externally strengthened using CFRP laminates.

It should be pointed out that simply strengthening corroding RC elements is not sufficient as corrosion will continue over time, thus requiring further treatment at a later stage and at a greater cost.

1.2 Statement of the Problem

Limited work on the fatigue performance of the RC elements strengthened using CFRP has been reported in literature. The few studies reported in literature focus on the performance of RC beams strengthened without introducing repair materials to the damaged RC elements. The fatigue performance of a structure is identified as the ability or duration of time to resist degradation due to continuous and consistent loads.

To the author's knowledge, no work on the fatigue performance of CFRP strengthening incorporating cementitious patch repairs has been reported in literature.

Thus it is recommended to address durability issues using appropriate corrosion inhibitors and cementitious repair materials and strength using CFRP.

1.3 Dissertation Objectives

The following objectives have been set for the study:

- Investigate the mechanisms of failure between the different interfaces of the materials present in the composite structure. Identify and discuss the possible failure interfaces, which include the bond between the patch repair mortar and original substrate, the bond between the CFRP and epoxy along the tensile face, and finally the debonding failure between the epoxy and patch repair at the midspan.
- Analyse the fatigue behaviour of each RC beam over the entire duration of the cyclic loading period and with the aid of a graphical representation illustrating the midspan deflection versus the number of cycles, as well as the number of cycles versus the percentage of cyclic load applied.

- Identify the relationship between the patch repair and original substrate during cyclic loading and the effective influence that CFRP strengthening has on the fatigue performance of each test specimen.
- Construct an empirical prediction failure curve to calculate the fatigue performance achieved due to the effect of the patch repair and CFRP strengthening system under varying degrees of cyclic loading.
- Investigate the internal damage of the internal corroded steel; describe the effects of the decreased internal steel versus the large increased bending capacity contributed by the presence of the externally bonded CFRP.

1.4 Outline of the thesis document

Chapter Two provides a critical analysis of previous research investigated which focuses on the core stages of the overall dissertation. Due to the uniqueness of the dissertation topic it is important that all stages related to the long term performance of the accelerated corrosion stage to the patch repair work, FRP strengthening and finally cyclic loading stages are efficiently covered in the literature review. The core of the literature review focuses on the fatigue performance of each stage which gives a better understanding of the importance and direction of this dissertation. Finally, a summary of the State of Art for the use of FRP as a repair and strengthening scheme is provided, followed by the various design guidelines and codes currently being implemented around the world relating to CFRP use.

Chapter Three provides an in depth summation of the methodology used during the laboratory stage. The stages included preparation for the accelerated corrosion phase, casting of the test specimens, the patch repair process, external FRP strengthening and finally the static and cyclic loading test program.

Chapter Four includes all test results for both static and cyclic load tests and provides a preliminary discussion of common trends and observations. All failure mechanisms are observed and documented throughout the tests. The results are graphically represented and compared. A critical discussion of the results is provided, which highlights the common failure mechanisms and trends as well as introducing the fatigue failure curve.

Chapter Five focuses primarily on the conclusion of the results, relating common trends observed in the graphical representation of results and visual observations made to similar

previous work that has been conducted. Finally, recommendations for further studies related to the dissertation topic are provided.

2 *Chapter 2:* LITERATURE REVIEW

2.1 Introduction

Over the past few decades extensive research has been conducted on investigating the long term effects internal steel corrosion of RC structures (Taljsten (2006), El Maaddawy (2005), Gussenhoven (2005)). This research has led to further investigation of possible repair techniques that could be implemented to minimize the damage caused by corrosion of steel in RC elements. The analysis of fatigue failure on CFRP strengthened concrete structures is a complex task to predict. It is not a simple problem to handle theoretically or experimentally since the progress begins in the atom structure and develops from the first load to over thousands or millions of intervals to a potential failure (Taljsten 2006). The strength at eventual failure is usually less than the strength observed for a single load cycle. The problem engineers' face is how to predict the time of eventual failure under repeated loading. The most common factor which influences the fatigue performance of a RC structure is the internal corrosion of the reinforcing steel. Corrosion of the reinforcement leads to a reduction of cross sectional area of internal reinforcement resulting in a decrease of the bending and shear capacities of the RC element.

Fatigue failure is a real threat to RC structures subjected to cyclic loading and therefore their safety for fatigue endurance must be evaluated. This requires knowledge about the material behaviour under cyclic loading. The quality of materials is ever improving and higher load bearing capabilities are being attained. Higher failure strength values often mean that the material becomes more brittle and the fatigue strength in relation becomes lower. New types of structures are being built where fatiguing loads occur to a greater extent than what has previously been common (Taljsten 2006). The most economical and sustainable method to ensure that a RC structures fulfil its intended design life span is to implement appropriate maintenance strategies, to repair and or strengthen the structures.

The most common form of concrete repair involves using a patch repair materials, whereby the existing damaged concrete is removed, the internal steel and damaged concrete is treated and finally the structural component is repaired using a modern repair mortar. Patch repairs are commonly undertaken to maintain or restore the durability of the existing structure by stopping or minimising further corrosion and introducing protection to steel

against corrosive agents (Malumbela 2010). After a patch repair, external strengthening maybe required to restore the structure to its original ultimate strength. The method of bonding fibre reinforced polymer (FRP) plates or FRP sheets to the tensile face of a RC beam has been shown to increase flexural capacity by an excess of 100% (Malumbela 2010). The use of externally bonded CFRP sheets or laminates has proven to be an excellent strengthening technology for RC structures, due to its high-strength, lightweight, corrosion-resistant, geometrically versatile, and aesthetically unnoticeable appearance (Parish 2011).

2.2 Reinforced Concrete Damage

2.2.1 Introduction

Damage of reinforced concrete structures refers to the deterioration of the structure from its original conditions. Structures deteriorate due to a number of external and internal factors, such as the simple aging of structures, environmentally induced degradation, reinforcement corrosion, poor initial construction and lack of maintenance (Taljsten 2006). Corrosion of reinforcing steel is one of the most common causes of deterioration of RC structures and is initiated by carbonation and chloride penetration (Badawi 2005). Steel corrosion can cause sudden catastrophic failure of RC structures. Although steel corrosion occurs over a long duration of time it is necessary to maintain and monitor the rate of corrosion in order to ensure the intended service life of the RC structure is reached. Various repair techniques can be implemented on the affected regions where internal steel corrosion has occurred on the concrete structure. This limits the rate of further internal steel corrosion which minimises the concrete damage leading to eventual failure. Since the steel corrosion damage progresses over a duration of time it is important to establish the relationship between the corrosion damage state, the fatigue life of the old and patch repair concrete as well as the long term or fatigue performance of the external fibre reinforced composites used for strengthening post repair.

2.2.2 Corrosion Damage

Corrosion of the steel reinforcement in RC structures affects both the steel and the concrete (El Maaddawy, Soudki 2005). Corrosion is a major problem for steel-reinforced concrete structures including bridges, parking garages, and coastal structures.

A good-quality concrete provides a high alkaline environment that forms a passive film on the steel surface, preventing the steel from corroding. Under a chloride attack, this passive film is disrupted and the steel begins to corrode (Masoud 2005). In typical RC structures, internal reinforcing steel is protected by a high pH (>12.5) of the concrete pore solution, which creates the passive film over the surface of the reinforcement. The reinforced steel bars in the concrete structures are depassivated when the chloride concentration reaches threshold levels on the rebar surface or when the pH of the concrete drops below critical levels due to carbonation (Badawi 2005). Depassivation also occurs if the alkalinity of the pore water in the concrete pores decreases or due to the penetration of the chloride ions (Tigeli 2010). When corrosion is initiated, it progresses by causing a volumetric expansion of the rust produced in the vicinity of the rebars (Badawi 2005). The volume of corrosion products produced in a corrosion reaction are at least twice the volume of steel that is dissolved, thus, rust formation involves a substantial volume increase (Tigeli 2010). From figure 1, a volume change due to rust production causes longitudinal corrosion cracks (Figure 2) to form along the corroding reinforcing bar when the tensile stress of the concrete surrounding the rebar exceeds the tensile strength of the concrete (Badawi 2005). The resulting cracks on the external surface of the concrete structure accelerate the risk and rate of further corrosion as there is a free access of moisture and corrosion agents to reinforcing steel, as the ability of concrete cover to act as a protective layer to steel has been remarkably reduced (Tigeli 2010).

Pitting corrosion may also reduce the ductility of the steel bar by introducing notches on the surface of the steel bars that lead to premature necking of the internal steel and weakening of the structure (El Maaddawy, Soudki 2005).

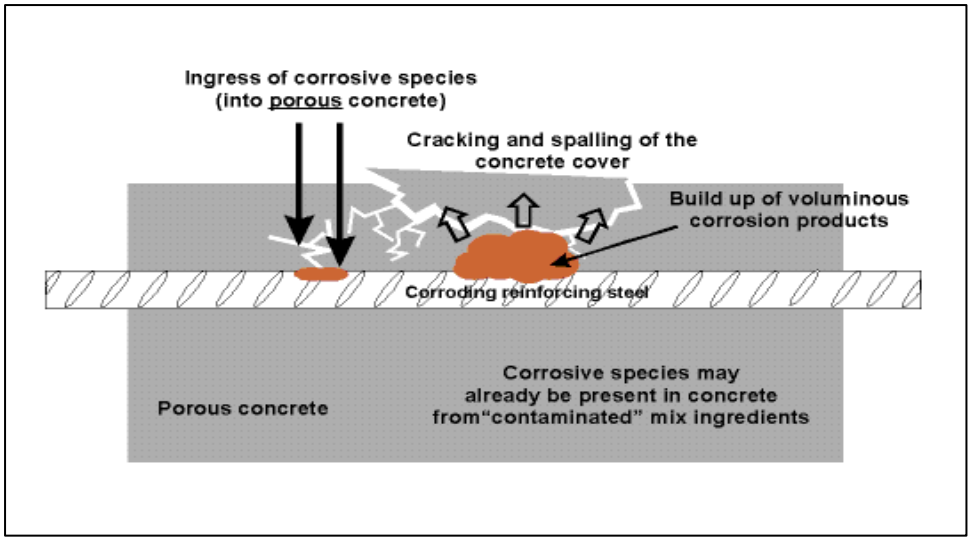

Figure 1: Progression of steel corrosion and concrete damage (www.corrosion-club.com)

Figure 2: Longitudinal corrosion cracking (www.nachi.org)

2.2.3 Bond Deterioration due to Corroded Steel

Previous studies conducted by Richardson (1995) and El Maaddawy (2005) concluded that there is a well-defined relationship between the bond strength and corrosion level of the internal steel. According to the FIB (2002), bond strength changes qualitatively and is illustrated in figure 3. El Maaddawy (2005) went on to state that the composite action of the steel and concrete is diminished because of deterioration of the bond at the steel-to-concrete interface caused by the lubricant effect of the corrosion products and by cracking of the concrete cover.

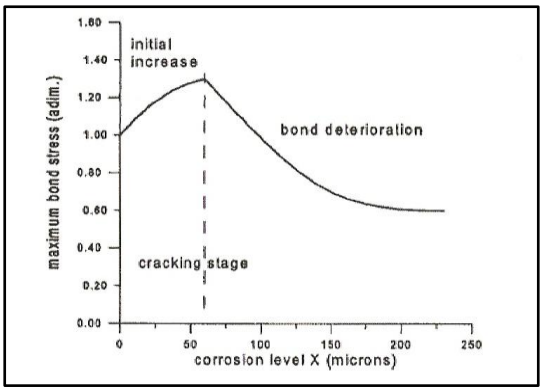

Figure 3: Bond Strength with Corrosion level (FIB 2002)

In order to maintain composite action induced loads on the RC structure need to be transferred between the concrete and steel. The load transfer is referred to as the bond and is idealised as a continuous stress field that develops in the surrounding area of the steel-concrete interface (Tigeli 2010). Therefore for RC structures subjected to loading, the bond stress capacity of the system should exceed the demand and there should be little movement between the reinforcing steel and the surrounding concrete.

2.2.4 Corrosion Initiation

The degree of corrosion is represented as a percentage which is defined as the mass loss of steel reinforcement due to corrosion (El Maaddawy, Soudki 2005). In order to obtain results within a certain period of time accelerated corrosion techniques are implemented. An accelerated corrosion technique is widely used to simulate corrosion in the laboratory with either an internal or external cathode terminal by impressing an electric current through the reinforcing bars. This method produces the desired mass losses in the reinforcing bars and damage in the concrete structural elements within a reasonable time frame (Badawi 2005). Current densities vary from 50 to 4000 $\mu A/cm^2$. After initial corrosion activation, oxygen and moisture must be provided at the surface of the cathode to allow the corrosion process to proceed. Wetting and drying of the concrete will also help accelerate the chloride ingress (Bohni 2005).

The chloride has a fourfold negative effect in reinforced concrete (Bohni 2005):

- It destroys the passive film of the steel rebar and makes corrosion attack possible.
- It reduces the pH of the pore water since it reduces the solubility of $Ca(OH)_2$.

- It increases the moisture content because of the hygroscopic properties of salts present in concrete (e.g. $CaCl_2$, NaCl).
- It increases the electrical conductivity of the concrete.

2.2.5 Corrosion monitoring techniques

There are various techniques to measure the degree of corrosion in RC structures. The most commonly used include the Linear Polarisation resistance (LPR), electrochemical impedance spectroscopy (EIS) and galvanostatic pulse measurement (GPM).

The measurement of the polarisation resistance R_p by means of electrochemical methods allows calculation of the corrosion rate according to:

$$\frac{B}{R_p} = i_{corr}$$

R_p = Polarisation resistance

i_{corr} = Corrosion current density

B = System constant

The reciprocal polarisation resistance is the slope of the current density-potential curve in the proximity of the corrosion potential. The system constant B contains the kinetics of the anodic and cathodic reaction and amounts to 26mV for corroding steel and 52mV for passive steel in concrete. The polarisation resistance can be determined by the following methods. All the methods have a similar set up with counter and reference electrodes on the concrete surface (Bohni 2005).

Linear Polarisation Resistance

In linear polarisation resistance (LPR) a constant potential voltage is applied, ξ (ξ=$ξ_{corr}$=±5mV and 10mV) directly to the steel in the concrete. After some time the resulting current is measured. The effective polarisation resistance $R_{p,eff}$ must be compensated by the ohmic resistance of the concrete, which can be determined by an impedance measurement (Bohni 2005). Figure 4 below illustrates the typical set up for electrochemical measurements on reinforced steel.

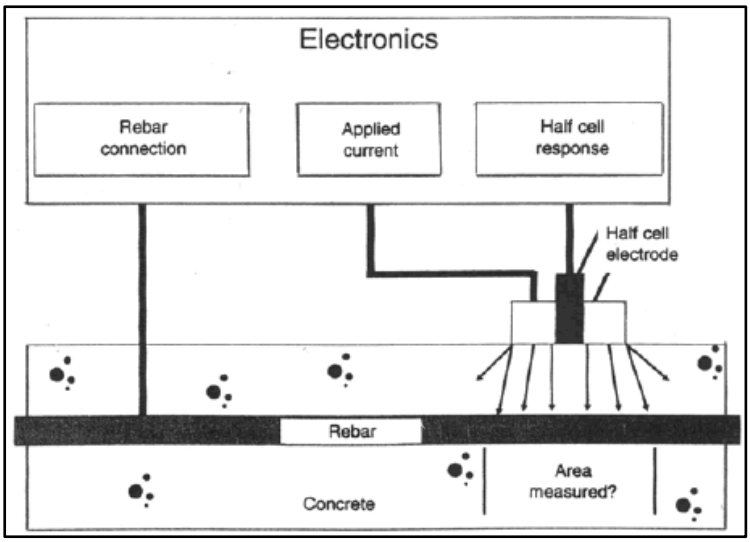

Figure 4: Schematic set-up for electrochemical measurements on reinforced concrete structures (fhwa.dot.gov)

Electrochemical impedance spectroscopy

The measurement set up of electrochemical impedance spectroscopy (EIS) is similar to that of LPR. An AC voltage signal in a frequency range from several MHz to approximately 100 kHz is applied and the resulting AC current is measured. By analysing the impedance spectrum the ohmic resistance of the concrete or the polarisation resistance can be determined. A disadvantage of this method is the time exposure for one measurement, depending on the lowest frequency and therefore EIS is barely applied on real structures (Bohni 2005).

Galvanostatic pulse measurement

Galvanostatic pulse measurement (GPM) is the most efficient method for determination of the polarisation resistance R_p (length of time per measurement approximately 10 seconds). A Galvanostatic current is applied to the reinforcement and the polarisation is recorded by a computer. The current of the pulse is selected in such a way that the change of the corrosion rate is less than 20mV. By curve fitting and extrapolation of time towards infinity the ohmic resistance of the concrete and the polarisation resistance R_p can be calculated (Bohni 2005).

2.2.6 Behaviour of Corroded RC Beams under Loading

Extensive research has been conducted in the specific field of further understanding the mechanisms which take place whilst a RC structure damaged due to corrosion whilst under a sustained load.

El Maaddawy performed a thorough experimental study designed to investigate the viability of using externally bonded carbon-fibre-reinforced polymer (CFRP) laminates to extend the service life of corroded reinforced concrete (RC) Beams. The work of El Maaddawy was extensively researched and summarised by (Malumbela 2010).

The experimental program involved corroding fifteen quasi-full-scale RC beams with dimensions of 152 x 254 x 3200 mm to four different accelerated corrosion periods of 50, 110, 210 and 310 days. Of the 15 test specimens: three beams were not corroded, two of them were strengthened by CFRP laminates, while one specimen was kept as a virgin beam. The remaining 11 beams were subjected to the different levels of corrosion damage up to 31% steel mass loss using an impressed current technique (El Maaddawy, Soudki 2005). Their specimens were reinforced with two 16 mm diameter steel bars in tension. The shear reinforcement was 8 mm-diameter stirrups spaced at 80 mm centre-to-centre in the shear span and 333 mm centre-to-centre in the constant moment region. Eight beams were tested under a sustained load equivalent to 60% of the ultimate load or yield moment of the virgin beam whilst corresponding seven were tested in the absence of a sustained load to act as controls.

The load was applied using a mechanical loading frame shown in Figure 5. The frame was designed and constructed at the University of Waterloo and was based on the work done at the University of Sherbrooke (El Maaddawy, Soudki 2005). The loading frame allows such that two beams were placed back-to-back and loaded simultaneously; the bottom beam with tensile face up and the top beam with tensile face down. The mechanical loading frame applied a constant four-point bending with a constant moment across the middle section of each beam. The frame applied loads on the test specimens by hanging weights on spate lever beam; the load is then transferred to another lever beam before being transferred to the test beams by a load distribution beam. Two lever arms were used to intensify and transfer an applied load (P) to the two concrete beams placed in the loading frame. The

loading arrangement was such that each test specimen experienced a constant bending moment region along the middle 1000mm section over a total span of 3000mm (Malumbela 2010).

To ensure corrosion of the test specimens, 2.25% chlorides by weight of cement were added to the concrete mixture used to cast the middle 1400 mm of the specimen and to a height of 100 mm from the tensile face of the beam, this section is referred to as the salted zone. The salted zone is indicated in Figure 9. A current density of 150 mA/cm^2 was used to accelerate steel corrosion. During accelerated corrosion, two fogging compressed air mist nozzles were used to spray mist over the test specimens to allow corrosion reactions to take place. To control the humidity around the test specimens, they were encased in a polyethylene cover. (Malumbela 2010).

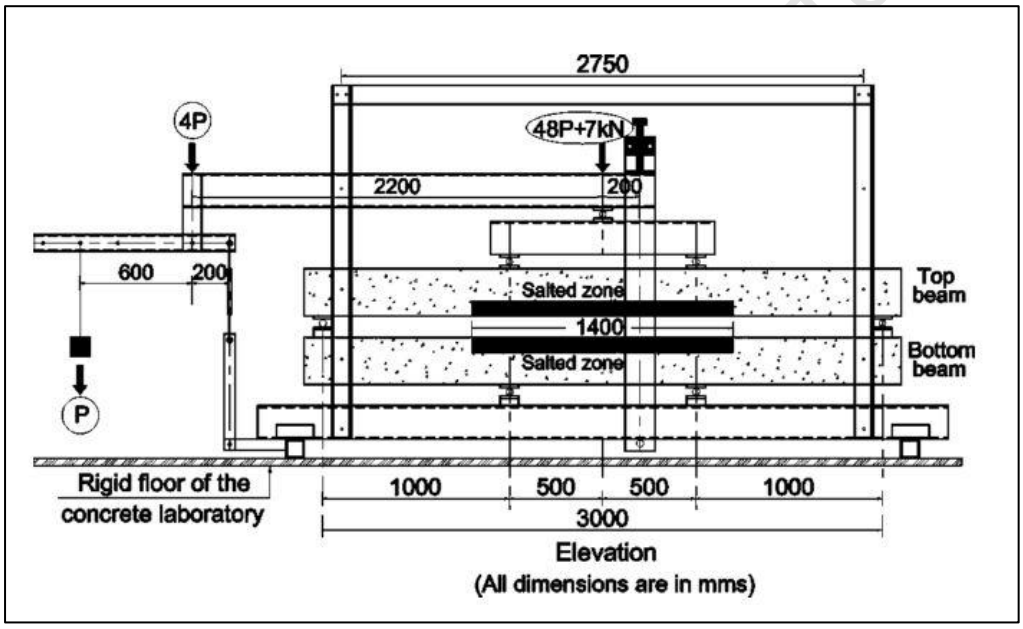

Figure 5: El Maaddawy - loading frame

El Maaddawy found that for beams corroded under load, the initial corrosion cracks appeared after 53 hrs whilst for beams corroded in the absence of a sustained load the initial corrosive cracks were observed after 95 hrs. It is important to note that the difference between 95 hours and 53 hours seem small but the test specimens in this particular experimental programme were corroded at a corrosion density which is close to a thousand times more than the corrosion density of in-service structures. El Maaddawy and Soudki (2005) suggest that if a current density of below 200 mA/cm^2 is used for the accelerated

corrosion, the corrosion damage they induced was proportional to typical damage experienced on in-service structures. Therefore the 50% reduction of the time to cover cracking due to a sustained load is very significant for in-service structures where the time to cover cracking is in the order of tens of years in relation. This particular study by El Maaddawy and Soudki (2005), suggest the variation in the thickness of the porous zone (amongst many other parameters) was found to be capable of causing a similar range in the time to cover cracking. It is therefore difficult to attribute the range in the time to cover cracking from El Maaddawy to the sustained load (Malumbela 2010).

After the appearance of the initial visible corrosion cracks, the rate of widening of these cracks at the middle of two beams that were intended to have the highest level of corrosion (310 days testing) was continuously monitored using a demec gauge. They reported a bi-linear rate of widening of corrosion cracks with time. During the first 50 days of accelerated corrosion, beams under a sustained load had a rate of widening of corrosion cracks of 22 µm/day compared to 18 µm/day for beams corroded in the absence of a sustained load. After 50 days, the rate of widening of corrosion cracks was about 7 µm/day for both loading regimens. Since the initial corrosion cracks were only continuously monitored on two beams and at a single point on each beam, it is not clear if other beams exhibited the same rate of crack widening (Malumbela 2010).

At the completion of the testing program, crack maps were developed for each corroded beam. A common trend developed whereby each test specimen has two longitudinal cracks on the tensile face and near each corroding bar. Smaller cracks were observed on the side faces of the beams, these cracks were intensified on the heavily corroded beams. Further investigation of the corrosion crack pattern map, and the fact that some specimens were corroded in the absence of a sustained load, it is evident that the sustained load had little influence on the pattern of corrosion cracks.

In drawing crack patterns, El Maaddawy and Soudki (2005), meticulously measured corrosion crack widths at 100 mm intervals along the beam span. Contrary to Ballim (2001) et al. where maximum crack widths were found at the beam ends, they observed maximum crack widths within 200 mm of the centre of the corrosion region. This emphasises the earlier notion that corrosion crack widths are influenced by the confinement of concrete. In

this case, more confinement was expected at the ends of the corrosion region from closely-spaced stirrups as well as the mass of the undamaged concrete. Maximum corrosion crack widths not necessarily being at the centre of the corrosion region implies that measuring crack widening only at the middle of the beam as done by the researchers does not always provide the maximum rate of widening of corrosion cracks. In fact the maximum crack widths on the specimens which they reported the rate of widening of corrosion cracks were 100 and 200 mm from the centre of the corrosion region (Malumbela 2010).

After testing beams to failure, six coupons of the internal reinforcement, three from each bar, each 30 to 50 mm in length were cut from the corrosion or salted zone. The coupons were then cleaned and weighed to determine the mass loss of steel. Specimens that were corroded in the absence of a sustained load had average mass losses of steel of 8.7, 14.2, 22.2 and 31.6% for 50, 110, 210 and 310 days respectively, of accelerated corrosion. The corresponding mass losses of steel for specimens corroded under load were 9.6, 15.6, 23.3 and 30.5%. Note that the expected respective levels of steel corrosion from Faraday's Law were 6.1, 13.3, 25.4 and 37.5%. At mass losses of steel below 15%, the mass losses of steel in beams corroded under load were around 10% larger than corresponding losses of steel in beams corroded in the absence of a sustained load. For these mass losses of steel, Faraday's Law underestimated the measured mass loss of steel by up to 36%. At higher mass losses of steel (>20%) however, the influence of sustained load on the rate of steel corrosion was negligible. To assess the magnitude of the differences in mass losses and hence the effect of sustained load on the rate of steel corrosion, these mass losses were plotted in figure 6

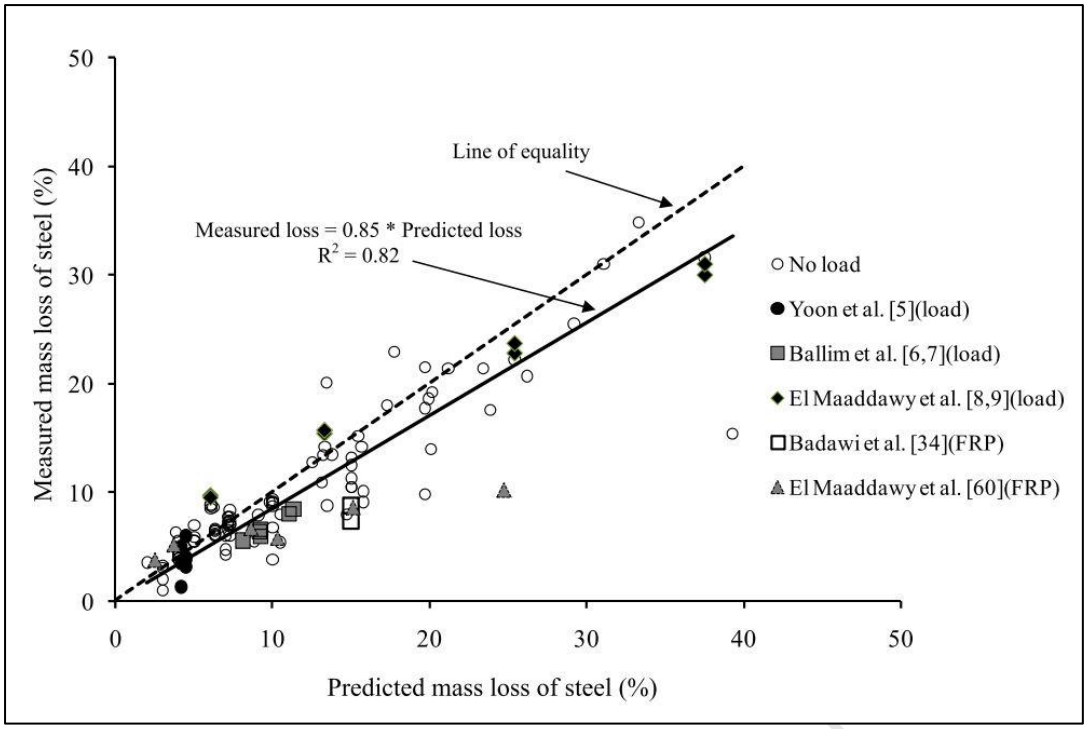

Figure 6: Measured versus predicted mass loss of steel using Faraday's Law

The errors from using Faraday's Law to calculate the steel mass loss (-3.5 to 7%) are within those found by other researchers on specimens that were corroded in the absence of a sustained load (-6.7 to 23.9%) (Malumbela 2010). The relations between mass losses of steel and maximum crack widths from various beams were found to be the same. It was found that, a 1% mass loss of steel corresponded to a maximum crack width of 0.1 mm. This relation is similar to those discussed earlier on specimens that were corroded in the absence of a sustained load by various researchers. It therefore emphasises the earlier notion that the level of sustained load had little effect of the rate of widening of corrosion cracks as well as the rate of steel corrosion (Malumbela 2010).

After the corrosion testing was complete, El Maaddawy (2000) tested some of their specimens to ultimate failure. The other specimens were repaired prior to ultimate load test. The interest here is on specimens that were not repaired. Even though it was not reported in their work, their results indicated that ultimate load-bearing capacity of the specimens linearly reduced (R2 ≈ 1) with an increase in the level of steel corrosion. For instance, a 1% mass loss of steel corresponded to 1.1% loss in the load-bearing capacity of beams. These findings are consistent with those found by other researchers where load-bearing capacity was related to average loss in the area of steel. Since the residual capacity

of beams were on the same curve regardless of the test conditions, residual capacity of corrosion-affected RC structures was affected by the level of steel corrosion and not the procedure of steel corrosion. This implies that relations between ultimate capacity and actual steel loss from accelerated laboratory tests are representative of relations on in-service structures (Malumbela 2010).

2.3 Localised Corrosion Repair of RC Beams

Concrete is a durable construction material and, if designed and placed properly, will give long service under normal conditions (Beushausen 2009). The problems that RC structures face are the natural elements which are exposed to which cause critical deterioration over duration of time. One of the main reasons for deterioration is insufficient cover depth to reinforcing steel, this along with poor concrete cover quality and exposure to harsh environmental elements result in steel corrosion, concrete cracking and spalling (Beushausen 2009).

The cost of repairing damaged concrete can often amount to greater than the original cost of the poor concrete, therefore the correct repair technique needs to be implemented to ensure that the repair effectively eliminates the original cause of damage, repairs the full extent of the damage and ensures the structure is protected from further damages or recurrence of the original cause for its intended service life.

Once the deteriorated concrete has been repaired it is crucial to strengthen the repaired section of the structure to alleviate the role of the corroded steel reinforcement which has ultimately lost strength due to deterioration over time. An effective method of external strengthening generally include application of external load bearing elements such as reinforced overlays, bonded steel plates, or fibre reinforced composites (FRC) sheets or plates (Beushausen 2009).

The following section of literature focuses on the effect of patch repairs and the influence of the repair on the structure as a composite.

2.3.1 Repair Techniques

The primarily objective of a repair technique is to increase the durability of the concrete structure. Durability refers to the ability of concrete to resist the ingress of deleterious

substances which may lead to corrosion of reinforcement while structural performance relates to the strength of the RC structure (Tigeli 2010). Therefore all repair materials used should assist in the reduction of further deterioration and the protection from further ingress of aggressive corrosive agents.

There are many different repair techniques that can be implemented, each of which has different application methods and materials used.

Examples of patching materials and applications are:

Cementitious repair mortars

Commonly used and designed for easy of application under a range of in-service conditions. The mortars have suitable consistencies and adhesion for ease of application either by hand or trowel. These repair mortars are claimed to have a low shrinkage. The major requirement of cementitious repair mortars is that their properties be compatible with the parent concrete in terms of modulus of elasticity, coefficient of thermal expansion, shrinkage movement and permeability (Tigeli 2010).

Free-flowing grouts and fluid micro-concrete

This form of patch repair is useful for extensive and large repairs where access for hand and trowelled mortars is difficult. The grouts are pumped or hand poured into formwork because their mixes are very workable and self-compacting.

Pre-packed dry aggregates which are grouted

Single sized course aggregates are packed into the repaired area, then grout is pumped from the furthest point to fill spaces between the aggregate within a simple formwork. The method does not require any vibration and it is suitable for underwater conditions (Tigeli 2010).

2.3.2 Patch Repair

The use of cementitious patch repair mortars will be adopted in the experimental work for this research. The cementitious mortar mix will allow for easy workability for small sample sizes, prevent further rebar corrosion and deterioration and limit or control the ingress of external threats, thus ensuring the repaired RC structure has a greater durability and

serviceability prior to the repair work. Patch repairs are prepared systematically following a step-by-step procedure which ensures proper and adequate surface preparation, method of application, curing and surface finishing.

In order to ensure that the patch repair does in fact limit the rate of deterioration it is important that there is compatibility between the repair mortar and the existing concrete structure so that the interaction with the substrate does not initiate another durability problem (Tigeli 2010).

To ensure compatibility between the repair material and the substrate there are several factors that need to be considered. Compatibility refers to the balance between the geometrical, chemical, permeable and electrochemical properties of the substrate and the existing concrete structure to ensure the forces experienced due to volumetric changes and electrochemical effects post patch repair do not cause premature deterioration. (Vaysburd 2006)

Keeping in line with the scope of the research, the literature specifically focuses on the volumetric changes experienced between the patch repair mortar and existing concrete substrate. Volumetric changes are a result due to the drying shrinkage of the repair material restrained by the existing concrete substrate which causes cracking and delamination between the two materials, the difference in elastic modulus causes unequal load sharing and strains resulting in interface stresses, creep properties and relative fatigue performance that cause stress that can crack the repair material or cause debonding between the repair material and substrate interface sometime after the patch repair was completed. (Vaysburd 2006).

The most common method of patch repairing involves cutting the deteriorated concrete 20mm below the corroded reinforcement, and cleaning off all corrosion products off the affected steel and preparing the concrete substrate. The remaining substrate should resemble a sound and strong material, which is a requirement for producing a repaired concrete structure with monolithic behaviour (Beushausen, Fultons Concrete Technology 2009). Finally, an appropriate steel primer and substrate bonding coat can be applied before the patch repair mortar is applied to rebuild the cut member to the original surface profile (Tigeli 2010).

Once the repair mortar has set and cured properly the next step is to provide external strengthening along the repaired section of the RC structure. Externally bonded fibre reinforced polymers are an easy and effective way to provide adequate strength to ensure the RC structure increased durability and serviceability, although we do not know how much. Therefore the primary objective of the research is to analyse the additional long term performance that the combination of FRP and the patch repair provide damaged RC structures.

2.3.3 Behaviour of corroded RC Beams after Patch Repairs

The test specimens for this dissertation comprise of a number of materials, these materials include the original substrate concrete, corroded and non-corroded internal steel reinforcement, patch repair mortar, epoxy bonding agents and finally fibre reinforced polymer laminates, therefore it is important to analyse each materials effect under certain loading conditions which will in turn all contribute towards a greater understanding of the failure mechanics of the system as a whole.

Patch repairs are implemented in an effort to restore the serviceability state of a damaged structure. The most common form of durability problems for RC structures within a marine environment emanate from corrosion of the internal reinforcing steel. The primary method of treating localised corrosion damage is patch repairs; therefore it is important to investigate the long term performance of the repair work. The most important factor to consider in repairs is the compatibility of the repair materials used with the original substrate concrete (Malumbela 2010). These compatibility factors refer to the balance of dimensional geometry, chemical, permeability and electrochemical properties between the repair and substrate that ensures the system as a whole withstands forced induced by restrained volume changes, chemical and electrochemical effects without premature deterioration over a designed period of time (Tigeli 2010). Focusing on the dimensional compatibilities of a repaired RC beam; the original substrate often constrains the repair mortar during hardening, thus resulting in localised drying shrinkage of the repair mortar which causes cracking and delamination between the two materials. Furthermore the difference in modulus of elasticity between the two materials causes an uneven distribution of loading and uneven strains, resulting in interface stresses, creep properties and relative fatigue performance which can cause cracking of the patch repair material or debonding

between the repair and substrate interface (Tigeli 2010). Shrinkage cracks that occur in the repair mortar often allow more ingress of corrosion agents which can speed up the rate of the corrosion process.

It has also been shown that some chloride contaminated concrete is left after the patch repair has been completed. The much stronger and harder repair mortar often offers more resistance to further steel corrosion compared to the substrate concrete, therefore a corrosion protective system should be applied to the original substrate before the repair mortar is applied. These protective systems include cathodic protection, corrosion inhibiting admixtures and electrochemical/physical barriers between the steel bars and repair mortar (Malumbela 2010).

Malumbela investigated the serviceability of corrosion-affected RC beams after patch repairs and FRP strengthening under serviceability loads. The experimental program included testing corrosion-damaged RC beams (153 x 254 x 3,000 mm) which were patch repaired and finally strengthened using FRP's under sustained service loads. Steel corrosion was induced using two sequential corrosion processes; firstly accelerated corrosion by impressing an anodic current followed by natural corrosion. The test specimens underwent a series of different corrosion and loading combinations. As a result of the different combinations, specific test specimens were either patch repaired and later externally strengthened with FRP's or purely strengthened without a patch repair to replace to the damaged concrete. After strengthening, further corrosion was induced and load applied at varying combinations once again.

Prolonged tests concluded that bonding FRP plates to a corrosion-cracked face of a RC beam was found to reduce the rate of corrosion crack widening on the strengthened face. Malumbela suggests that strengthening with FRP plates prevents further corrosion cracking if the plates are bonded directly over the cracks and along the same line of the propagation of the cracks. It was also found that the use of FRP strengthening to reduce local corrosion cracking resulted in an increased rate of crack widening on other already-cracked sections that were not strengthened on the beam. Also, the effect of the localised FRP strengthening also induced new cracks on previously uncracked faces of the unstrengthened beam. Therefore concluding that purely strengthening with FRP's on corrosion damaged RC beams

under loading further deteriorates the service life of the RC beams based on the criterion of corrosion crack widths. Despite the increased rate of crack widening due to the FRP strengthening, the load bearing capacity of the beams was greatly improved.

Therefore, to fully-restore the service life of a corroding RC structure based on the criteria of crack widths and load bearing capacity, corrosion-damaged concrete should be replaced with a patch repair and the reduced area of steel should be compensated by strengthening with FRP's (Malumbela 2010).

2.4 Fibre Reinforced Polymers (FRP)

2.4.1 Introduction

Specific studies relating to the advantages and uses of individual fibre reinforced polymers (FRP) are relatively new. Although FRP's were first introduced into the civil engineering field in the 1980's, very little was known about their properties and specific uses. Initially, the use of FRP's was limited to strengthening structural buildings in bending and shear because the individual FRP fibres have excellent strength to self-weight ratio which could easily be formed into any shape when used as a FRP matrix.

There are commonly three main types of FRP's that are used for structural applications namely Glass (GFRP), Carbon (CFRP) and Aramid (AFRP). Each of these FRP's has their own significant advantages over classical materials such as steel and wood.

FRP is a composite material made of high-strength fibres and a matrix for binding these fibres to fabricate structural shapes. The individual fibres provide the essential strength and stiffness required while the matrix provides the transfer of the stresses and strains between the fibres. The matrix also helps to provide a barrier against the environment which protects the surface of the fibres from mechanical abrasion (Keller 2003), (Balaguru 2009).

2.4.2 Uses of FRP in Civil Infrastructure

Studies carried out over the last ten years have revealed that different FRP composites provided different advantages (Taljsten 2006). Thus care should be taken when selecting FRP's for a given application. Certain FRP fibres can be combined in order to suit a required structural objective whether it is to repair or strengthen a structure.

FRP's are applied to existing structures to increase any of the following properties (Buyukozturk et al 2004), (Taljsten and Elfgren, 2000):

- Axial, flexural, or shear load capacities
- Ductility for improved seismic performance
- Improved durability against adverse environmental effects
- Stiffness for reduced deflections under service and design loads

FRP composites are also useful for the repair of existing concrete structures to provide additional strength. The most common reasons for repair and strengthening of concrete structures include the need to compensate for design errors, correct deterioration problems, or improve the performance according to design codes.

Most common applications of FRP repair work include (Balaguru, 2009):

- Strengthening of reinforced and pre-stressed concrete beams for flexure
- Shear strengthening of reinforced and pre-stressed concrete beams
- Column wrapping to improve the ductility
- Strengthening for improved blast resistance
- Strengthening of un-reinforced masonry walls for in-plane and out of-plane loading

2.4.3 Types of Fibres

Fibres are produced in three different forms, firstly, roving, comprises of continuous parallel bundles of untwisted filaments, secondly, a yarn consists of bundles of twisted continuous filaments and thirdly, short fibres produced from chopped or ground filaments limited lengths of 3-50mm.

In order to obtain sheet like elements with several reinforcement directions, the fibres are further worked to textile products (Keller 2003). One differentiates between directional roving products like woven and non-woven fabrics, grid and mesh products and non-directional sheet products like mats with random chopped filaments, mats with continuous fibres and surfacing fleeces (Keller 2003). As reinforcing elements for FRP construction: elements at the present time woven and non-woven fabrics as well as reinforcing mats and fleeces are mainly used (Keller 2003).

In order to achieve high tensile strengths, FRPs' are arranged in complicated polymer matrices. A polymer matrix forces the individual FRP fibres to exercise the actual load bearing function of the matrix. The polymer matrix has four functions:

- Fixing the fibres in the desired geometrical arrangement
- Transferring the forces to the fibres
- Preventing buckling of the fibres under compressive actions
- Protecting the fibres from humidity

The mechanical properties of fibre polymer bonds are mainly determined by the adhesion and the mechanical compatibility between fibres and the matrix as well as the angle between the fibres and the direction of loading (Keller 2003).

The linear elastic deformational behaviour of the composite is governed primarily by the reinforcing fibres. In order to prevent the development of micro-cracks in the matrix before reaching the fibres elongation limit, the failure strain of the matrix should be greater than that of the fibres. Under compression, a minimum stiffness of the matrix is required to prevent buckling of the fibres (Keller 2003).

The stiffness and strength of a fibre-matrix bond depend greatly on the angle between the fibres and the direction of loading. The highest load values are obtained for a constant loading and a corresponding arrangement of the fibres in this direction (so-called uni-directional UD laminates). If the loading direction is subject to the changes, multi-layered structures (woven and non-woven multi-axial fabrics, etc.) exhibiting quasi-isotropic behaviour are used (Keller 2003).

2.4.4 Types and Production of Fibre Reinforced Polymers (FRP)

There are three types of FRP's, namely glass fibre FRP, carbon FRP and aramid FRP, each having different compositions, characteristics and advantages.

Glass Fibres

GFRP's are the most commonly used of all reinforcing fibres. There are four types of glass fibres, namely, S-glass (Structural glass), E-glass (Electrical glass), C-glass (Chemical glass) and AR-glass (Alkali-resistant glass). Glass fibres are manufactured by fusing silicates with

silica, potash, lime or meal oxides. This produces a molten mass which is passed through micro brushing and rapidly cooled to produce the glass fibres filaments. The filaments are then bound into closely packed strands or loosely packed roving, whilst being covered with a coating, known as sizing, see figure 7. The coating used minimizes the abrasion-related degradation of the filaments. Advantages of glass fibre include low cost, high tensile strength, chemical resistance and high temperature resistance. The disadvantages include low tensile modulus, sensitivity to abrasion while handling, relatively low fatigue resistance and brittleness. (Miller, 1987; Gurit Composite Technologies, 2008)

E-glass is most commonly used and makes up 90% of all GFRP used. It is a family of glasses with a calcium aluminoborosilicate composition and an alkali content (<2.0%) which allows good strength at very low cost. (Miller, 1987)

S-glass has the highest available tensile strength for a GFRP. It comprises of magnesium aluminosilicate which is difficult to manufacture and therefore the cost is considerably higher than that of E-glass (Miller 1987; Gurit Composite Technologies, 2008).

C-glass and AR glass are more specific to certain conditions. C-glass is used in corrosive environments and has a soda lime-borosilicate composition. It is commonly used as a surface coating or laminate to pipes and water tanks.

AR-glass is specifically developed for use in concrete or applications requiring greater chemical resistance to alkaline chemicals, such as cement substrates and concrete. AR-glass is composed of alkali-zirconium silicates (Miller 1987; Gurit Composite Technologies, 2008).

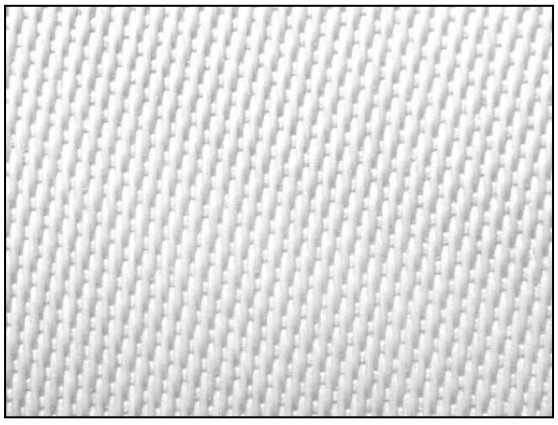

Figure 7: Glass fibre (www.glassfiber-fabric.cn)

Carbon Fibres

CFRP's are often used for strengthening because they offer the highest modulus of all the FRP's. Carbon fibres have a wide range of grades all of which offer different tensile-strengths-to-weight-ratios as well as high tensile-modulus-to-weight ratios. Among the top commercial grades of CFRP's, the fibres have a high fatigue strength and very low coefficient of linear thermal expansion. All GFRP's possess a high electrical conductivity, they are also not susceptible to corrosion and oxidation at low temperatures (<400'). The cost of the GFRP's is a major disadvantage as well as the low impact resistance. (Amateau, 2003; Mallick, 1993)

Carbon fibres tensile moduli range from 207GPa – 1035GPa for top grade. Carbon fibre is renowned for its low density, this is achieved due to the fact that individual fibres are generally stiff, and thus a matrix requires less overall layers to achieve the balance between rigidity and strength (See figure 8). High modulus and high strength weigh the same but an important advantage of a high modulus is the increased rigidity, thus less material is required and a lighter weight composite structure for application that require stiffer components (Competitive cyclist, 2003).

There are three main feed-stock or precursor sources used to produce carbon fibre: Rayon, polyacrylonitrile, and petroleum pitch.

A method called, Carbonization is used to produce carbon fibres of a high tensile strength. It is a process whereby a precursor material is chemically changed into carbon fibre by the action of heat. This method is used with the aid of a rayon precursor. The disadvantage of this process was the relatively low conversion yield to carbon fibre, although it is widely available. Only 25% of the rayon precursor is yielded into carbon fibre, thus making it more expensive than carbon fibres made from other materials (Hansen, 1987; Pebly, 1987).

Carbon fibre yielded from polyacrylonitrile (PAN) precursor, during the carbonization process, generally has a higher tensile strength. This is due to the lack of surface defects; these defects tend to accentuate the stress experienced, therefore reducing tensile strength (Hansen 1987).

Petroleum pitch often yielded the most amount of carbon fibre after the carbonization process. It is a much cheaper and widely available precursor, which made the carbon fibres yielded relatively cheaper. A major disadvantage was the non-uniformity from batch to batch during production (Hansen, 1987; Mallick, 1993).

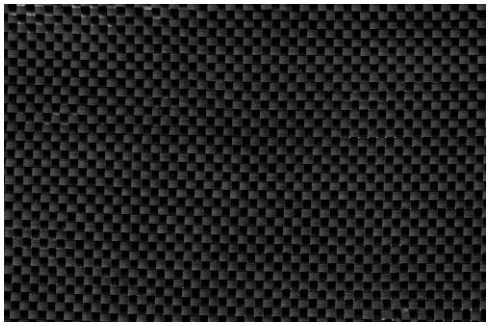

Figure 8: Carbon fibre (www.alibab.com)

Aramid Fibres

Aramid fibre, a synthetic organic polymer, more commonly known as Kevlar is produced by spinning a solid fibre from a liquid chemical blend (See figure 9). A significant characteristic of the Aramid fibres includes having the lowest specific gravity and the highest tensile strength-to-weight ratio among all FRP. AFRP is 40% lighter than GFRP and 20% lighter than CRFP. Advantages of AFRP include high strength, good resistance to abrasion and impact, as well as chemical and thermal degradation (Mallick, 1993; Smith, 1996; Gurit Composite Technologies, 2008).

There are many different grades of Kevlar, each differing in tensile and modulus strengths. Different types of Kevlar are also used for specific requirements in practice.

The disadvantages of aramid fibres are the low compressive strength (500 – 1000 MPa), the reduced long-term strength as well as their sensitivity to UV radiation (Keller 2003).

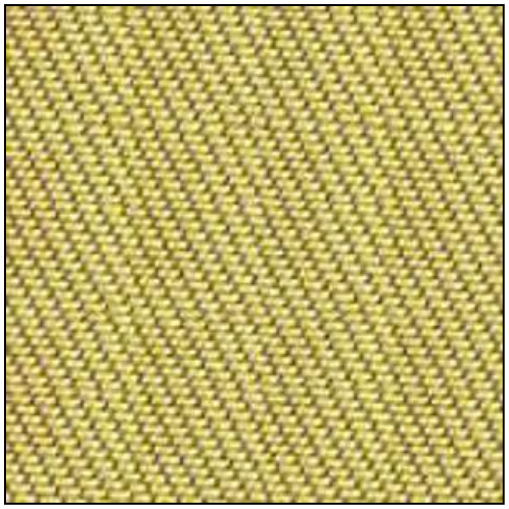

Figure 9: Aramid fibres (www.nauticexpo.com)

2.4.5 Properties of Fibre Reinforced Polymers

Mechanical Properties

The mechanical properties of FRP's described above are given in table 1.

Table 1: Mechanical Properties of common FRP's (Keller 2003)

		GFRP	CFRP	AFRP
Property	**Unit**	**E-Glass Fibre**	**Carbon Fibre**	**Aramid Fibre**
Tensile strength	MPa	3.500	2.600-3.600	2.800-3.600
Young's modulus, E	GPa	73	200-400	80-190
Elongation at failure	%	4.5	0.6-1.5	2.0-4.0
Density	g/cm^3	2.6	1.7-1.9	1.4
Co-efficient of thermal expansion	$10^{-6}/K$	5/6	Axial-0.1–(-1.3) to, radial 18	-3.5
Fibre diameter	µm	3-13	6-7	12
Fibre structure	-	Isotropic	Anisotropic	Anisotropic

Fire Resistance

FRP resistance to fire is a critical characteristic because FRP's are often used in environments where exposure of FRP to fire is possible. In general, FRP materials are in principle combustible, however advances have been made in the technologies of the FRP's which now allow for FRP's to be fire-retarded, self-extinguishing and not emit any toxic

fumes. Very little is known about the loss of strength to the FRP's once heated (Keller 2003).

CFRP's are able to achieve near zero expansion to temperatures as high as 300°C. If the carbon fibres are protected from oxidation, the fibres will be able to withstand temperatures as high as 2000°C. Anything above this temperature and the fibres will decompose (Balaguru 2009).

Sustainability of FRP Materials

The main indicator for determining the sustainability of fibre reinforced polymers is to compare the amount of energy required to manufacture FRP's with respect to the amount of energy required to manufacture steel. Glass fibres can be described as sustainable and ecological because the manufacturing of GFRP's requires a quarter of the amount of energy needed to produce steel. The glass fibres themselves are made mainly of quartz powder and limestone, both of which are environmentally friendly and basic resources are inexhaustible.

On the other hand, the production of carbon fibre requires a large amount of energy, which in turn affects the sustainability of this particular polymer.

Polymers in essence are waste products from the oil industry. In their use for structural components, however, the energy possessed by the starting materials is stored for several decades. The required amount of material, even if their application increases in the future, is comparatively insignificant. Therefore the application of polymers for structures can be of the most sustainable uses of fossil fuels today (Keller 2003).

FRP Durability

FRP materials will experience a wide range of climate conditions. The durability of each particular FRP is indicated by the resistance to attack when placed in particular environments. Common glass fibres are especially vulnerable to humidity and alkaline attacks and Aramid fibres are susceptible to ultraviolet attacks. Only carbon fibres are generally considered to be resistant to most forms of attack (Keller 2003).

Three tests were conducted and the following results were recorded:

- C-fibres and CFRP bars exhibit good durability, but external UV protection is required.
- AFRP bars exhibit good durability, with the exception to stress rupture and of UV and acid influence.
- GFRP bars exhibit poor durability, with the exception of acid resistance and freeze-thaw resistance.
- GFRP bars are not suitable as concrete reinforcement.
- Carbon fibre/ epoxy systems exhibit good durability.
- Glass fibre systems: loss of strength 20% (humidity absorption), no negative effect of salt water and alkali solutions.

2.4.6 CFRP Installation

In practice, FRP's are applied to existing structures in many different ways with varying techniques. The growing technology of using CFRP composites to strengthening existing structures is particularly promising for bridge applications because of the large number of existing bridges across the world that need repair or replacement (Gussenhoven 2005).

Installation of a CFRP involves the correct method of application along with a suitable strengthening scheme. The bond between the CFRP and existing RC structure is the most crucial since this is often the first bond of failure and the weakest. Figure 10 illustrates the different mechanics of failure between the FRP and concrete bond. Mode 1 illustrates brittle concrete crushing failure, this occurs when the compressive strain in the concretes compressive zone is exceeded. Modes 2 and 3 illustrate when the internal reinforcement steel yields in tension and compression. Cracks at the midspan of the RC beam in the tension zone often result in brittle tensile failure of the FRP laminate, this mode of failure would occur after considerable concrete damage is visible. Mode 5 is a result of anchorage failure in the bond zone of the laminate, this type of ductile failure can be avoided with sufficient anchorage lengths which provide a forewarning of the propagated failure. Failure mode 6 is a result of the FRP laminate debonding failure at the laminates cut off end against the concrete beam. Mode 7 is the most common and illustrates typical FRP laminate debonding from the original concrete surface. When designing composite structures, it is preferred to design for ductile failure since the failure mode in most cases will be followed by a large deformation.

McSweeney and Lopez (2005) conducted pull off tests to investigate the failure loads of FRP-concrete systems. It was concluded that failure mode depends primarily on the width of the bonded region and the thickness of the FRP repair. Increasing the bonded width of FRP had the greatest effect on increasing the failure load of the system, but this is limited due to the geometry of the repaired section. Increasing the thickness of the bonded FRP also significantly increased the failure load of the system. Failure between the FRP-concrete bond occurs in stages, provided there is enough bonded length to develop the full capacity of the bond in more than one region. Furthermore, localised cracks in the structure under loading results in the failure of the bond at the specific cracked region and results in a pull out of concrete before the bond begins to fail at the epoxy-concrete interface. Eventual failure of the FRP-concrete bond is extremely brittle, the energy release is sufficient to also fail the FRP itself in some cases (McSweeney, Lopez 2005).

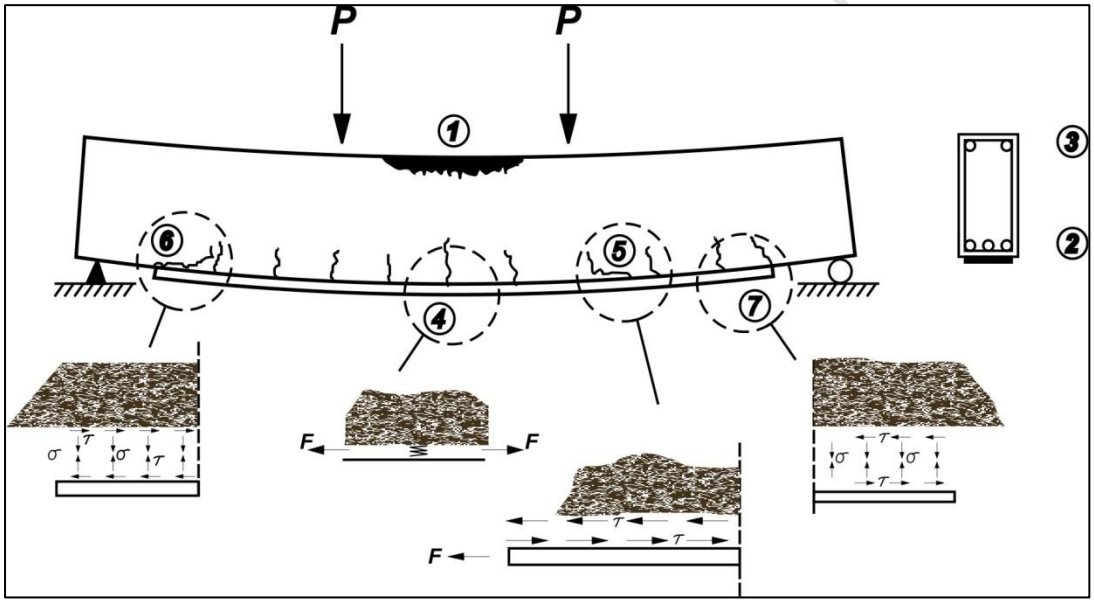

Figure 10: Possible failure modes for a RC beam strengthened for bending using CFRP

2.5 CFRP Strengthening

2.5.1 Introduction

The use of advanced composite materials in the form of externally bonded fibre reinforced polymer laminates have been successfully used in structural retrofitting and upgrading of existing RC members (El Maaddawy, Soudki 2005). Extensive research conducted by Soudki

(2005), has indicated the structural benefits that may be obtained when externally bonding CFRP laminates onto existing corrosion-damaged RC structures.

The method of externally bonding the CFRP is a repair technique with the intention of restoring and exceeding much of the original flexural or shear capacity lost due to the internal corrosion of the steel. Externally wrapping an existing RC structure with FRP laminates may reduce the corrosion activity because FRP wraps act as a low-permeability barrier to further ingress of water and oxygen into the concrete. The physical confinement that the FRP wrap reduces the dispersion of corrosion products and thus limits the corrosive reaction itself. Furthermore, effectively wrapping a concrete section with FRP laminates provides an external pressure of corrosion products and thus decreases the corrosion and splitting cracks. Therefore, the structural performance of corroded RC members could be improved if they were repaired with FRP laminates (El Maaddawy, Soudki 2005).

Extensive research has been conducted by many engineers to investigate the study of externally bonding CFRP's onto existing RC structures with the intention of increasing the flexural and shear capacities of these RC structures (Balanguru 2009) (Keller 2003) (Chen, Teng 2003) (Taljsten 2006). This idea has been introduced into many applications in-service today, such FRP applications include; reduction of corrosion damage in RC structures, minimization of crack propagation as well as most commonly externally strengthening or retrofitting existing structures. However there is limited reported research on the long term behaviour of corrosion damaged RC structures that have been repaired and externally strengthened using CFRP's. El Maaddawy (2005) explains that there is insufficient research available concerning the feasibility and viability of using externally bonded FRP laminates to repair already corroded RC beams at various levels of corrosion damage. Gussenhoven (2005) also states that an understanding of the factors affecting the fatigue performance of strengthened beams is required to develop appropriate design guidelines for bridge applications.

Currently there is an abundance of literature available regarding the short term effects of FRP strengthening as well as the advantages that these FRP applications provide (Gussenhoven, Brena 2005). The extensive literature of the short term effects of FRP applications has been concluded through extensive testing which involved simulated

experimental programs involving static loading of simplified RC structures strengthened using CFRP.

The next step of investigation and the primary objective of the dissertation include analysing the long term fatigue performance of composite RC structures. A composite RC structure refers to a structure that has undergone a patch repair as well as external CFRP strengthening due to the effects of corrosion damage. Therefore the structure comprises of the original substrate concrete, the patch repair mortar, the epoxy bond and CFRP laminate. This type of composite structure is commonly seen in-service where a localised patch repair has been performed on a corrosion damaged section of a service nearing its end of service life.

The advantages of understanding the failure mechanisms and long term performance behaviour of such a composite RC structure will go a long way to contribute in the study of extending the service life of an existing RC structure. If a structures extended service life can be qualitatively calculated and predicted, the method of patch repairs and FRP strengthening can ultimately be used as a typical repair technique for damaged RC structures as well as to stagnate and prolong maintenance plans for structures such as bridges and dams.

2.5.2 CFRP Application

There are many ways to externally bond FRP onto reinforced concrete structures. The different application modes or techniques provide different outcomes depending on the specific requirements and demands of a project. Throughout this thesis we will refer to four main methods to apply the carbon fibre composite onto reinforced rectangular beams, namely, U-Jacketing, Fully Wrapped, Side Strips and a relatively new method called Near Surface Mounting (NSM). Each application method has its own benefits with respect to the amount of strengthening of the RC beam as well as their own subsequent disadvantages.

Different strengthening schemes fail under different circumstances. Typical failure modes include FRP rupture, and debonding of FRP where the FRP wrap delaminates completely off the RC beams. Careful consideration must be taken when deciding on an appropriate type of strengthening scheme. The selection of a strengthening scheme usually depends on the additional strength increase required, type of repair work required or retrofits work needed.

The location of the project and application manoeuvrability also have an influence in the FRP arrangement applied.

Specific strengthening schemes are designed according to a damaged structures needs. Often localised repair work is done on a structure, whereby a specific installation technique can offer additional bending strength or shear strength or a combination of both. Below the different methods of installations are described as well as the design guidelines for bending, shear and torsion.

2.5.2.1 Shear Strengthening

In the principle of design, the shear capacity should always exceed the flexural capacity for a given reinforced concrete section; therefore a typical RC beam should fail in flexure before it fails in shear. But when the shear capacity is less than the flexural capacity after flexural strengthening, shear strengthening must be implemented. Previous researchers have investigated and proven the effectiveness of using FRP as a suitable method of strengthening RC beams in shear.

According to ACI 440.2R-08,effective design requirements stipulate that the fibre orientation should be in the same direction as the principle stresses, which is approximately 45° to the member axis but in practice it is generally accepted to bond the FRP in the perpendicular direction to the member axis. The FRP can be orientated in many different strengthening patterns both along the axis of the beam and the plane of the cross section. The strengthening scheme can also be continuous or discontinuous in the longitudinal direction. Different modes of strengthening yield different results; the most common form of shear strengthening involves wrapping sheets around the cross section.

To calculate and analyse the effect of FRP shear strengthening of existing RC structures, there are several different approaches to predict the actual addition shear capacity. Modern design modes include the shear friction method, the compression field theory, various truss models including Morsch truss analogy and the design guidelines that have been adopted by *fib*, ISIS Canada, ACI and The Concrete Society (Hollaway 2010). All possible failure mechanisms need to be understood before a suitable strengthening application can be applied. Normal concrete structures are designed in such a way that they experience large deformations before failure, which means that the failure is often bending failure. However,

for a concrete beam with conventional steel stirrups the shear failure can be characterised in the following main categories (Taljsten 2006):

- Web shear failure; cracking occurs in the regions where the beam is not affected by bending cracks. Cracking occurs when the principle tensile stress exceeds the concretes tensile strength in the web; a result of insufficient shear reinforcement.
- Bending shear failure; initiated from bending cracks to inclined shear cracks. Cracking grows from the tensile zone to the compression zone.
- Compressive failure in web; failure is caused by the compression failure in the inclined concrete struts in the truss. This typical failure is a result of excessive shear reinforcement; therefore the steel reinforcement does not reach its yield limit before the concretes compression strength is reached.

Figure 11 illustrates a further two modes of failure once a RC beam is strengthened using CFRP.

- Fibre failure in the composite; this typical failure occurs when the critical strain capacity is exceeded. The failure is usually brittle; however the fibre orientation of the CFRP affects the ductility of the beam.
- Anchorage failure; this failure occurs when the concretes external strength is too low or the anchorage area is too small to transfer the shear forces between the reinforcement and the concrete.

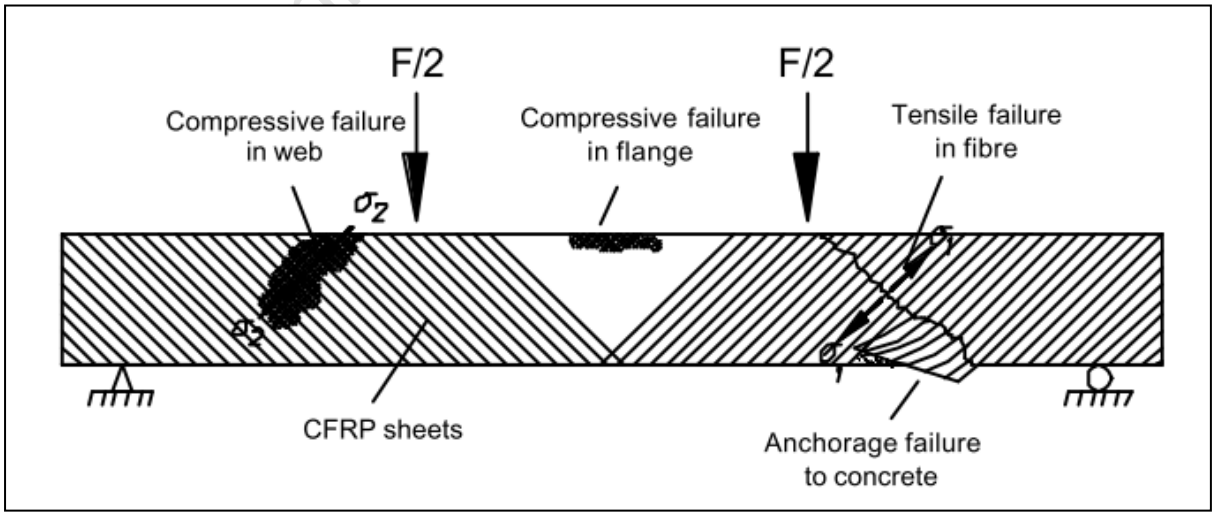

Figure 11: Different failure mode in shear (Taljsten 2006)

Side Laminates

The most effective way to increase the shear capacity of an existing structure is to apply CFRP strips externally at the regions of desired increased shear capacity, as shown in figure 12. The strips are often placed at a calculated equidistant spacing from each other and positioned at all concerned areas of sheer failure and at the points of loading. This bond technique is highly susceptible to CFRP debonding but ultimate failure will be due to rupture (Chen, Teng 2003). Side strips can be orientated at any required angle but it is recommended that the strips are aligned at 45° or 90° to the longitudinal base of the RC beam. This will allow the strips to intersect any propagating cracks, effectively reducing the damage and potential failure of the beam. The fibres are effectively aligned in the direction of the principle stresses and normal to the propagating cracks which lead to failure.

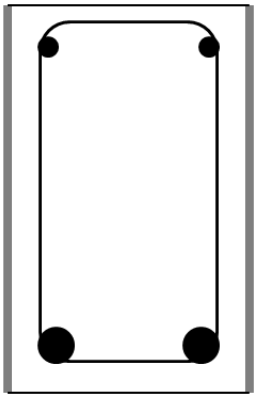

Figure 12: CFRP Side Laminate Strips

Design for shear strengthening

Taljsten differentiates equations for the two different application modes, namely, fully wrapped and side strips. The proposed design equations also account for the different fibre orientations that the FRP can be externally bonded onto the RC beam in. Taljsten understood that the combination of the effect of shearing together with the shear force influences creates a multi-axial stress-state in the beam, where tensile stresses are generated at angles between 30°-60° (depending on reinforcement and loading) in relation to the construction's longitudinal axis. This leads to the formation of inclined shear cracks and ultimately failure. Taljsten (2006) derived his FRP shear equation based on the principle that the capacity of the beam is obtained by for external composite

reinforcement. The external reinforcement is angle at β from the horizontal plane. The greatest principle tensile strain occurs at right angles to the crack plane.

Taljsten (2006) analyses the stresses and strains experienced in the carbon fibres and derived equations based on the type of application depending on the orientation of the fibres. A general equation to calculate the shear capacity of CFRP has been formulated:

Tests by Caroline (2001) have shown that a factor of 0.6 of the ultimate strain gives a goo estimate of the shear capacity for rectangular beams strengthened with carbon fibre composite sheets (Taljsten 2006).

Modified Shear equations for different strengthening schemes:

Case 1: Entire side strengthened with inclined fibres, ß=45°

Case 2: Entire side strengthened with vertical fibres, ß=90°

Case 3: Strengthening with inclined strips, ß=45°

Case 4: Strengthening with vertical strips, ß=90°

2.5.2.2 Flexural Strengthening

The most common form of CFRP repair and strengthening is flexural strengthening. Flexural strengthening involves increasing the flexural capacity for damaged or under designed structures. There are many application methods for flexural strengthening, some of which provide both additional flexural and shear strength as a combination.

The following methods are the most common and effective for CFRP flexural strengthening:

U-Jacketing

In order to increase both the bending and shear capacity of a damaged RC beam, CFRP's are wrapped around the RC beam along the bending and shear faces. The CFRP is fully bonded using a high tensile strength bonding agent. This specific application mode is often used for Tee and Rectangular sections. The positioning of the FRP is often at the most likely point of sheer failure or near the supports and mid-span. Failure of the U-Jacket is not very common to FRP rupture but more susceptible to the FRP debonding off the beam because of the discontinuity (J.F Chen 2003). U-Wrapping provides a good anchor, however they are not as effective in the negative moment region because shear cracks initiate at the top of the beam. Providing a mechanical anchor at the junction of the beam and slap will considerably increase the effectiveness of the U – Jacket (Balaguru 2009).

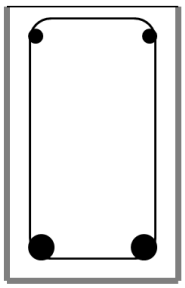

Figure 13: CFRP U-Jacketing

Wrapped

A more effective method increasing both the shear and bending capacities of a damaged RC beam. CFRP fibres are completely wrapped around the entire cross-section of the RC beam, covering all tensile and compressive faces. Often used for rectangular RC beams and positioned near all supports to provide anchorage or along the entire beam to ensure continuity and maximum strength. CFRP debonding is very unlikely for this particular application mode and therefore is highly susceptible to sudden CFRP rupture (Chen, Teng 2003).

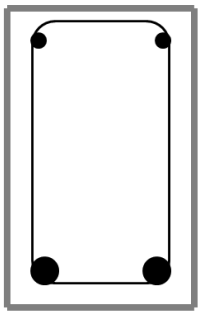

Figure 14: CFRP Fully Wrapped

Near Surface Mounting (NSM)

NSM is not a very common strengthening application mode. The application of NSM introduces CFRP laminate strips that are placed into grooves using an epoxy adhesive which is cut out into the cover concrete along the sides of the RC beam. The position of the cuts along the sides of the beam is determined by the expected positions of the shear failure cracks as seem in Figure 16. In the case of sheer strengthening, the CFRP strips will be spaced equidistantly along the side of the RC beam and fixed into the groves using an epoxy adhesive. The CFRP strips can be aligned at any angle relative to the RC beam, similar to when externally bonding side strips. Different orientations of the strips allow for variations of additional sheer strength. Figure 15 represents a typical RC beam which has been strengthened by the near surface mounting method to increase the bending capacity of the RC beam.

This is not a very common or effective application mode for shear strengthening since the fibres within the laminates are not specifically aligned along the line of the primary tensile forces and therefore external bonding with side strips would be more effective.

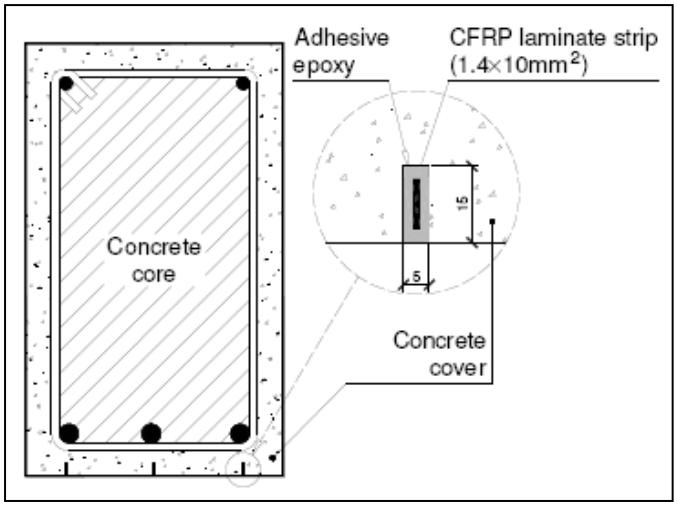

Figure 15: Near Surface Mounting of CFRP

Design for strengthening in flexure

The design for CFRP flexural strengthening can only begin once the strain diagram is known for the concerned section (See figure 16). With regard to strengthening, it is then assumed that the composite structure either reaches crushing in the compression zone or that the laminate reaches ultimate limit strain. For a double reinforced cross section the following design cases are concerned (Taljsten 2006):

- Failure in laminate with yielding in the compression steel reinforcement.
- Failure in laminate without yielding in the compression steel reinforcement.
- Crushing of concrete as well as yielding in the compression steel reinforcement.
- Crushing of concrete without yielding in the compression steel reinforcement.

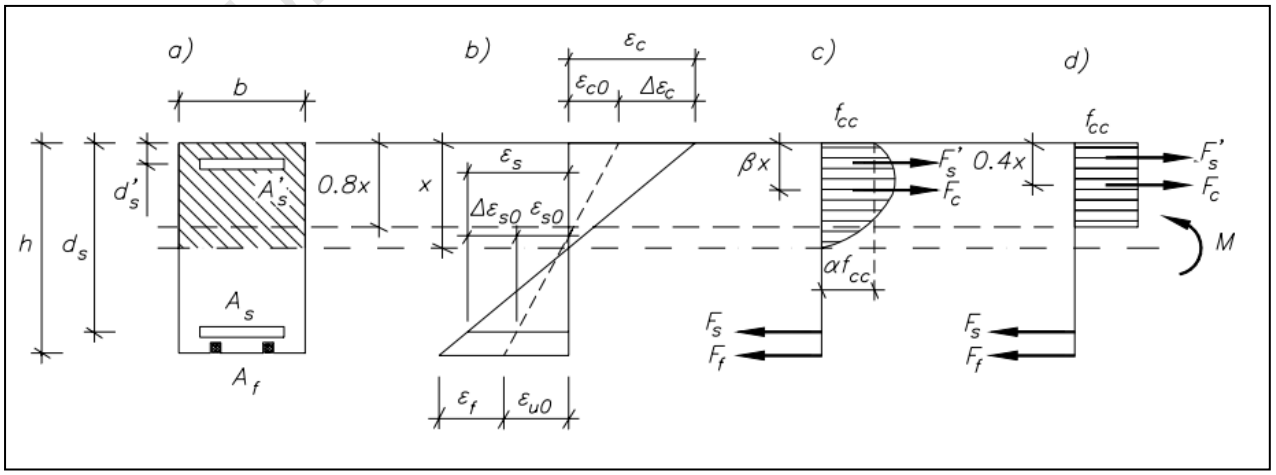

Figure 16: Principles for strengthening in bending (Taljsten 2006)

For general compressive stress distribution, horizontal equilibrium equation gives:

The desired moment capacity depends on the failure type.

1. Failure in laminate with yielding in the compression steel reinforcement

Moment equilibrium gives:

So *x* can be solved;

2. Failure in laminate without yielding in the compression steel reinforcement

Moment equilibrium gives:

X can be solved with the use of quadratic equations

Where,

3. Crushing of concrete as well as yielding in the compression steel reinforcement

Moment equilibrium gives:

X can be solved with the help of the quadratic equations

Where,

4. Crushing of concrete without yielding in the compression steel reinforcement

X can be solved with the help of the quadratic equations

Where,

2.5.2.3 Torsional Strengthening

The most effective way to strengthen for torsional damage is to follow a similar application mode to that of shear strengthening. It is evident that cracks in the concrete due to torsional loading usually follow the same mechanism as concrete cracking under shear loading (Taljsten 2006). Therefore application modes like side strips or fully wrapped are best suited for torsional loading, although he design values differ.

Design for torsional strengthening

The following equations were derived with the principle similar to shear strengthening, concentrating on the engineering-related origins of strengthening in torsion, considering that only the stress fibres build up perpendicular to the crack plane (See figure 17).

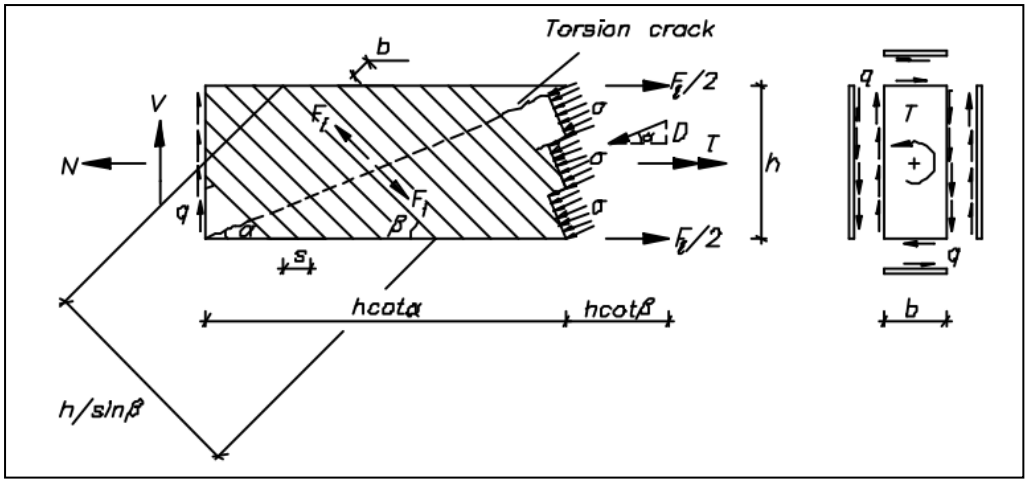

Figure 17: Principle for torsion capacity for FRP (Taljsten 2006)

Modified Torsional equations for different strengthening schemes (Taljsten 2006):

Case 1: Entire side strengthened with inclined fibres, ß=45°

Case 2: Entire side strengthened with vertical fibres, ß=90°

Case 3: Strengthening with inclined strips, ß=45°

Case 4: Strengthening with vertical strips, ß=90°

These equations are the basis for design of strengthening in torsion with CFRP materials. A RC structure subjected to torsion can fail in one of the following ways (Taljsten 2006):

- Compression failure in the concrete struts
- Exceeding the ultimate strain in the fibre or steel
- Anchorage failure between the concrete and composite

2.5.3 Behaviour of FRP Strengthened RC Beams under Fatigue loading

The following papers discussed tested the long term performance of non-corroded or repaired, FRP strengthened RC beams. The aim of the fatigue analysis is to determine the modes of failure, advantages and additional extended life span of FRP strengthened RC beams versus un-strengthened control RC beams.

2.5.3.1 Shahawy and Beitelman (1999)

This paper focused on both the static and fatigue performance of RC beams strengthened with CFRP laminates. The aim of the static testing was purely to show that the application of CFRP to reinforce concrete beams results in increased strength and enhanced performance. Fatigue tests were conducted on several of the test specimens, the degree of CFRP lamination system was varied for each specimen, including one member this is fatigued for over half of the expected fatigue life, then rehabilitated with the CFRP, and fatigue again until failure. Comparisons are made for the standard section and equivalent sections with two and three layers of CFRP involving the improvements in fatigue behaviour, stiffness and capacity.

The fatigue experimental program consisted of seven T-Section RC beams; a t-section was selected as being the most suitable for the use in the study since it provided a large surface area for application of the CFRP laminates, as well as a relatively large compressive resistance area of the flange. Six of the test specimens were strengthened using CFRP laminates and one was un-strengthened and used as the control beam.

The fatigue loading program was achieved using an electro-hydraulic actuator programmed to deliver a sinusoidal load ranging from 25% to 50% of the ultimate capacity of the static control specimen at a frequency of 1Hz. The loading arrangement was a four-point set up (See figure 18) which ensured a constant bending moment being applied across a 1930mm mid-section (Shahawy, Beitelman 1999).

Section properties are as below:

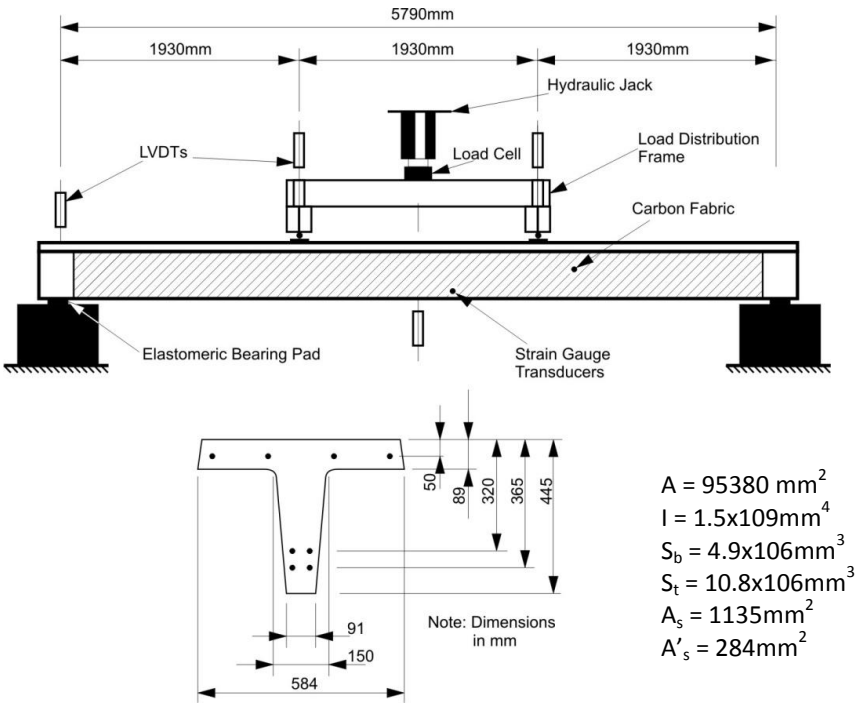

Figure 18: Details of specimen and test set up

The fatigue test program is tabulated as below:

Table 2: Fatigue Test Program

Specimen	Number of Cycles	Description
C-OL5-FA	295,000	Control specimen fatigued to failure
C-OL5-FB	150,000	Cycled for 150 000 (Approx. half fatigue life)
C-2L5-FB	2,000,000	Previously fatigued C-OL5-FB reinforced with two layers of web section
F-2L5-A	1,800,000	Two layers along entire web section
F-2L5-B	1,756,000	Two layers on entire web section
F-3L5-A	3,000,000	Three layers on entire web section
F-3L5-B	3,215,000	Three layers on entire web section

Elastomeric bearing pads were used at the supports. The load was monitored using a combination of load cells on the beam and digital pressure gauges on the hydraulic lines. For the case of fatigue loading, load cells resistant cell resistant to cyclic degradation was used. RC beam deflections were measured at the supports, load points, and midspan using linear voltage displacement transducers. Strains within the RC beam were monitored at load points and midspan using electrical resistance strain gauge transducers.

The fatigue test program included rehabilitating an initially damaged RC beam (C-OL-FB) with two layers of CFRP fabric and again testing it to ultimate failure. The objective of the specific test is to study the effect of strengthening an already fatigued RC structure and measuring the additional fatigue life contributed by the externally bonded CFRP layers. Four other beams were strengthened, namely (F-2L5-A, F-2L5-B, F-3L5-A and F-3L5-B) using two

or three layers of CFRP fabric, these tests were compared to the un-strengthened control specimen (C-OL5-A) with the intension of measuring the additional fatigue life provided from the CFRP layers (Shahawy, Beitelman 1999).

All specimens were initially loaded statically beyond the cracking moment up to the maximum level of fatigue loading before commencing application of the fatigue loading cycles. The control specimen failed at 250,000 cycles, this value was considerably lower than the expected value for the stress ranges of the reinforcing bars were subjected. Beam C-OL-FB, was tested to 150,000 cycles, noticeable cracking had occurred at this stage, the beam was then reinforced with two layers of CFRP fabric and further fatigue loaded. The reinforced beam reached a total of 2,000,000 cycles of loading before the specimen failed following rupture of the CFRP fabric. It can be seen that the beam experienced an increase in stiffness upon the external reinforcing and remained at this constant stiffness until failure. It can obviously be noted that the repaired beam performed exceedingly well under fatigue loading, even though it has been damaged before rehabilitation. (Shahawy, Beitelman 1999)

Beams F-2L5-A and F-2L5-B that were reinforced with two layers of fabric experienced a large shift in the deflection between 1,200,000 and 1,800,000 cycles, reflecting sever degrading of the specimen. Once again the stiffness of each beam remained approximately constant, and the fatigue life of each team was relatively the same at approximately 1,800,000 cycles.

The two RC beams that were reinforced with three layers of CFRP fabric differed in terms of the moment versus deflection graph and deflection profiles, beam F-3L5-b was stiffer than F-3L5-B, however both test specimens survived 3,000,000 cycles of applied loading, compared to the 2,000,000 applied cycles for the specimens with two layers of CFRP fabric.

A summary of the rehabilitated beam exhibited a prolonged fatigue life compared to those that were strengthened from the outset, demonstrating that severely cracked beams in service could be effectively rehabilitated with CFRP (Shahawy, Beitelman 1999).All the test specimens which were either strengthened or rehabilitated using CFRP fabric exhibited stiffness equal or greater than that of the control RC beam (Shahawy, Beitelman 1999).

Shahawy and Beitelman (1999) concluded that the full wrapping of beams with CFRP fabric is an effective method of rehabilitating and strengthening fatigue critical concrete structures.

2.5.3.2 R. Gussenhoven and S.F Brena (2005)

This work focused on the fatigue behaviour of small scale beams strengthened using carbon fibre-reinforced polymer composites. The test specimens were strengthened using different thickness and widths of composite laminates to identify parameters that would generate different failure modes under repeated loads. Varying factors that all have an influence on the long term behaviour of the test specimens include CFRP laminate width and thickness, amplitude of cyclic loading, and pre-existing damage in the beams.

The experimental program included thirteen small-scale beams were cast with identical geometric properties. Two of the test specimens were used as a control, and the remaining eleven beams were strengthened using carbon fibre-reinforced polymer laminates. The strengthening scheme for each test specimens depends on the group, each group varied with respect to their specific CFRP laminate orientation and properties.

The results of the experimental program have been tabulated in Table 3.

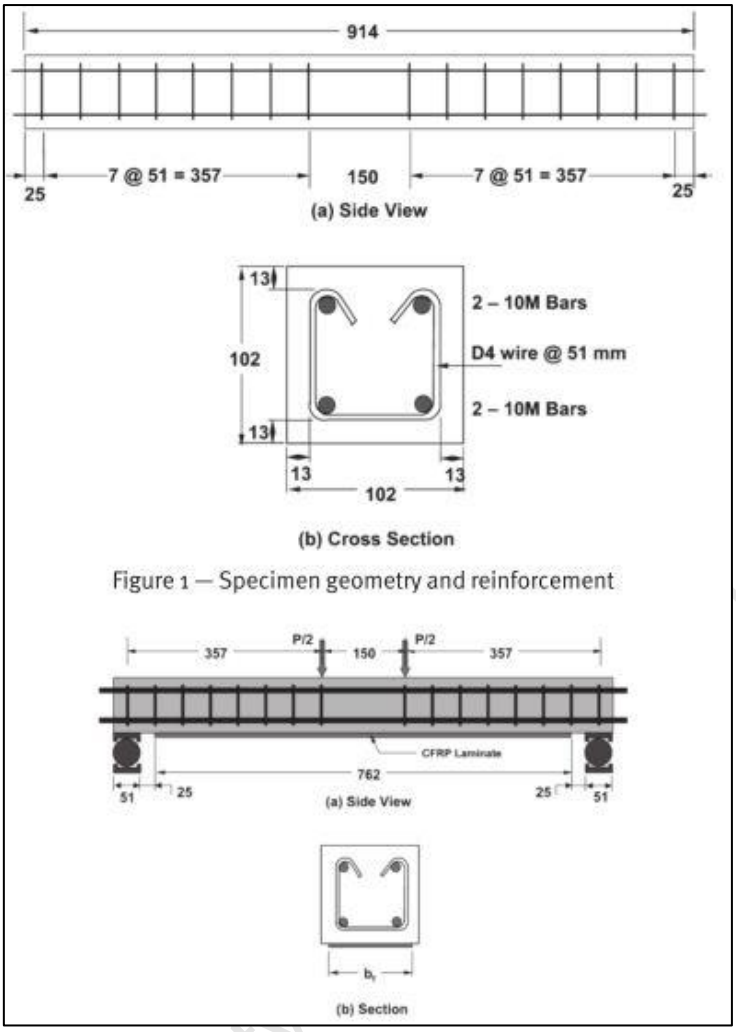

Figure 19: Gussenhoven and Brena (2005) - Test set up and CFRP Strengthening Configuration

The groups were categorised according to each ones cast date.

Group A, consists of five small-scale beams strengthened using a one-ply, 89mm wide laminate. The primary variable for these specimens was the loading amplitude therefore all the specimens have the identical laminate configuration. For the testing of the specimens, load amplitude close to that of the expected fatigue limit of the reinforced steel was used. At this limit, it was possible to investigate the advantages that the CFRP laminate might have in the fatigue life of the beams as a result of increased stiffness, reduction of crack width, and larger crack spacing at service loads (Gussenhoven, Brena 2005). All of these attributes have been commonly reported on by previous researchers.

Of the five test specimens of group A, two beams were used as a control, one unstrengthened specimen and one strengthened specimen. The unstrengthened specimen

was tested using repeated loading that generated peak stresses in the tension steel equal to 80% of the yield stress. The strengthened control beam contained the same geometric properties as the rest of the specimens in the group, and was tested statically to failure to provide a static-load baseline for the repeated loads (Gussenhoven, Brena 2005).

Group B consisted of five beams which were strengthened using CFRP laminates of equal 51mm width but different thickness. The primary focus for this group of test specimens was the influence of the different composite thicknesses on the fatigue behaviour. These test specimens were strengthened using 2-ply CFRP laminates, therefore the applied stress was increased in the beams in order to generate the same peak stress in the reinforcing steel as group A. The laminate surface contact area for the double-ply laminate, group B, test specimens has approximately 14% more area than the 54% of that for the single ply Group A test specimens. The interface stresses in beams with 1-ply laminate in group B would be theoretically equal to those beams in group A. Due to the fact that the 2-ply specimens have a higher thickness and smaller contact surface, the interface stresses would be twice as large as those generated in the beams in group A at equal laminate strains (Gussenhoven, Brena 2005).

Group C consisted of three test specimens, each subjected to 500,000 cycles of repeated loads generating a stress equal to 50% of the yield stress on the tensile reinforcement prior to strengthening. After damaging the beams, all the beams were strengthened using identical CFRP configurations to those used in beams with 1-ply in group B. Once again the loading applied after strengthening was designed to generate the same stress levels as those during group B testing (Gussenhoven, Brena 2005).

Table 3: Load Parameters and Failure Modes

Specimen	Peak Stress, MPa	Stress Range, MPa	No, of Cycles to Failure	Failure Mode
A – Control	368	310	183,674	Fatigue of reinforcement
A-1-4-80	332	295	131,619	Concrete Clear Cover Peel off
A-1-4-70	316	272	287,594	Fatigue of Reinforcement followed by CFRP Debonding
A-1-4-60	265	224	778,734	Fatigue of Reinforcement and Concrete Cover peel off
B-1-2-80	347	300	290,307	Fatigue of Reinforcement

				followed by CFRP Debonding
B-1-2-70	309	268	336,873	Fatigue of Reinforcement followed by CFRP Debonding
B-1-2-60	283	236	4,000,000+	Statically Loaded to Failure after 4 Million Cycles
B-2-2-70	328	270	150,000	Concrete Cover Clear Peel Off
B-2-2-60	256	199	2,000,000+	Statically Loaded to Failure after 2 Million Cycles
C-1-2-80U	220	175	500,000	No Failure
C-1-2-70U	229	182	500,000	No Failure
C-1-2-60U	193	137	500,000	No Failure
C-1-2-70S	320	326	326,775	Fatigue of Reinforcement followed by CFRP Debonding
C-1-2-70S	298	226	440,193	Fatigue of Reinforcement followed by CFRP Debonding
C-1-2-60S	227	189	4,000,000+	Statically Loaded to Failure after 4 Million Cycles

All members were simply supported and subjected to a four-point bending using an 8500 Instron testing machine. Direct loads were measured using a 50kN load cell mounted to the machine piston. All beam deflections were measured using linear potentiometers which were positioned at midspan and at the support centrelines to account for flexibility of the supporting beam. An LVDT integral to the hydraulic actuator was used to measure the deflection at the load points.

Each beam was also instrumented with a series of strain gauges. In order to measure the strain across the entire cross-section of the beam, gauges were positioned at the midspan to measure the tension in the reinforcement, the compression face, and the CFRP laminate for each of the strengthened beams.

The repeated load followed a sinusoidal variation between the minimum and maximum values at a load frequency of approximately 4Hz. The minimum load which is reprehensive a dead load to avoid shifting of the beams equalled 2.7kN, the maximum load in the tension reinforcement was calculated to as a percentage of the nominal yield stress (60, 70 or 80%). A peak stress in the region 60% of the yield stress is intended to represent service-load stress conditions that would typically be experienced in practice. The 80% maximum yield stress represents the upper strengthening limit recommended by the ACI Committee 440 (2002).

On the completion of the testing, visual inspections were conducted throughout the testing and concluded that most of the new cracks that developed on the beams occurred during the early cycles of loading (up to 20,000 cycles); these cracks did not increase substantially. Throughout the testing, no imminent failure was observed, especially in the beams where the reinforcing bars failed due to fatigue failure.

The observed failure modes were a result of the selected peak stress levels in the tension reinforcement and the configuration of the CFRP laminates. Test specimens that reached 2,000,000 cycles without failing were considered to have an infinitive fatigue life and were then loaded statically to failure. These beams did not experience any strength degradation after the cycling.

Test specimens that were cycled at peak stress levels equal to 70% or 80% of the yield stress exhibited one of two failure modes depending on the stress amplitude and the CFRP laminate configuration. Failure modes in these beams were characterised by fatigue fracture of the reinforcement with subsequent debonding of the CFRP laminate or failure of the concrete cover along the bottom reinforcement. During this type of failure mode, after the reinforcing bars fracture the excess force generated in the CFRP laminate causes the bond between the laminate and concrete surface to separate. A point worth noting is that failure due to fatigue fracture did not show any signs of distress prior to fracture of the reinforcement, since the cracks had stabilised and ceased to elongate in length.

Another mode of failure which occurred in a small number of the beams which exhibited failure along the concrete cover were characterised by visible indications of damage as loading progressed. Initial cracks form at the ends of the CFRP laminate during early stages of the repeated loading, and later propagate along the plane just below the tension reinforcing bar level. The end crack propagated sometimes in the form of a diagonal cracks within the beam shear span; this typical crack s causes severe crack widening to occur within this region (Gussenhoven, Brena 2005).

The above mentioned failure modes are for non-composite or damaged test specimens where accelerated corrosion was not induced and therefore no patch repair is present. Currently there is very little literature which focuses on the fatigue behaviour of a patch

repaired-CFRP strengthened beam, and therefore we can only predict that similar failures mode will be observed.

Gussenhoven and Brena (2005) investigated the influence of laminate geometric parameters on fatigue life by plotting the ratio of laminate force to laminate width or laminate thickness as a function of number cycles to failure. Results showed that only one of the two specimens that were strengthened using twice the laminate thickness than the rest failed in fatigue, and therefore the conclusive evidence of any effect of laminate thickness on fatigue life could not be obtained in this research (Gussenhoven, Brena 2005).

Further results proved that laminate thickness did in fact have an influence on the fatigue performance of the test specimens. As figure 20 below indicates, the two test specimens who experienced the highest laminate force during the first loading cycle eventually failed by concrete clear cover peel off. Two distinct trends are easily plotted on the graph and indicate a distinct line per laminate width.

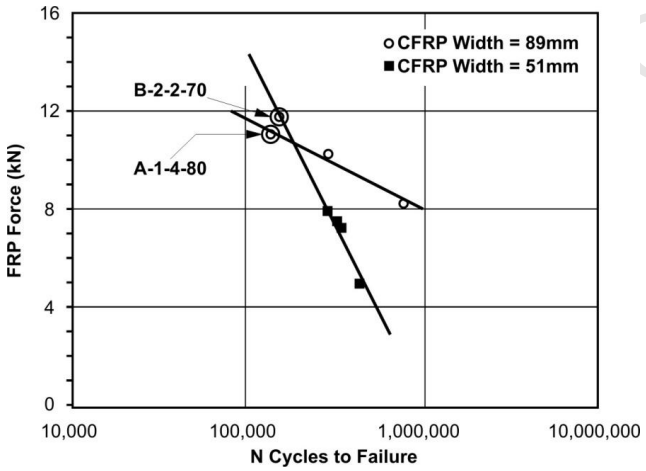

Figure 20: Fatigue life as a function of CFRP laminate force on first cycle

Figure 21 below indicates the ratio of laminate force versus laminate width. It can be seen that, to achieve similar increased in fatigue life between each of the test samples, a higher decrease in laminate force per unit width is required in specimens with 51mm laminates compared to those with 89mm laminates. The graph also shows that for all test specimens strengthened with the 51mm laminate width, there fatigue life increased approximately 3 times for a laminate unite force decrease of 0.13 kN/mm, while specimens strengthened with 89mm laminates increased the fatigue life by six times for a laminate unite force

decrease of only 0.03kN/mm. This behaviour could attribute to wider laminates being able to restrain opening more effectively than narrower laminates, therefore delaying fatigue failure of reinforcing steel (Gussenhoven, Brena 2005).

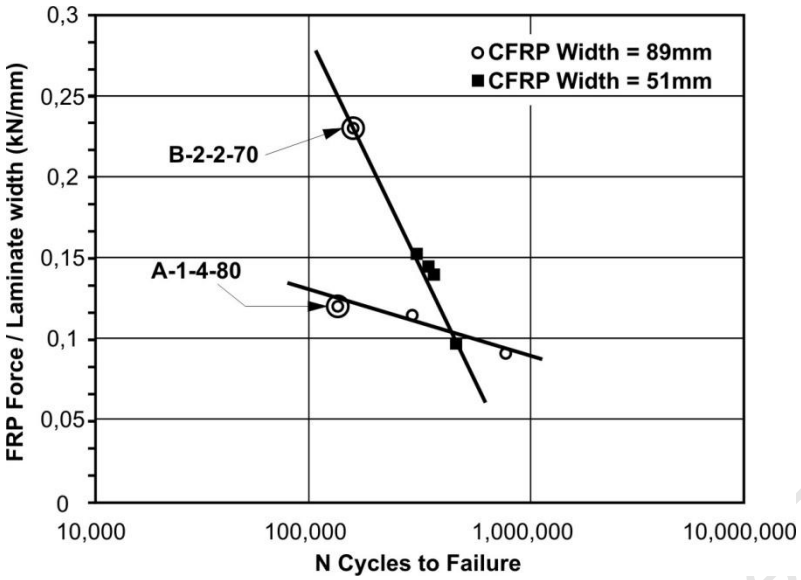

Figure 21: Fatigue life as a function of CFRP laminate force/width in first cycle

Finally Gussenhoven and Brena (2005) conclude that additional tests in larger beams are needed to verify the results obtained, as well as to identify other parameters that might affect fatigue behaviour.

Gussenhoven and Brena's (2005) work agreed with the concluded research by Ferrier and Hamelin (2000) whereby they tested FRP strengthened beams for fatigue, from the tests they showed that FRP strengthening increases the fatigue behaviour and that the fatigue in the steel bars and concrete is the dominant factor governing failure. Therefore the stress range should be limited to that of an un-strengthened beam.

2.5.4 Influence of External CFRP Strengthening of Corrosion Damaged RC Beams

All the above experimental programs mentioned were conducted on non-corroded or damaged RC beams and therefore do not simulate in-service conditions of a repaired damaged structure. All previous work discussed in this chapter has either focused on the long term performance of accelerated corrosion on a RC structure or the fatigue analysis of existing CFRP strengthened RC structures. The next logical step is to analyse literature that focuses on corrosion-damaged reinforced concrete structures that have been strengthened

using CFRP laminates. Much research has been developed in this specific area and below is a summary of concluded works.

Simple research carried out by Lee (1999), Craig (2002), Sherwood (2000) and Masoud (2002) confirmed that bonding fibre reinforced polymer laminates to the external surface of RC members in one of the new methods being considered to minimize the corrosion crack width and rate of corrosion activity (Badawi 2005), although limited amount of studies have been carried out to investigate the effect of concrete confinement by FRP laminates to control corrosion induced crack widths and corrosion propagation (Badawi 2005).

Masoud (2005) later identifies that research on the effect of FRP strengthening on the fatigue performance of uncorroded reinforced concrete beams has been addressed by many researches (Heffernan and Erki (2004); Barnes and Mays (1999)), but limited information is available on the fatigue performance of FRP-strengthened or repaired corroded beams (Masoud 2005).

A previous research study by Masoud (2001) investigated the fatigue performance of corroded, CFRP strengthened small scale beams. The FRP strengthened beams resulted in increased fatigue lives up to six times that of the un-strengthened corroded beams. A draw back to that study was the fact that the beams were only subjected to one level of corrosion and the specimens were tested to failure directly after the FRP strengthening; their post repair was not addressed (Masoud 2005).

Soudki and Sherwood (2000) studied the effect of bonded CFRP laminates confined the corrosion expansion. It was concluded that CFRP laminates confined the expansion of steel reinforcement due to corrosion by up to 15% mass loss (Badawi 2005).

El Maaddawy (2005) identifies that further practical experiments need to be conducted; the tests should involve the repair of already corrosion-damaged RC beams. Also, in previous studies, accelerated corrosion was not accompanied by external load in corrosion tests of RC beams. The presence of a sustained load during corrosion exposure would aggravate both the concrete damage and the bond deterioration by corrosion under a sustained load (El Maaddawy, Soudki 2005).

Soudki (2007) did further research of Masoud's (2001) findings and concluded that the effect of using CFRP laminates to repair corroded RC beams under fatigue loads was investigated and it was found that strengthening with CFRP was capable of increasing the strength and the flexural stiffness to a level higher than that of the control beam (M. Badawi, K. Soudki 2010).

Masoud (2010) summarises for flexural members, it has been reported that applying FRP laminates reduces the stress carried by the tension reinforcement and increases the flexural strength of corrosion-damaged beams. For example, an increase of 16% in the flexural capacity was achieved in a CFRP strengthened beam with 10% mass loss in the total area of the reinforcing bars and bonding the CFRP laminate increased the load carrying capacity by 10-35% with respect to the control beam (M. Badawi, K. Soudki 2010).

Recent studies complied by Parish et al (2011), mention that there is considerable information in the literature about CFRP materials and their immediate repair benefits when bonded to concrete, relatively little is known about the long-term durability of this material or repair technique (Parish 2011).

The research carried out by Parish concluded the following (Parish 2011):

- ACI guidelines are probably conservative for newly repaired girders but may not be conservative for girders that continue to deteriorate over time.
- Complete concrete cover replacement with polymer-modified concrete prior to FRP strengthening provides a repair that is much more durable than epoxy filling alone.
- Cyclic loading appears to weaken the FRP-Concrete interface and to induce an interfacial failure mode in static failure
- The most effective combination of reinforced concrete bridge repair techniques studied in this research was; the removal of all deteriorated concrete from the cover level, thorough cleaning of steel reinforcement, application of an epoxy containing corrosion inhibitor, complete cover replacement using polymer-modified concrete with corrosion inhibitors, flexural strengthening with CFRP sheets, and use of at least two CFRP U-Wrap anchor sheets.

According to the literature, no significant research has been published which used a patch repair technique to repair the damaged corroded beam and concrete prior to FRP strengthening and long term performance testing. The test methodology will follow this procedure.

2.6 State of Practice of FRP Application

Early research and development led to many innovations in structural and civil engineering advanced polymer composite (APC) systems. This interest dates back more than 30 years and is instrumental in the current research projects investigated currently. In civil engineering APC is generally referred to as the fibre-reinforced-polymer (FRP) composite (Hollaway 2010). The present and future development of structural systems that have been developed as a result of the unique physical and in-service properties of FRP composite materials has been illustrated in figure 22.

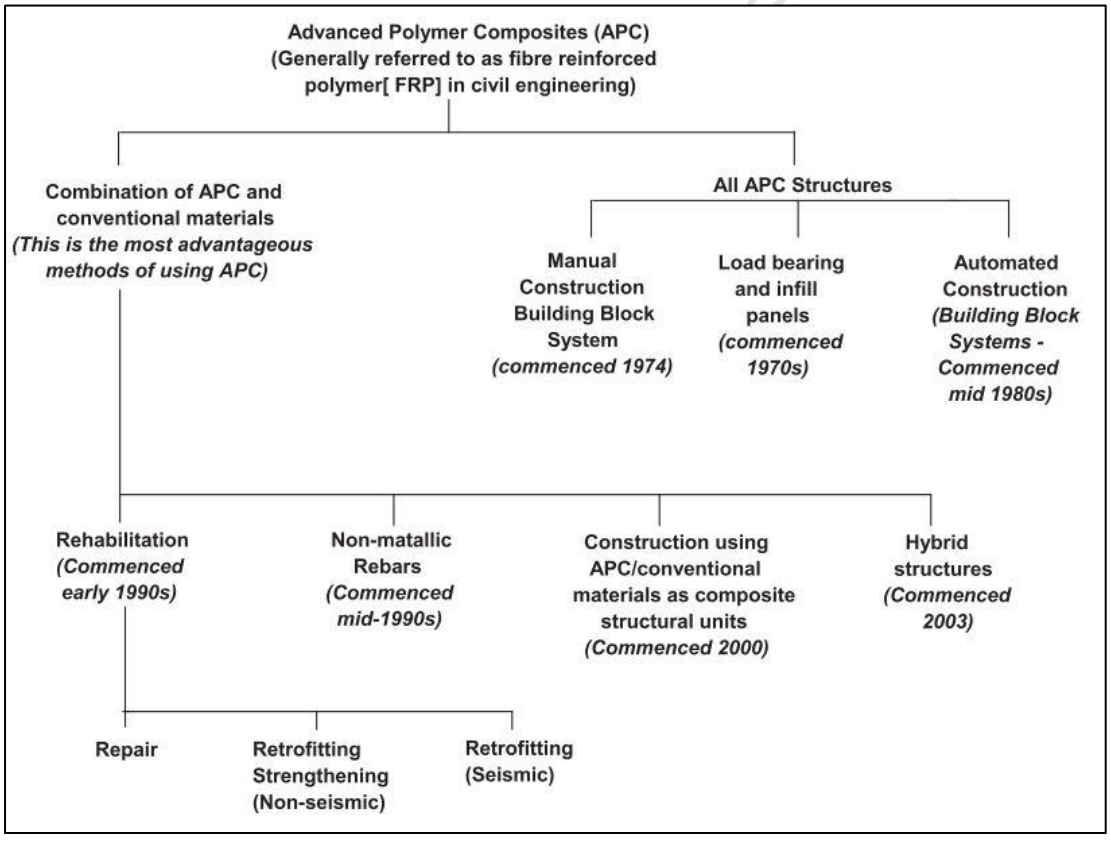

Figure 22: The development of the fibre matrix composite from early 1970 into the 21st century (Hollaway 2010).

During the 1950's and 1960's very little was known about FRP materials but there remained a great need for the material and therefore many manufacturers did one of two operatives,

either manufacturing the material without fully understanding the fundamentals of fabrication or the importance of correct procedure for curing the material.

It was only in the 1970's when consulting architects and civil engineers considered FRP composites as a building material and start to design composite building structures. The origin of FRP in construction began with simple FRP fabrication of semi-load bearing and infill panels for houses and larger constructions. In the mid 1980's engineers began to use FRP composites as a structural material and this was driven by the need for durable, high-strength and high stiffness materials that could replace more conventional materials that were being used in aggressive and hostile environments at the time. The new desires for FRP lead to newer methods of automated manufacturing of structural components for 'all composite' structures; the primary method of manufacturing was pultrusion. The pultrusion technique included using isophthalic polyester resin and uni-directional, bi-directional and chopped up strand mat glass fibre reinforced for the main structural members. From the mid to late 1980's the use of FRP composite materials continued to be widely used on a variety of civil and architectural applications (Hollaway 2010).

2.6.1 The Use of Advanced Composites in Civil Infrastructure

2.6.1.1 The rehabilitation of RC beams by the technique of external plate bonding (EPB)

The deterioration of some civil engineering structural elements and the need to upgrade others to service requirements and capacities beyond those for which the original structure was initially designed for, has placed demands on owners and highway authorities to effect rapid renewal (Hollaway 2010). Proper maintenance and management of these degraded structures has become increasingly important to ensure the longevity and full utilization of the structure. The use of FRP's to repair existing damaged structures is not a new technique at all; there are many forms of FRP application which can be implicated to ensure that a damaged building can fully restore its serviceability life span.

Hollaway describes a structurally deficient building as one whose components may have deteriorated or have been damaged, resulting in restrictions on its use. A functionally obsolete bridge refers to the geometrical characteristics of the bridge in terms of the load carrying capacity of it.

Civil engineering structures that are deficient can be split into two groups;

- Changes in the use of a structure, so that it needs to carry different loads from those originally specified
- Degradation of a structure, so that it cannot carry the loads for which it was originally intended

Both groups of deficient structures can be addressed with the use of externally bonding CFRP. The externally bonded CFRP laminates will provide the additional strength required in shear or flexure depending on the orientation and application method used.

There are many common forms of structural deficiencies for which FRP is used as a repair or retrofit technique. Below is a brief summary for common FRP strengthening techniques used in modern civil engineering practice.

2.6.1.2 Unstressed FRP soffit plate for flexural strengthening of concrete structures

External strengthening of concrete structures is now routinely considered a viable alternative to rather costly replacement of these structures. The first upgrading applications of this nature used wet lay-up sheets or pre-cured pultruded plates bonded to the tension face of the beam with the fibre direction aligned to the beam axis. The high-strength-to-weight ratio and good corrosion resistance of FRP materials provides considerable advantages over that steel for rehabilitation (Hollaway 2010). The effectiveness of flexural strengthening has been well published by many researchers and there is a large database of experimental results to reinforce this argument.

Currently, governments and engineering associations worldwide are cooperating to standardise workable international design parameters and guidelines. The most commonly used standards for external FRP strengthening is the American Concrete Institute; ACI 440-2R-08, this guide is for the design and construction of externally bonded FRP systems, ACI 440.5-08, is a guideline towards specification for construction with fibre-reinforced polymer (FRP) reinforcing bars, and ACI 440.6-08 specifies for carbon and glass fibre-reinforced polymer (FRP) bar materials for concrete reinforcement.

2.6.1.3 Failure areas of an upgraded RC beam

There are nine different failure areas of a RC beam that has been externally strengthened with an unstressed FRP plate. Hollaway describes each mode of failure below:

- For an un-strengthened and over-reinforced RC beam, the flexural failure occurs as a concrete compression failure at the top flange (mode 1).
- For an un-strengthened and under-reinforced RC beam, the initial failure occurs at yield of the steel tensile reinforcement (mode 2), with an increasing deflection but without any additional load carrying capacity, the beam fails in concrete compression in the top flange, (mode 1), due to excessive deflection.
- For an un-strengthened and under-reinforced beam and if the beam remains under-reinforced when strengthened with an FRP plate, the failure mode could be a tensile rupture of the laminate, (mode 3).
- For a beam over-reinforced after plate bonding, flexural failure occurs as a concrete compression failure in the top flange (mode1). Yielding of the steel reinforcement is likely to occur before either the concrete or the CFRP plate fails and whilst this may contribute to the ultimate failure of the beam it is not the prime cause of failure. At the termination of the plate (plate free end)there are high normal stresses to the plate, these will cause the plate to peel off towards the centre of the beam; this is known as end anchorage peel, (mode 6 – anchorage peel/shear in cover zone)and (mode 7 – peel failure)
- For upgraded beams there is also a peel failure mode at a shear crack, (modes 4 – shear failure), (mode 5 – peel due to vertical movement at the shear crack) and (mode 8 – adhesive failure at concrete/adhesive interface), where there is a possible complex mechanism of de-bonding due to strain redistribution in the plate at the crack and/or the formation of a step in the soffit of the beam thus causing shear peel. The delamination can then propagate towards the end of the plate. Whether modes 5 or 8occur depends upon the structure of the shear reinforcement in the un-strengthened beam.

Another mode of failure which has been reported in previous literature but is not very common is the delamination of the composite plate or of the area within the glue line, this mode of failure is very uncommon since the strength of the composite if much greater than

that of the concrete and therefore failures will only occur of the installation has been poorly performed or there is a defect in the FRP plate.

There are several design guidelines which are discussed in section 2.9.4 to calculate for retrofitting of FRP composites to reinforced concrete structures.

2.6.1.4 Composite patch technology

Adhesively bonded FRP composite patch techniques have been successfully applied to military aircraft repair. The technique is applied to extend the service life of aluminium aerospace components and the method is now of interest to the civil engineering industry to repair cracked metallic materials (Hollaway 2010).

The fatigue of steel sections and the ultimate fracture under cyclic loading is a problem common to many industries but particularly to aging metallic bridges. Recent research has shown that CFRP patches provide an efficient and a relatively easy repair technique. Research has been conducted and has proven that externally bonding CFRP laminates onto existing damages RC structures effectively increased the service life of the structure. Currently, the numerical software programme BEASY was adopted to calculate stress intensity factors, crack propagation and fatigue lives of steel plates and the adhesive layer was simulated as interface elements to connect the patch and steel plate. It was also found that, prestressing the CFRP composite patch induced compressive stresses that acted into the opposite direction to the principle stresses therefore creating a crack closure effect.

2.7 Codes of Practice

In recent years a number of design codes and specifications have been published by technical organisations which provide guidance for design with FRP materials for civil engineering. The key publications listed by Hollaway include:

2.7.1 British and European Codes

- Structural Design of Polymer Composites Eurocomp Design, Code and handbook. Edited by John L Clarke., (1996).
- fib Task Group 9.3, FRP Reinforcement for Concrete Structures, Federation Internationale du Beton (1999).

- fib Bulletin 14, Design and use of externally-bonded FRP Reinforcement for RC Structures, Federation Internationale du Beton.
- 'Strengthening Concrete Structures using Fibre Composite Materials: Acceptance, Inspection and Monitoring' TR57, Concrete Society, Camberley, UK [46].
- 'Design Guidance for Strengthening Concrete Structures Using Fibre Composite Materials', TR55, 2nd ed., Concrete Society, Camberley, UK.
- 'Strengthening Metallic Structures Using Externally Bonded Fibre-Reinforced' Cadei, J.M., Stratford, T.K., Hollaway, L.C., and Duckett, W.G. CIRIA Report, C595, (2004).
- Eurocrete Modifications to NS3473 – When Using FRP Reinforcement, Report No. STF 22 A 98741, Norway (1998).

2.7.2 USA

2.7.2.1 FRP reinforcing rebars and tendons

- ACI (2004) 'Prestressing Concrete structures with FRP Tendons, ACI 440.4R-04, American Concrete Institute, Farmington Hills, MI.
- ACI (2006) 'Guide for the Design and Construction of Structural Concrete Reinforced with FRP Bars' 440.1R-06, American Concrete Institute, Farmington Hills, MI.
- ACI [3],'Report on Fibre Plastic Reinforcement for Concrete Structures' 440.R-96 (Re-approved 2002).
- ACI (2004), 'Guide Test Methods for Fibre-Reinforced Polymers (FRP) for reinforcing or Strengthening Concrete Structures' 440.3R-04, American Concrete Institute, Farmington Hills, M

2.7.2.2 FRP strengthening systems

- ACI [3] ,'Guide for the Design and Construction of externally bonded FRP Systems for Strengthening Concrete Structures', 440.2R-02 American Concrete Institute, Farmington Hills, MI.

2.7.3 Canada

- AC 125 (1997), Acceptance Criteria for Concrete and Reinforced and Un-reinforced Masonry Strengthening Using Fibre-Reinforced Polymer Composite Systems ICC Evaluation Service, Whittier, CA.

- AC 187 (2001)Acceptance Criteria for Inspection and Verification of Concrete and Reinforced and Un-reinforced Masonry Strengthening Using Fibre-Reinforced Polymer Composite Systems ICC Evaluation Service, Whittier, CA. Canada
- CSA (2000), 'Canadian Highway Bridge Design Code', CSA-0600, Canadian Standards Association, Toronto, Ontario, Canada.
- CSA (2002), 'Design and Construction of Building Components with Fibre-Reinforced Polymers', Canadian Standards Association, Toronto, Ontario, Canada, CSA S806-02 (2002).
- ISIS Canada, Design Manual No. 3,'Reinforcing Concrete Structures with Fibre-Reinforced Polymers', Canadian Network of Centres of Excellence on Intelligent Sensing for Innovative Structures, ISIS Canada Corporation, Winnipeg, Manitoba, Canada (Spring 2001).

2.7.4 Japan

- Japan Society of Civil Engineers (JSCE), 'Recommendation for Design and Construction of Concrete Structures Using Continuous Fibre-Reinforced Materials', Concrete Engineering Series 23, ed. by A. Machida, Research Committee on Continuous Fibre-Reinforcing Materials, Tokyo, Japan, (1997).
- BRI (1995),Guidelines for Structural Design of FRP Reinforced Concrete Building Structures, Building Research Institute, Tsukuba, Japan
- JSCE (1997), Recommendation for Design and Construction of Concrete Structures using Continuous Fibre-Reinforcing Materials. Concrete Engineering Series 23, Japan Society of Civil Engineers, Tokyo.
- JSCE (2001), Recommendations for Upgrading of Concrete Structures with Use of Continuous Fibre Sheets. Concrete Engineering Series 41, Japan Society of Civil Engineers, Tokyo.

2.8 Summary

Chapter 2 identifies the different components of a composite CFRP patch repaired and externally strengthened system.

Each component is critically identified and studied; with special attention focused on the fatigue performance and failure mechanisms during sustained loading and ultimate failure.

The chapter identifies the need for further research of corrosion-damaged RC structures which have been repaired using a patch repair mortar and later strengthened using CFRP laminate and wrap. The emphasis of the future research is to focus on the critical fatigue performance analysis and failure mechanisms under cyclic loads.

3 *Chapter 3:* EXPERIMENTAL INVESTIGATION

3.1 Introduction

The experimental test program included six large scale reinforced concrete beam specimens of dimensions 150 x 250 x 3200 mm. All RC beam specimens were subjected to an identical estimated 10% degree of accelerated corrosion, using a 5%NaCl solution, after which, all the damaged concrete was removed, the internal steel was treated and the RC beams were repaired using a self-leveling patch repair mortar across the entire damaged section. CFRP laminates were externally bonded onto the tensile face to restore the reduced tensile capacity due to the reduction of the internal steel corrosion.

All six of the beams were subjected to a four point load while the accelerated corrosion phase and patch repair was implemented. At the time of testing all the RC beams had similar degree of corrosion, patch repair and CFRP strengthening application scheme. The six test specimens were split, two of which were statically tested and four were cyclic tested. The static tests were implemented to determine the relative static loads at failure for each of the 40MPa and 50MPa RC beams; this failure load was later used to calculate the degree of cyclic loading to apply. The four cyclic loaded RC beams that were subjected to fatigue loading were tested under varying degrees of three point bending cyclic loads, and the different degrees of loading was a percentage of the ultimate static loads at failure under three point loading. Stress ranges ranged from low (45% of ULS), medium (55% of ULS) and high (67% of ULS).

3.1.1 Specimen Details

A schematic of the test specimen is shown in Figure 23. All specimens had identical dimensions of 3200mm length, height of 250mm, and a width of 150mm. Each specimen had identical internal reinforcement, for the tension reinforcement, the beams were reinforced with two Y16 bars and for compression reinforcement, two Y8 bars were used. To avoid a shear failure, 8mm diameter plain stirrups having a 25mm cover depth were used 80mm spacing in the shear span and 333.3mm spacing in across the constant moment region. The middle stirrups exposed to the accelerated corrosion pond were not coated with anticorrosion epoxy resin, and therefore localized corrosion took place at the regions of the mid-span stirrups. Table 4: Mix Quantities/1m3 for beams S40 and F401

Aggregate type	**Quantities per cube of concrete**
Binder	355kg
Water	195l

Stone	1000 kg
Sand	705kg

Table 5: Reinforcement Requirements per RC beam

Reinforcement	Size (mm)	Spacing (mm)	Shape Code	Length (mm)	
Tension steel	2 x Y16	25	20	3150	
Compression steel	2 x Y8	25	20	3150	
Shear steel	28 X R8	Varies	60	A	B
				200	100

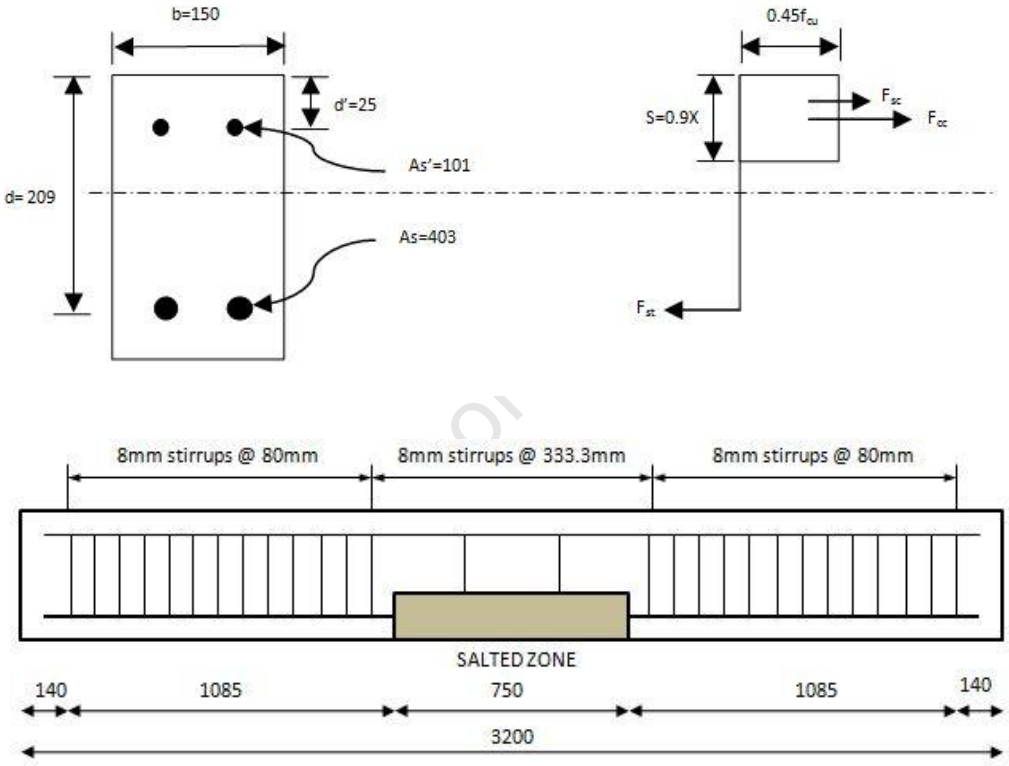

Figure 23: Test specimen reinforcement arrangement

3.1.2 Material Properties

All test specimens were cast using ordinary Portland cement (OPC), with mix proportions by weight as follows: cement/sand/gravel/w:c - 1 : 1.98 : 2.8 : 0.55. A maximum aggregate size of 19mm was used. The mould for casting is illustrated below in figure 24. The average compressive strength of the concrete cubes for Group 1 after 28 days was 40 MPa, while Groups 2 used Ready-mix concrete from Afrimat Readymix; the average compressive strength after 28 days of the ready mix concrete was 49 MPa.

The concrete, for Group 1, was mixed in a 100*l* concrete mixer and cast horizontally in the moulds, and then compacted with a poker vibrator and leveled with a trowel, while group 2 used delivered ready mix concrete. After casting, the concrete was covered in plastic sheets for 2 days, then demoulded and cured by covering the specimens with large damp hessian cloth for 28 days.

The tensile and compression reinforcement was supplied by Winelands Reinforcing and had documented yield strengths of 450 MPa and an ultimate strength of 585 MPa. The 8mm plain bars used for the compression reinforcement and stirrups had a yield strength of 340 MPa and ultimate strength of 300 MPa.

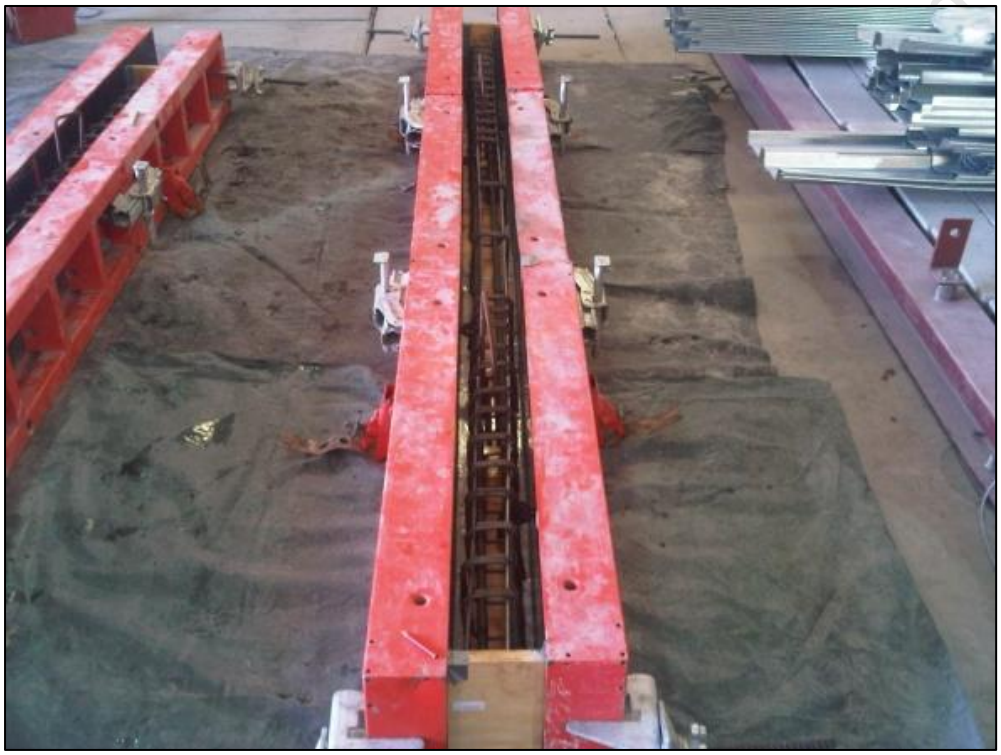

Figure 24: Moulds with internal reinforcement

Table 6: Summary of Concrete compressive strengths per batch

Concrete Batch	Beams	Average Compressive Strength (MPa)
1	S-40, F-401	40
2	S-50, F-501, F-502, F-503	49

3.1.3 Test Specimen Notation

The codes below are used to annotate each test specimen for the experimental investigation;

Sample Number	Code	Description
1	S-40	Statically loaded until failure, 40MPa concrete
2	S-50	Statically loaded until failure, 50MPa concrete
3	F-401	Fatigue loaded until failure, 40 MPa concrete, Sample 1
4	F-501	Fatigue loaded until failure, 50 MPa concrete, Sample 1
5	F-502	Fatigue loaded until failure, 50 MPa concrete, Sample 2
6	F-503	Fatigue loaded until failure, 50 MPa concrete, Sample 3

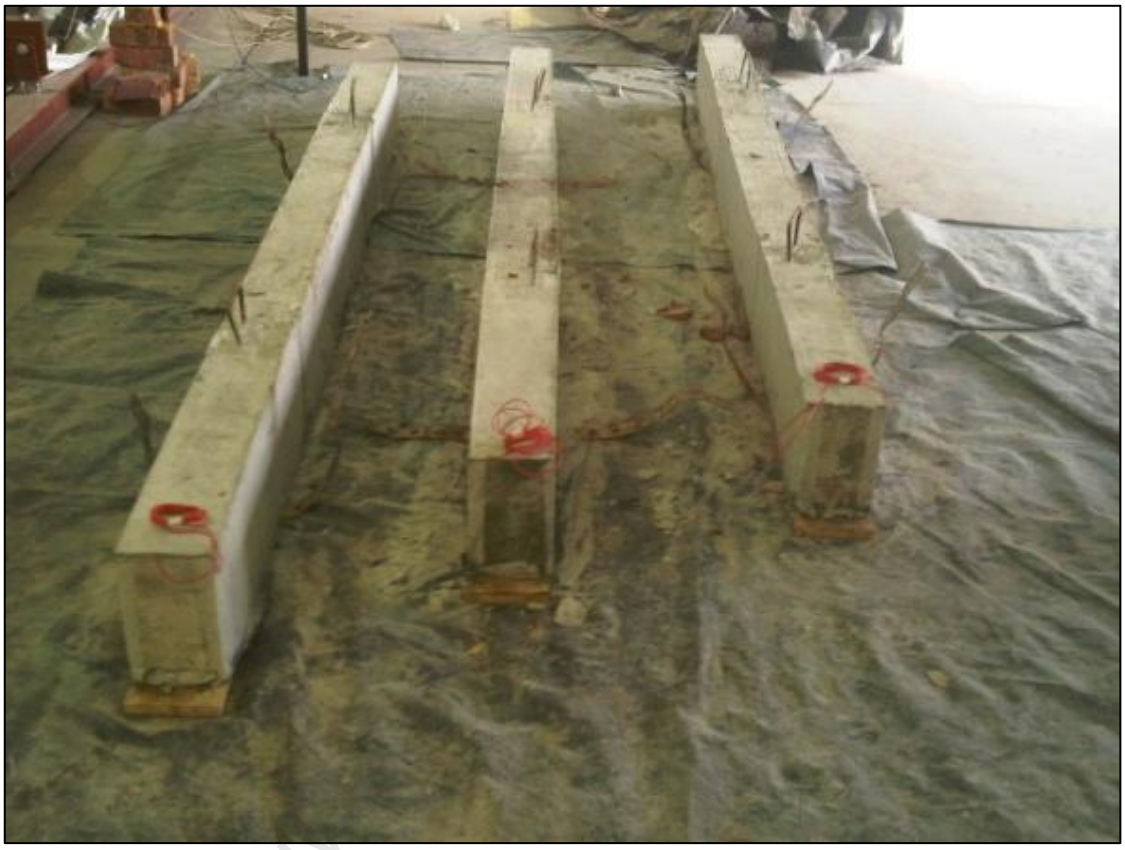

Figure 25: Cast Test specimens

The following Sika products were used for the corrosion treatment, patch repair and CFRP strengthening stages:

Corrosion Treatment

- *Sikatop Armatec 110 EpoCem* is a three component cement modified epoxy resin based anti-corrosive product containing corrosion inhibitors. It has been specifically formulated as a reinforcement coating and bonding primer for concrete repair mortars.

Patch Repair Products

- *SikaCrete 214* is a one component, free flowing, high strength, cement based concrete with a maximum aggregate size of 10 mm. The patch repair mortar boasts high early age compressive strengths after 7 and 14 days and eventually reaches approximately 75 MPa after 28 days of curing.

CFRP Strengthening Products

- *SikaCarbodur S512/80* Plates was used for the external strengthening of all test specimens, data sheets from the manufacturers specifies a typical ultimate strain of 1.7%, modulus of elasticity equals 165 GPa, thickness of 1.2mm and a width of 50mm for cured CFRP laminate.
- *SikaWrap 230C/45* was used to anchor the test specimens at the supports; according to the data sheets from the manufacturers the dry strain properties of the fibers offer ultimate strain of 1.8% and a modulus of elasticity of 238GPa.
- *Sikadur30* was used to bond the CFRP laminates to all six of the RC beams.
- *Sikadur31 CF Normal* was used to bond the CFRP wrap at the support ends for anchorage.

Table 7 summarises the compressive strengths of the two different concrete batches that were used to cast all 6 test samples. Batch 1 was delivered as a Readymix; therefore only one set of samples were taken. Batch 2 consisted of two separate mixes of the same concrete properties and therefore 2 samples for Batch 2 (A and B) were collected.

Table 7: Compressive Cube Strengths

Day	Mass 1 (kg) 100x100mm cube	Comp. Strength Batch 1 (MPa)	Mass 2 (kg) 100x100mm cube	Comp. Strength Batch 2A (MPa)	Mass 3 (kg) 100x100mm cube	Comp. Strength Batch 2B (MPa)
7	2.475	44.0	2.400	29.8	2.290	26.9
14	2.410	48.4	2.350	36.8	2.280	31.8
21	2.435	51.6	2.320	37.8	2.315	35.7
28	2.450	53.5	2.310	42.2	2.310	36.8

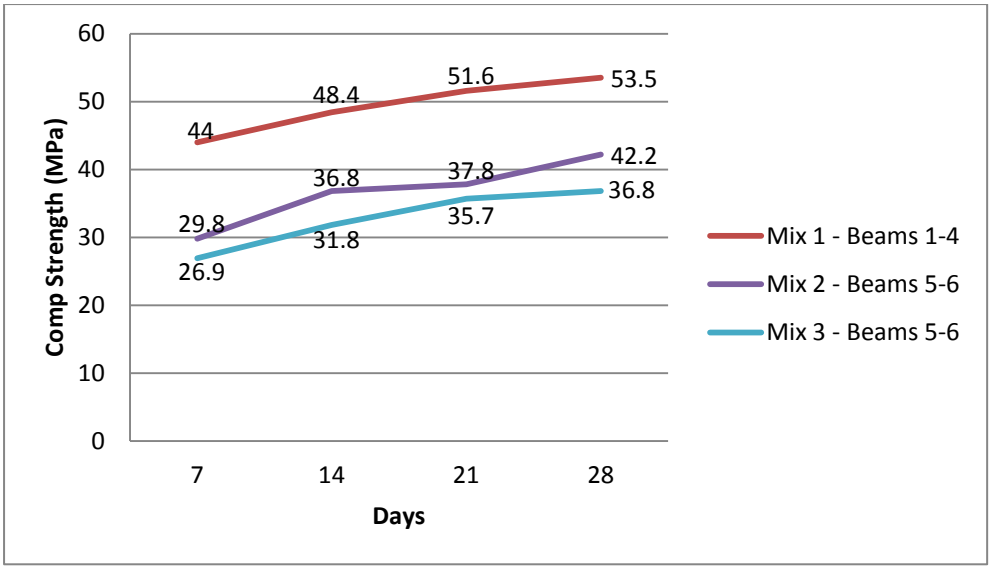

Figure 26: Concrete Compressive Strengths

3.1.4 Accelerated Corrosion

Accelerated corrosion is a very common technique to simulate the effects of long term corrosion on RC structures which are exposed to harsh environmental conditions; the accelerated corrosion technique can be varied for each system to allow for a shorter duration of testing in order to achieve the desired degree of corrosion for a specific RC structure.

The preparation for accelerated corrosion shown in Figure 27 involved cutting a grove into the tensile reinforcement and bending the wires in place, the wire was then insulated with a layer of cling wrap, then electrical tape and finally duct tape to ensure that no moisture would access the point of contact. A hole was drilled in the stainless steel rod which was submerged in the 5% NaCl solution, the cathod wire was connected at this point and then to the power supply.

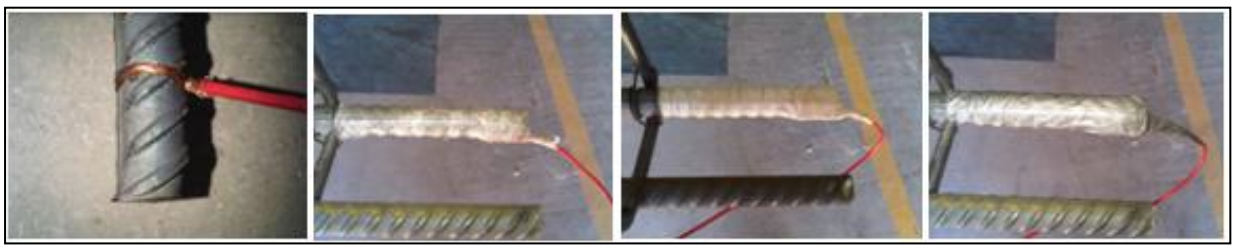

Figure 27: Accelerated corrosion preparation

The steel reinforcement acted as the anode and the stainless steel bar as the cathode. In order to induce the accelerated corrosion, PVC ponds of dimensions 140 x 30 x 750 mm were placed along the mispan of all six of the test specimens. A 12mm stainless steel rod was placed along the bottom surface of the PVC pond, which was later filled with a 5% NaCl solution. In order to initiate the accelerated corroison, a potential difference was applied across the tensile reinforcement steel bar and the stainless steel bar using electric copper wires. The tensile bars were connected to the positive terminal of the power supply to act as the anode whilst the stainless steel bar was connected to the negative terminal of the power supply to act as the cathode.

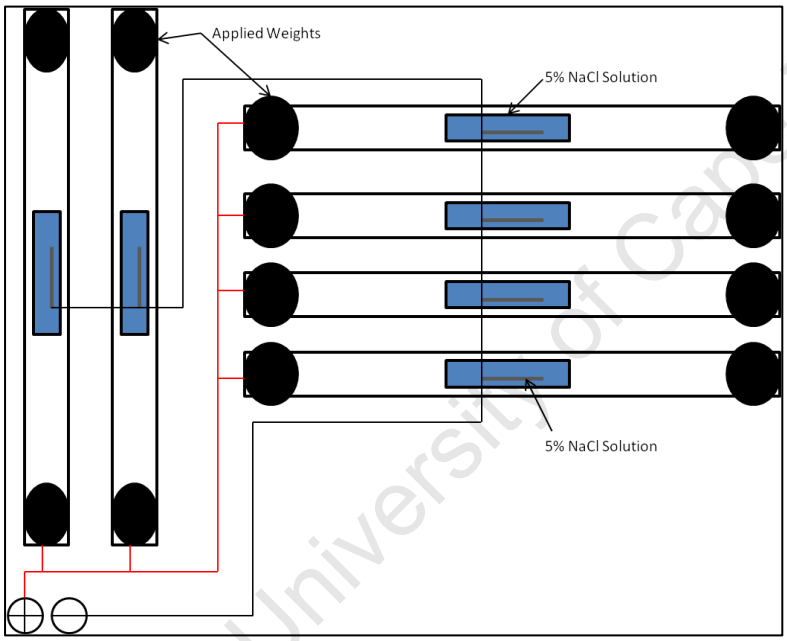

Figure 28: Accelerated Corrosion series layout

Figure 29: Accelerated corrosion under sustained load

To monitor the rate and degree of corrosion more effectively, all corroded beam specimens were supplied with the same current of 480 mA/cm^2 which was divided equally between the two bars in a series arrangement (See Figure 28). The duration of accelerated corrosion depended on the desired degreee of corrosion for each specimen and was calculated using Farady's Law.

Figure 30: Constant current of 480 mA/cm^2 supplied.

3.1.4.1 Faraday's law

Calculating the amount of current required to achieve an estimated amount of steel lost during the accelerated corrosion process:

Mass of steel consumed (g); Atomic weight of steel (56g); Current (A); time (s); Ionic charge (2); Faradays constant (96 500 A/s).

From the specimen, there are 2 x 16mm bars in the tension zone to be corroded; the length of the corrosion is 750mm. The mass of the steel bars to be corroded is calculated as follows:

Density of steel,

Mass of two steel bars of length 750mm:

Based on the required mass loss of 10%, the current required to achieve the corrosion level can be calculated using Faraday's law.

Table 8: Accelerated Corrosion Program

Group	Beam No.	Mass Loss (%)	Mass loss (g)	Current (mA)	Duration (Days)
1	1	10	237	480	20
	2	10	237	480	20
2	3	10	237	480	20
	4	10	237	480	20
3	5	10	237	480	20
	6	10	237	480	20

Note: The mass loss is dependent of Faraday's Law; it can be observed that after the accelerated corrosion stage, the total mass loss of the internal steel was significantly less. This can be attributed to the localized pitting which occurred.

Example for all six test beams:

Figure 31: Internal corrosion of the RC beams

3.2 Repair Process

3.2.1 Repair preparation

The corrosion damaged RC beams were prepared by removing all the damaged concrete that had been affected. The damaged concrete was removed by cutting out the affected area using a grinder and jack hammer, the affected area removed totaled to a depth of approximately 25mm below the internal tensile steel reinforcement. The damaged reinforcement was then cleaned with a wire brush thus removing all excess corrosion products, then any loose existing concrete particles were removed by sand blasting the cut away surface, finally the concrete and steel surfaces were cleaned of all contaminates. The exposed beam was then wetted overnight to ensure full saturation for preparation of the patch repair application.

Figure 32: Damaged Concrete removed and internal steel treated

3.2.2 Patch Repair

The repair technique of patch repairing was implemented for all six test specimens. After the damaged concrete was removed and the surface and internal reinforcement was adequately coated with *Sikatop Armatec 110 EpoCem* adhesive bonding agent, *SikaCrete 214* repair mortar was mixed with 3*l* of water and poured in the formwork, no vibrating was necessary. Once the repair mortar was at the same level as the existing concrete the beams were covered with a polythene sheet overnight and demoulded after 24 hours. The repaired section was covered with wet hessian to ensure that the section cures properly for the remaining 3 days. *SikaCrete 214* is a rapid hardening repair mortar which boasts compressive strengths of 55MPa after just 24 hours.

Figure 33: Internal steel pitting and treatment technique

Figure 34: Treatment of surface and internal reinforcement with the Sikatop *Armatec 110 EpoCem*

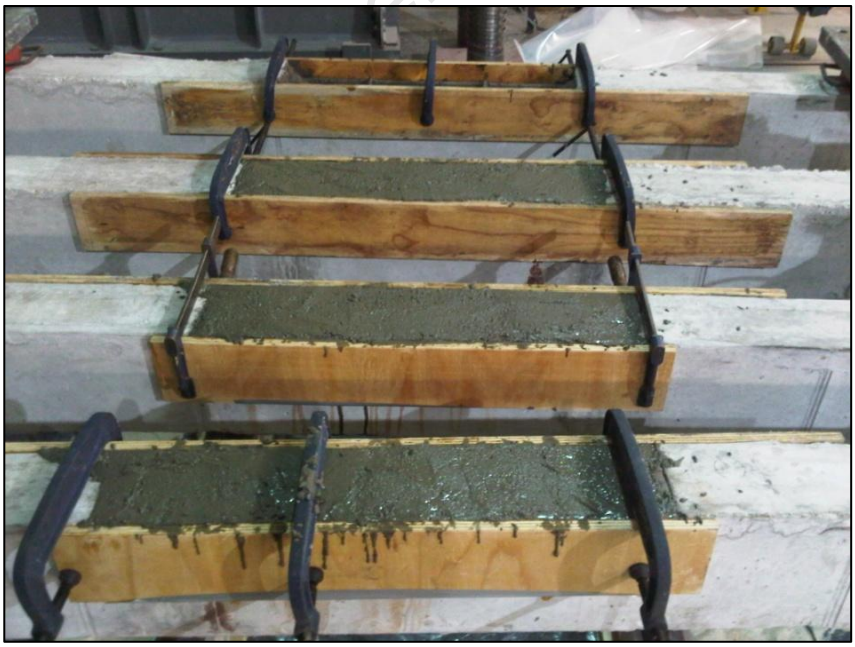

Figure 35: Patch repair casting and moulds under sustained loading

Figure 36: Cured Patch repair under sustained loading

Table 9: SikaCrete 214 Patch Repair mortar compressive strength

Mix Batch 1	Compressive Strength (MPa)	Flexural Strength (MPa)*	Tensile Strength (MPa)*
Day 7	60.8	7.5	5.5
Day 14	88.2		
Mix Batch 2	Compressive Strength (MPa)	Flexural Strength (MPa)*	Tensile Strength (MPa)*
Day 7	69.8	7.5	5.5
Day 14	94.9		

* As supplied by the Sika manufacturers hand book at 28 days of curing.

3.2.3 CFRP Strengthening

In order to restore the tensile strength lost due to internal steel corrosion, CFRP laminates are bonded onto the external surface of the tensile faces to provide the additional tensile strength required to restore the RC beams to its initial design strength.

The eventual success of the CFRP strengthening relies on the process of application. For the six RC beams, the following process was followed for each to ensure that the CFRP laminates were fully utilized.

Only once the patch repair had cured for 3 days were the CFRP laminates applied to all six test specimens. The following method of application was followed:

- Hand wire brush the concrete surface and patch repair where the CFRP is to be bonded.
- Remove any excess dust from the concrete surface with a damp cloth.

- Clean the CFRP *SikaCarbodur* laminate surface which will be bonded to the concrete with *SikaColma* Cleaner and leave for 10 minutes before application.
- Using Sikadur-30, Mix part A and part B (3:1) of Sikadur30 and stir until a uniform light grey colour is visible.
- Apply the epoxy onto the CFRP laminate cleaned surface.
- Epoxy thickness should be approximately 3mm prior to bonding.
- Bond the laminate onto the concrete and press down until the thickness of the epoxy is approximately 2.5mm and can be seen all around the edges of the laminate once in position.
- Leave to set and harden in the desired position, time to harden depends on the ambient temperature and the initial temperature of the epoxy.

Two CFRP laminates were bonded parallel to each other along the entire length of the tensile face for each RC beam (Figure 37). A Light weight, uni-directional 200mm CFRP wrap was bonded around the entire beam at the location of the supports to provide adequate anchorage during the testing phase (Figure 38). The test beams were finally coated with white paint in an effort to easily identify early stage cracking.

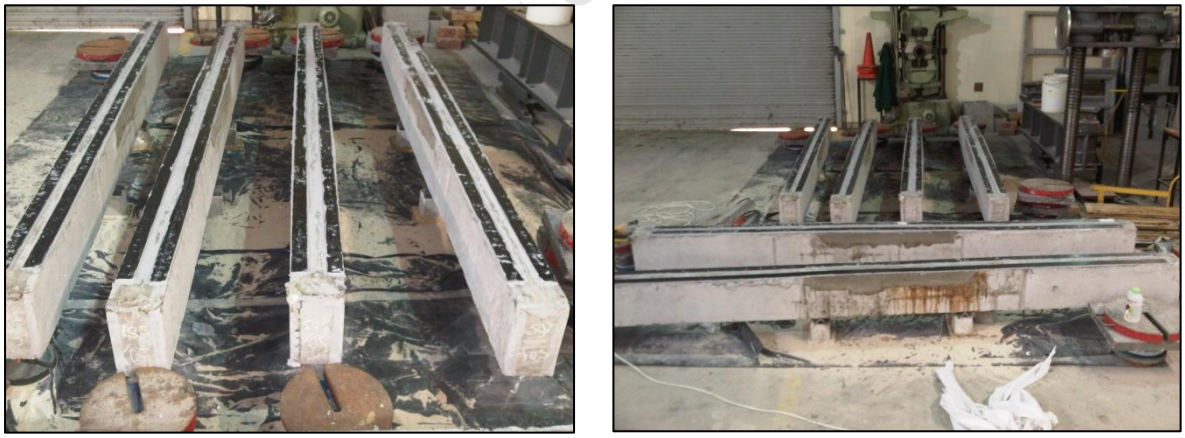

Figure 37: CFRP laminate application along the tensile face

Figure 38: CFRP Wrap applied at support ends for anchorage

3.3 Testing

3.3.1 Sustained Load during preparation

During the accelerated corrosion phase and patch repair process all the test specimens, were statically loaded under a four point loading scheme. The static load applied increased the rate of corrosion due to the increased stress experienced in the test specimens. The static load applied, see figure 37, W = 1.96kN, this caused a constant moment across the midspan section equalling 2.21kNm. The constant moment applied is approximately 56.5% of the cracking moment (3.9kNm).

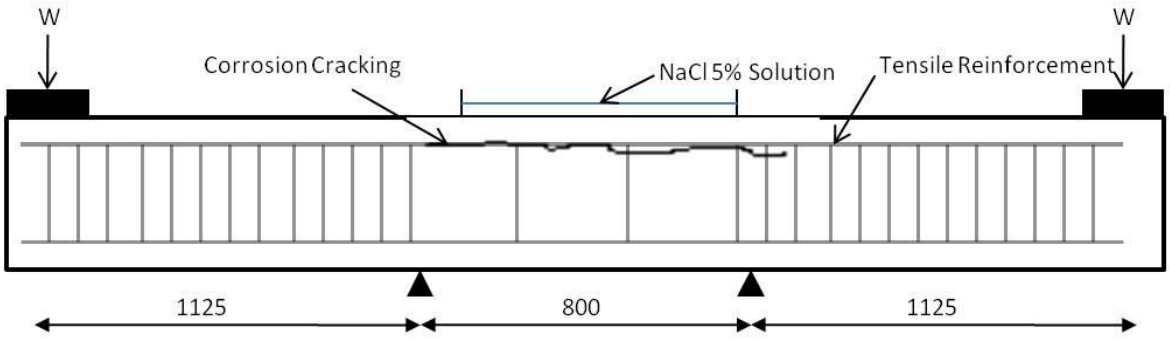

Figure 39: Set up for accelerated corrosion stage

Figure 40: Static load set up and accelerated corrosion phase

3.3.2 Data Acquisition

The program Wave Matrix was used to form the applied load waves for the cyclic and static test sequences. The Instron is connected to the 250kN actuator which applied the desired cyclic and static loads, throughout the loading sequence; Wave Matrix collects load and displacement data according to the position of the actuator whilst performing the desired load. The data captured was used to graphically represent the deterioration of each test specimen over a period of time. The graph displays the number of cycles versus midspan displacement throughout the entire test sequence.

Figure 41: Data acquisition and Instron set up

3.3.3 Dynamic Testing

To assess the fatigue performance of the test specimens under various stress levels, cyclic loading tests were performed. The cyclic load test was designed to simulate the ideal life span cycle of a common RC structure up until 3,000,000 cycles or ultimate failure. Ultimate failure is described as the point when the RC beam can no longer support any further loads, this point is identified when the CFRP has ruptured or debonded and there is excessive concrete cracking. The design life of a typical RC structure is estimated at around 50 years, cyclic loading tests are able to simulate a typical 50 year life span in a couple days of testing using repetitive load cycles at a constant frequency and amplitude.

For the cyclic load tests, a sinusoidal load was applied at varying amplitudes, depending on the desired stress range, resulting in an imposed repetitive cycle of maximum and minimum stress levels at a constant frequency of 2Hz. The tests were set up to apply a cyclic load until failure, throughout the test, the beam cracks were analysed. Refer to Table 10 for the fatigue testing program.

Figure 42: Dynamic test set up

3.3.3.1 Test Program

The test program includes three different degrees of testing, ranging from low, medium and high. The loading was applied in a three-point bending arrangement, therefore causing a maximum bending moment at the midspan and point of loading.

The frequency for each test sequence was identical, with varying amplitudes. Studies have shown that a frequency of 1.7 Hz best simulates the typical frequency for vehicle loads on bridge decks (Parish 2011), but due to time constraints the test program used a frequency of 2 Hz.

All test specimens were subjected to an initial minimum cyclic load which equaled 10% of the static failure load for each RC beam category (Parish 2011); this load was applied for a short period of time before a sinusoidal load cycle was applied at varying amplitudes. The amplitude for each test varied depending on the desired stress range to be achieved.

Table 10 and 11 summaries the applied cyclic and static loads as well as the corresponding number of cycles performed and the visual observations of each test. The failure mechanisms are discussed in depth in Chapter 4: RESULTS.

After the completion of the dynamic load tests, the internal reinforcement was analysed. Discontinuities in the results suggested that the internal steel had in fact fractured prior to the eventual fatigue failure of the entire RC beams.

Table 10: Fatigue Test Program

Beam Description	Min Load (kN)	Max Load (kN)	Amplitude	% of ULS	# of Cycles
F-40-1	9.6	45	35.4	55	439,790
F-50-1	10.8	41.5	30.7	45	3,010,000
F-50-2	10.8	51	40.2	55	704,108
F-50-3	10.8	61.5	50.7	67	355,000

Table 11: Static Load Program

Beam Description	Load Type	Rate	Load at Failure	Observations
S-40	Load cont.	0.33kN/min	96kN	Bending failure
S-50	Displacement cont.	1.5mm/min	107kN	Shear failure

Figure 43: Internal steel fracture

Figure 43 clearly indicated that the internal steel in fact fractured. This is clear as there is no evidence of steel elongation at the point of fracture. This indicated that the failure of the steel was sudden, which is expected as fatigue failure is often brittle. This mode of failure is described further in the following chapter.

3.4 Summary

The test methodology described in this chapter was designed with the intention of analysing the fatigue performance of a patch repaired and CFRP strengthened RC structure.

The methodology describes the process of accelerated corrosion and the technique used to perform a successful patch repair. After the patch repair, the method of using CFRP laminates as a strengthening scheme is described.

Finally, the method of testing is described, focusing on the sustained load applied during the accelerated corrosion phase and finally the method of data acquisition. The methods of static and dynamic testing that were implemented were designed in such a way to achieve the desired results. The results of the proposed methodology are interpreted in the following chapter.

4 Chapter 4: RESULTS

4.1 Introduction

Due to the empirical nature of the investigation, the methodology which was implemented successfully determined the fatigue performance of the corrosion damaged RC beams which were repaired and finally strengthened using CFRP. The results are presented, discussed and shown by graphically representing the fatigue behavior of the beams and describing the observations of the failure mechanisms during failure.

4.2 Accelerated Corrosion and Patch Repair

Static load tests conducted on both the 40MPa and 50MPa RC beams showed that their ultimate static capacity at failure had doubled after the patch repair and CFRP strengthening. Therefore the 10% accelerated corrosion initiated on the steel prior to strengthening had very little or no influence on the final ultimate capacity of the CFRP strengthened beam. The only influence the corrosion would have on the CFRP strengthened beam was if the tensile corrosion cracks propagated after strengthening, but since the damaged concrete was removed and replaced with a patch repair mortar and the internal steel was treated prior to the concrete replacement, this problem was avoided totally.

Due to limitations of the methodology it was impossible to study the long term effect of further corrosion cracking after the patch repair and CFRP strengthening whilst under a cyclic load. Further corrosion cracking could however have an influence on the strength of the beam after a repair was done. If corrosion cracks propagate whilst under cyclic load the corrosion cracks would in fact have weakened the bonds between the patch repair, substrate and CFRP and ultimately weakened the entire composite as a whole.

Figure 44 below indicates the expected long term performance that further internal steel corrosion would have on a repaired and strengthened RC beams' ultimate load capacity whilst under cyclic loading after a patch repair and CFRP strengthening. It can be noted that the beam has an improved ultimate capacity due to the CFRP strengthening and the curve is the gradual decrease in capacity due to the ingress of corrosion cracks which ultimately weaken the beam.

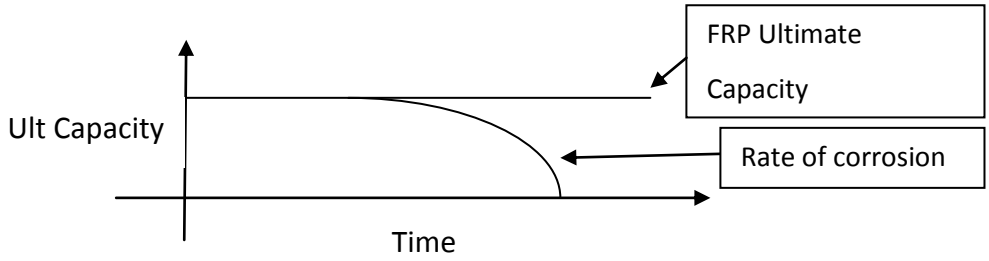

Figure 44: Loss of Ultimate Capacity due to long term corrosion

Unlike the accelerated corrosion, the patch repair did have an influence on the failure mechanisms of the cyclic load tests.

In the majority of the cyclic load tests; initial cracks appeared between the substrate concrete and patch repair interface at the extreme tensile face. The crack patterns along the patch repair mortar were very common, and since the mortar had very high strengths, the material is very brittle and would therefore crack at early age.

The early age cracking was a combination of initial shrinkage cracks and the loading that was applied on the extreme ends of the repaired structure. The accentuated early age cracking was a result of the combined shrinkage cracking due to the confined area that the patch repair cured in and the bending moment that was applied across the curing section).

These cracks often propagated upwards along the interface and eventually would propagate through the substrate and joined the midpoint cracks which had propagated towards the point of loading at the mid-span.

Although the interfacial cracks were often the first noted cracks, they did not lead to the primary mode of failure, which was failure due to the ultimate moment capacity being exceeded which lead to extreme mid-span cracking under the loading point. During the patch repair process, while under early monotonic loading, small cracks developed in the patch repair mortar, these cracks propagated through the patch repaired section when the loads were increased.

When the cyclic loads were introduced, these early age cracks propagated upwards and slowly through the patch repaired sections and into the original substrate interface. Over a period of time these cracks would widen and propagate further into the substrate, these

cracks eventually contributed towards the eventual modes of failure once the ultimate bending or shear capacities were exceeded.

Figure 45; shows the crack propagation along the patch repaired section and eventually into the original substrate interface. At failure, the original cracks at the mid-span had significantly propagated and eventually contributed to the final mechanisms of failure when the bending moment was exceeded.

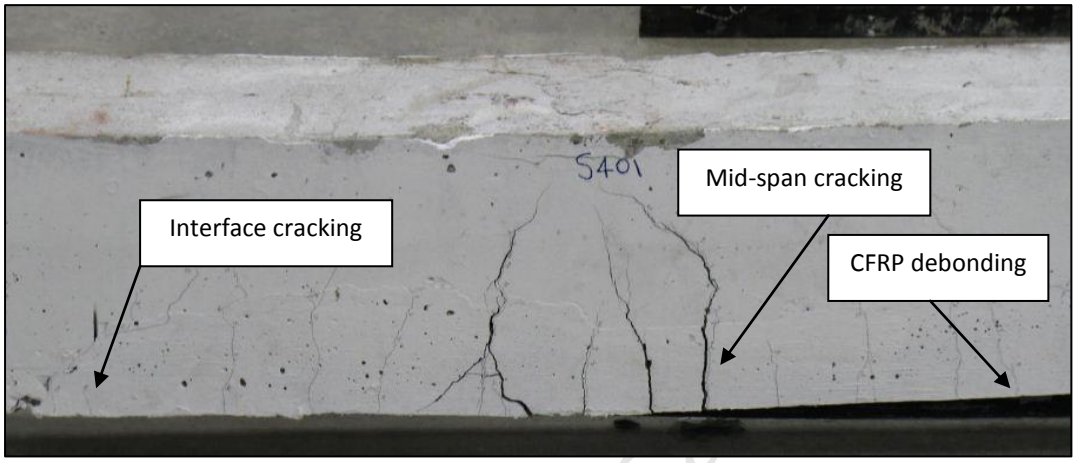

Figure 45: Patch repair crack propagation

4.3 Static Loading

4.3.1 Introduction

The applied loads for the cyclic load tests are a function of the ultimate static failure load of a previously tested identical RC beam. The static failure loads are therefore an important tool to determine what the increased static load at failure is of the patch repaired and CFRP strengthened RC beams. A static load test was each conducted on a 40MPa and 50MPa repaired and strengthened RC beam; the results showed that the ultimate bending moment at failure for both beams were double that of the design strength for an unrepaired and unstrengthened identical RC beam according to the simplified stress block method.

- Unrepaired and unstrengthened RC beam had calculated design strength of ≃ 41.3kN (See Appendices 1)
- Static load at failure for the 40Mpa patch repaired and strengthened RC beam ≃ 96kN (See Static Load Test: S-40 below)

- Static load at failure for the 50Mpa patch repaired and strengthened RC beam ≃ 107kN (See Static Load Test: S-50 below)

The influence of the patch repair and CFRP laminate combination more than doubles the total ultimate moment capacity for identical repaired and strengthened RC beams.

4.3.2 Results

4.3.2.1 Static Load Test: S-40

S-40 refers to the static load testing of a 40MPa RC structure until ultimate failure. Failure was identified as the point when the CFRP ruptured or debonded or the structure could no longer resist any further loading.

S-40 was load controlled at a rate of 0.33kN/min. The slow rate of applied force allowed for a thorough investigation of the crack propagation and failure mechanisms. The problem with the load controlled testing scheme was that once the beam began to fail, the load was applied at a constant rate and force. Therefore failure was sudden and it was difficult to analyse all aspects throughout failure.

Typical 3-point bending failure was experienced. Initial cracking was first observed in the patch repaired section. Cracking then developed along the patch repair and substrate interface as well as along the entire length of the patch repair (See Figure 47: S-40 Crack failure pattern). These cracks began to propagate with the increased load until the cracks propagated into the original substrate. The cracks experienced in mid-span of the substrate began to widen significantly, at this point a large majority of the load is carried by the still bonded CFRP strips. Therefor the bending moment of the original RC structure had been exceeded and the CFRP strengthening was resisting the increased load allowing for a stronger repaired structure. At a certain moment, the tensile CFRP-concrete bond was exceeded and the strips debonded from the repaired structure, confirming the ultimate failure of the RC structure.

The eventual analysis and observations confirmed that the RC beam failed with large cracking at the mid-span at an approximate load equalling 70kN, but with the aid of the still fully bonded CFRP the structure transfers the load fully onto the CFRP. Finally, sudden

bending failure occurred at 98kN when half of the CFRP bond delaminated from the patch repair and substrate along the entire tensile face, as seen in Figure 46.

Figure 46: S-40 Bending Failure

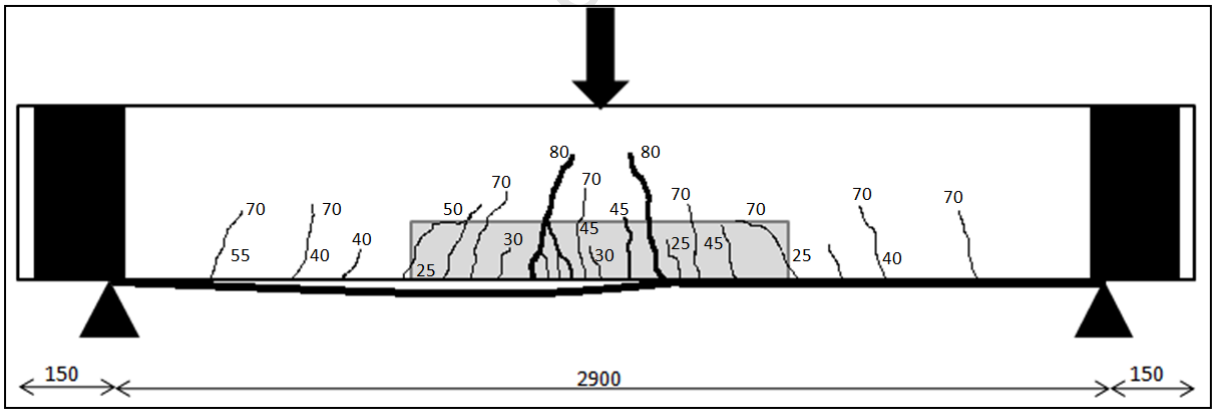

Figure 47: S-40 Crack failure pattern

4.3.2.2 Static Load Test: S-50

S-50 refers to the static load testing of a 50MPa RC structure until ultimate failure. Failure was identified as the point when the CFRP ruptured or debonded or the structure could no longer resist any further loading.

The static load test for S-50 was displacement controlled at a rate of 1.5mm/min. This allowed for a much faster test, but in the case with displacement controlled fatigue testing,

the failure mechanisms during failure can better analysed and understood since the test is better controlled throughout. The method of load controlled testing, as for S-40, was not recommended as the results were not accurately captured and therefore displacement controlled testing was preferred for the static loading of S-50.

S-50 did not exhibit the same type of failure as S-40. In this case there was a shift of failure mode from the expected bending failure to an unexpected shear failure (See Figure 48). The shift in failure mode was due to the external CFRP strengthening which increased the bending moment capacity to such a degree that it exceeded the shear capacity for the strengthened RC beam which ultimately led to shear failure.

A flaw with the RC beam design was that the stirrups across the patch repaired section were designed for a 4-point loading system, but due to limitations with the study all static and cyclic tests were performed in a 3-point loading system, this contributed to the lack of shear capacity and eventual shear failure of the S-50 RC beam.

Soon after the initial load was applied, initial cracks were observed at the interface between the patch repair and original substrate. Further cracks were noticed along the entire length of the patch repair, once again these cracks were present during the curing of the patch repair mortar. The cracks along the repaired section propagated up towards the original substrate at the mid-span. Due to the increased mid-span displacement the cracks began to propagate along the entire length of the patch repair boundary and finally up towards the point of loading in a shear failure pattern of 45 degrees (See Figure 49).

Once again, the RC beam showed significant degradation before it was judged to have reached ultimate limit state. This was due to the fact that the CFRP laminates were all still fully bonded along the entire tensile face, even while the beam exhibited large shear and bending cracks. After the observation of the significant diagonal shear cracks the beam was still able to regain strength; this was achieved by the composites internal mechanics shifting the total force of the increased load directly into the CFRP strips. The ultimate failure load of the RC structure was finally determined once the CFRP laminate suddenly debonded from the repaired and strengthened structure at 108kN.

At the point of failure, the laminate debonds at the positions where the most excessive cracks are visible. The CFRP laminate then debonds along the entire length of the tensile face until reaching the CFRP anchorage wrap. Therefore, even when the concrete has failed due to excessive cracking, the bonded CFRP is able to carry the tensile loads until ultimate failure occurs when the laminates debond from the concrete.

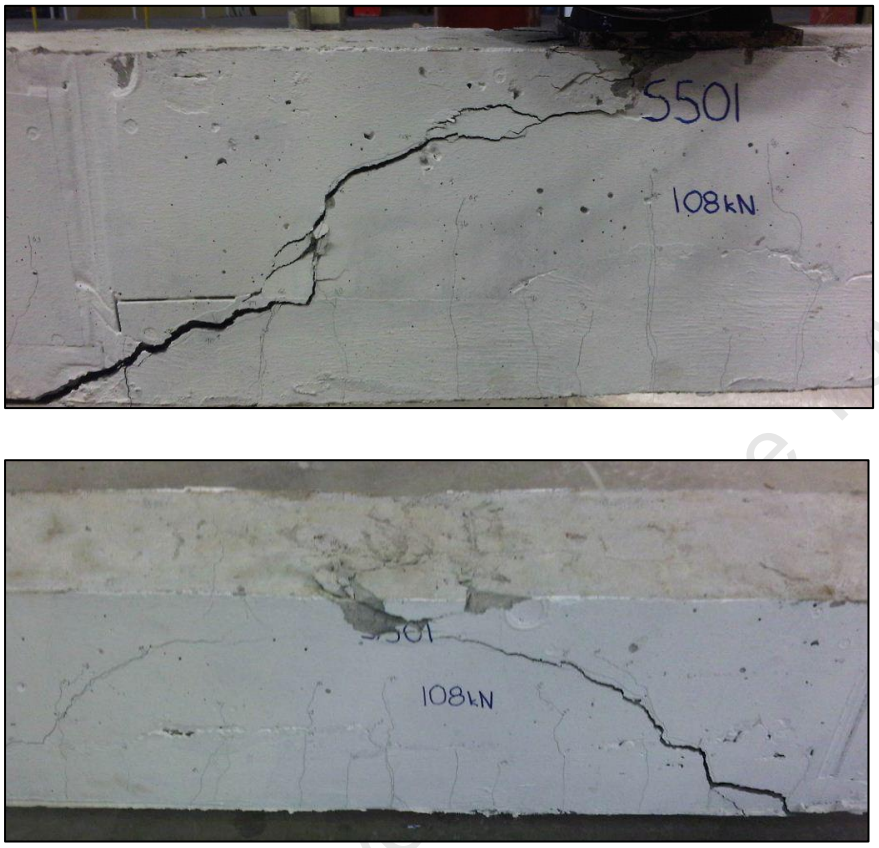

Figure 48: S-50 Shear Failure

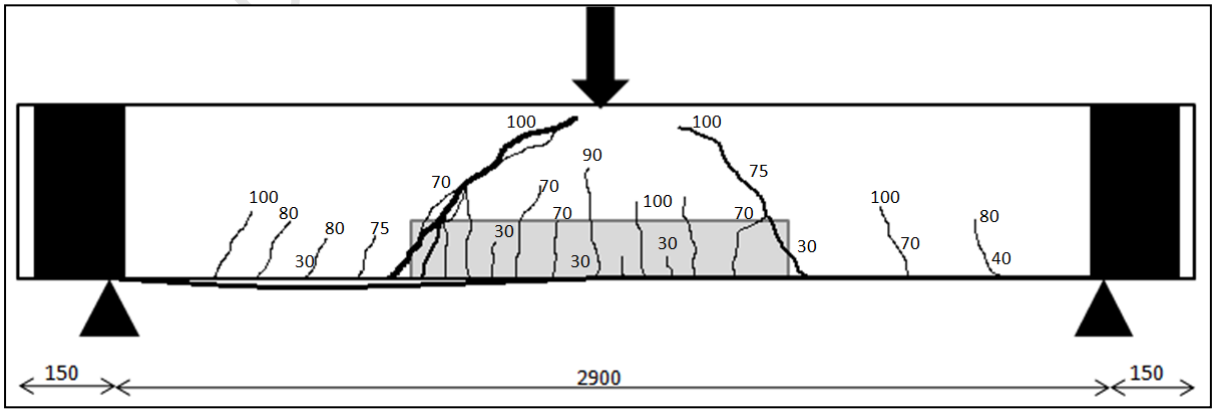

Figure 49: S-50 Crack failure pattern

4.4 Fatigue Loading

4.4.1 Introduction

In order to successfully analyse the fatigue performance of the repaired and CFRP strengthened RC beams, a varying range of amplitudes were used to derive a relationship between the beams fatigue performances based on the number of cycles achieved versus constant cyclic load applied over duration of time.

The amplitudes used were derived as a function of the ultimate static loads experienced for an identical RC beam at failure. The 40MPa RC beams failed at a maximum static load of 98kN and the 50MPa RC failed at 108kN respectively.

Therefore to determine the maximum and minimum amplitudes for the cyclic loads applied, we set the minimum cyclic load as 10% of the corresponding maximum static load experienced for an identical repaired and CFRP strengthened beam at failure. So, for each of the low, medium and high cyclic load cases, the minimum value of the sinusoidal wave is a percentage (10%). The maximum value of the cyclic wave to form the low, medium or high amplitude was 85% of the maximum static load for the relevant identical beam multiplied by a factor (0.45, 0.55 or 0.67) to give rise to the varying amplitudes for testing.

The cyclic test was run in two stages, stage 1, a monotonic load was applied at a rate of 2kN/min until the minimum value of the cyclic sinusoidal wave was reached (10% Static failure load), at which point stage 2 applied a sinusoidal wave load formation at the desired amplitude (low, medium or high) until ultimate fatigue failure was reached. Fatigue failure was determined when the CFRP finally debonded from the RC beam and the maximum set deflection was exceeded.

4.4.2 Results

4.4.2.1 Cyclic Load Test: F-50-1

F-50-1 refers to low amplitude range (1) of fatigue load testing of the 50MPa RC structure until ultimate failure was reached. Failure was identified as the point when the CFRP ruptured or debonded or the structure could no longer resist any further loading.

F-50-1 was tested under cyclic loading conditions at low amplitude of approximately 15.15kN. This was in the range equalling 45% of the ultimate static load capacity for the patch repaired and CFRP strengthened 50MPa RC beam (S-50).

It is evident from Figure 51 that F-50-1 exhibited a common 3-point loading bending crack trend along the extreme tensile face of the beam during the initial stages of testing. After only 100 000 cycles, the cementitious patch repair mortar began to crack along the entire length (Figure 50), only few cracks are evident outside of the patch repaired section.

An interesting trend which develops at an early stage is the cracking which propagates between the patch repair and original substrate bond (See Figure 51). Very little to none of the cracks which develop in the patch repaired section protrude into the substrate at the midspan. The early age cracking along the repaired section was often a result of the early age cracking which developed after the patch repair work was done; these cracks were only observed and began to propagate once an external load was applied.

After 800 000 cycles, the mid-span cracks protrude into the original substrate and diverge towards the point of loading. These cracks were only noticeable when the sinusoidal load was applied. After a period of time, further cracks were observed outside of the patch repaired section as well as along the interfacial bonds between the patch repair mortar and original substrate. The interfacial bonds then propagated further along the patch repair boundary and joined the original mid-span cracks which had now since protruded into the substrate below the point of loading. No CFRP debonding or rupture was detected at this point.

At the low amplitude no further CFRP or concrete damage was detected for almost 1,500,000 cycles. The reason no further damage was detected is due to the fact that the CFRP laminate was resisting any additional loads.

Nearing the point of failure, the majority of the entire mid-span cracks had propagated towards the point of loading and had increased significantly in width, thus suggesting that the beam might have already reached a point of fatigue failure due to the excessive concrete cracking. At this point though, the CFRP resists the majority of the tensile stress

applied until eventual CFRP debonding occurs and the beam ultimately fails after 3,010,817 cycles due to the ultimate bending capacity being exceeded.

Figure 50: F-50-1 CFRP debonding at failure

Crack Patterns	Description
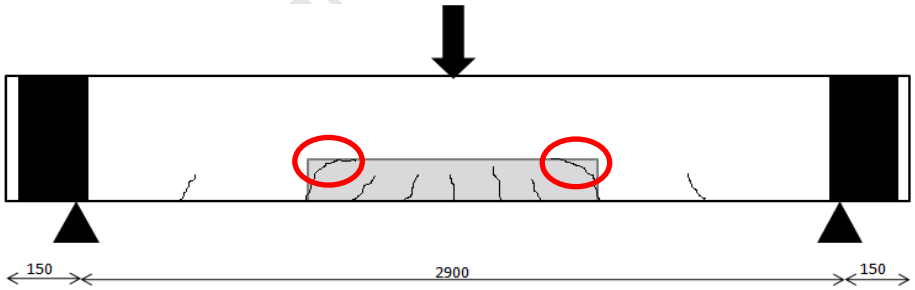	Crack patterns after **100,000** cycles. Common cracking occurs along entire patch repair section.

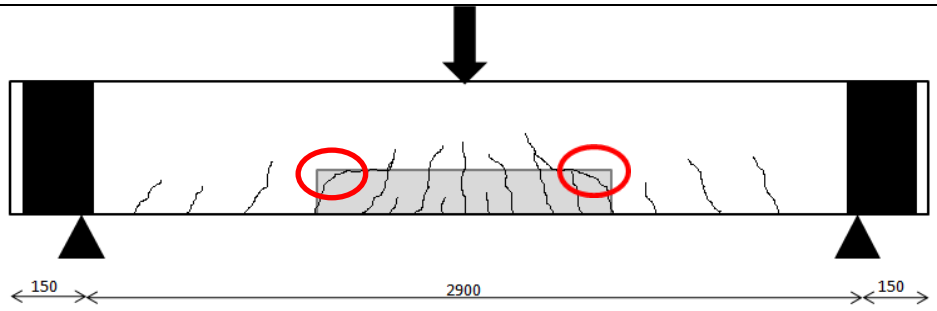	Crack pattern after **800,000** cycles. Initial cracks have propagated and begin to converge towards the midspan.
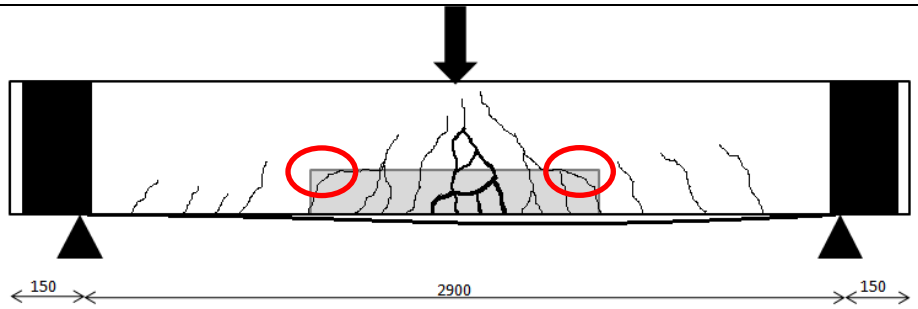	Crack pattern at failure, **3,010,817** cycles. FRP debonded at failure.

Figure 51: F-50-1 Crack distribution

It can be noted that the eventual mode of failure was due to the eventual debonding of the CFRP, although prior to the debonding, the beam had failed in bending due to excessive mid-span cracking. Figure 53 below, graphically illustrates the long term fatigue behaviour of F-50-1's. From the graph, it can be clearly observed that the beam displays a consistent increase in displacement for the majority of the fatigue test until the sudden discontinuity in displacement at approximately 2 400 000 cycles. At this point, it was observed that excessive cracking occurred at the mid-span. The CFRP bond was still fully bonded but it was suspected that the discontinuity in the displacement was a result of the internal steel which fractures under the continued cyclic loading (See Figure 52). After the steel reinforcement had fractured, it was observed that the test specimen was still able to resist the cyclic loading for a further 600,000 cycles.

Soon after 3,000,000 cycles the test specimen experienced ultimate fatigue failure due to the excessive mid-span concrete cracking. At the point of excessive concrete cracking, the CFRP was still fully bonded along the tensile face and therefore was able to resist the majority of the cycling loading.

After 3,010,817 cycles the test specimen experienced sudden CFRP debonding along the most of the tensile face. At this point of ultimate fatigue failure, pieces of the patch repair mortar were spalling and the beam exceeded the maximum allowed displacement which resulted in total fatigue failure of the test specimen.

Figure 52: Internal Steel fractured after approximately 2,400,000 cycles

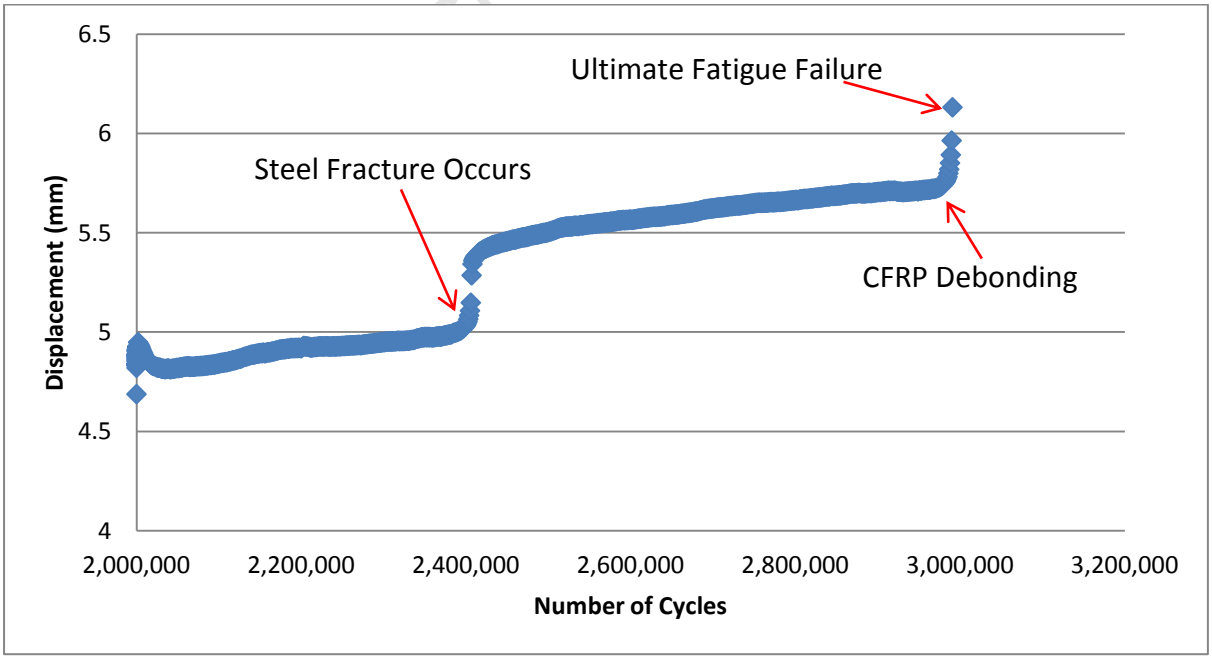

Figure 53: F-50-1 - Number of Cycles versus Displacement

4.4.2.2 Cyclic Load Test: F-50-2

F-50-2 refers to medium amplitude range (2) of fatigue load testing of the 50MPa RC structure until ultimate failure was reached. Failure was identified as the point when the CFRP ruptured or debonded or the structure could no longer resist any further loading.

F-50-2 was tested under cyclic loading conditions at medium amplitude of approximately 20.65kN, this was in the range equalling 55% of the ultimate static load capacity for the patch repaired and CFRP strengthened 50MPa RC beam, S-50.

It is evident from Figure 51 that F-50-2 had very similar early age crack distribution to that of F501 despite the increased amplitude. Once again, the RC beam displayed typical bending cracks to that of a 3 point loading across the patch repaired section. Since the preparations of all the F50 RC beams were identical, the initial cracks are once again a combination of the shrinkage cracks from the brittle patch repair mortar and the cyclic load imposed. Very few cracks are visible outside of the repaired section and once again early age cracks have formed at the patch repair – substrate interface after 100 000 cycles.

After 500 000 cycles more cracks have developed along the patch repaired section and the original cracks have propagated into the original substrate and towards the point of loading. Further cracking has developed outside of the repaired section due to the duration and nature of the imposed load.

F502 shows a very similar failure pattern to that of F-50-1, where by the cracks propagate towards the point of loading and increase in width with the increase of cycles. The mechanics of failure are also very similar, as F-50-2 nears the 704 000 cycles the RC beam fails due to concrete fatigue failure which is indicated the large midspan cracks, but the CFRP is still bonded at that time and withstands the tensile strains for a further 4 000 cycles until failure.

Finally the concrete is fully cracked and the CFRP debonds from the patch repair and original substrate, resulting in ultimate fatigue failure at 704,137 cycles.

Figure 54: F-50-2 Cracking and debonding at failure

Crack Patterns	Description
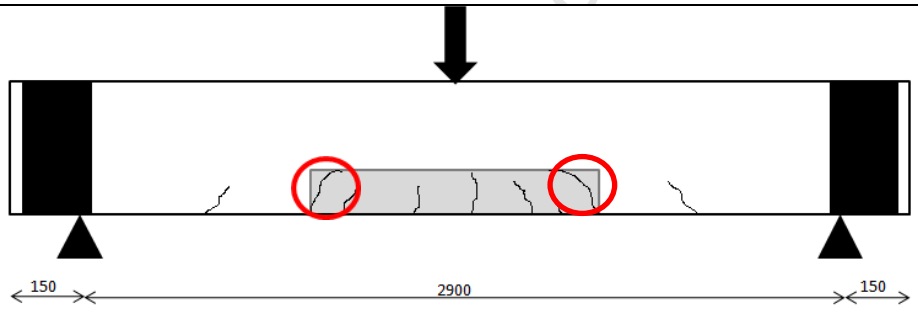	Crack patterns after 100 000 cycles. Common cracking occurs along entire patch repair section.
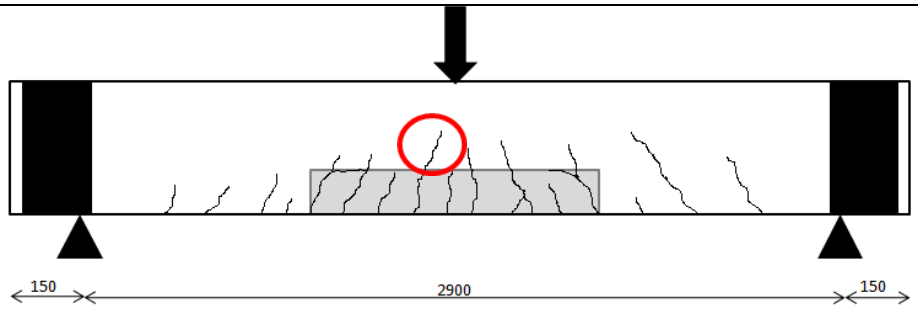	Crack pattern after 500 000 cycles. Initial cracks propagate and begin to converge at the centre.

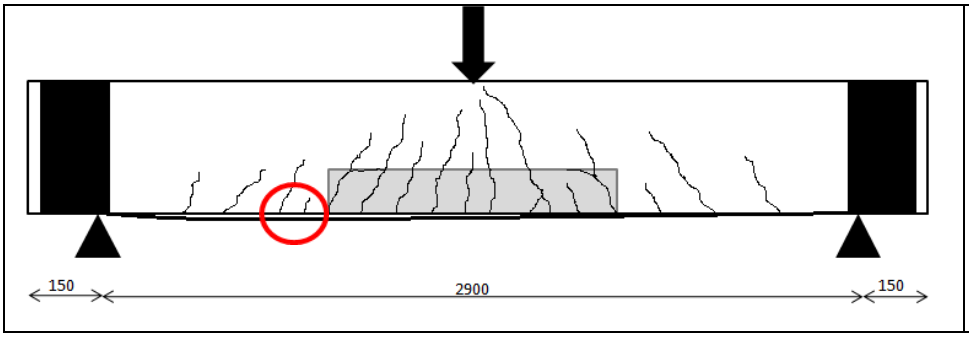

Crack pattern at failure, 704 000 cycles.
FRP debonded at failure.

Figure 55: F-50-2 Crack Distribution

Figure 57 below graphically illustrates the fatigue performance of F-50-2. It is clear to see the long term behaviour of the patch repaired and CFRP strengthened RC beam throughout the cyclic load testing phase. Similar to F-50-1, the RC beam reached a point where the displacement increased at a relatively consistent rate, but due to the fact that F-50-2 experienced greater amplitude the displacement gradually increased at a faster rate over time. Therefore the test specimen reached fatigue failure at a significantly less number of cycles. There is no indication along the curve that the concrete failed and CFRP recovered the strength, thus possibly implying that the CFRP debonded at the same time that the concrete failed. An inspection after the cyclic loading revealed that the internal steel in fact fractured but it is not clear in the graph.

Figure 56: Internal steel fractured

Based on the observations and the graph below it can be concluded that at failure, the internal steel fractured, CFRP debonded and excessive concrete cracking occurred at the mid-span. The ultimate failure of the test specimen was reached after only 704,137 cycles.

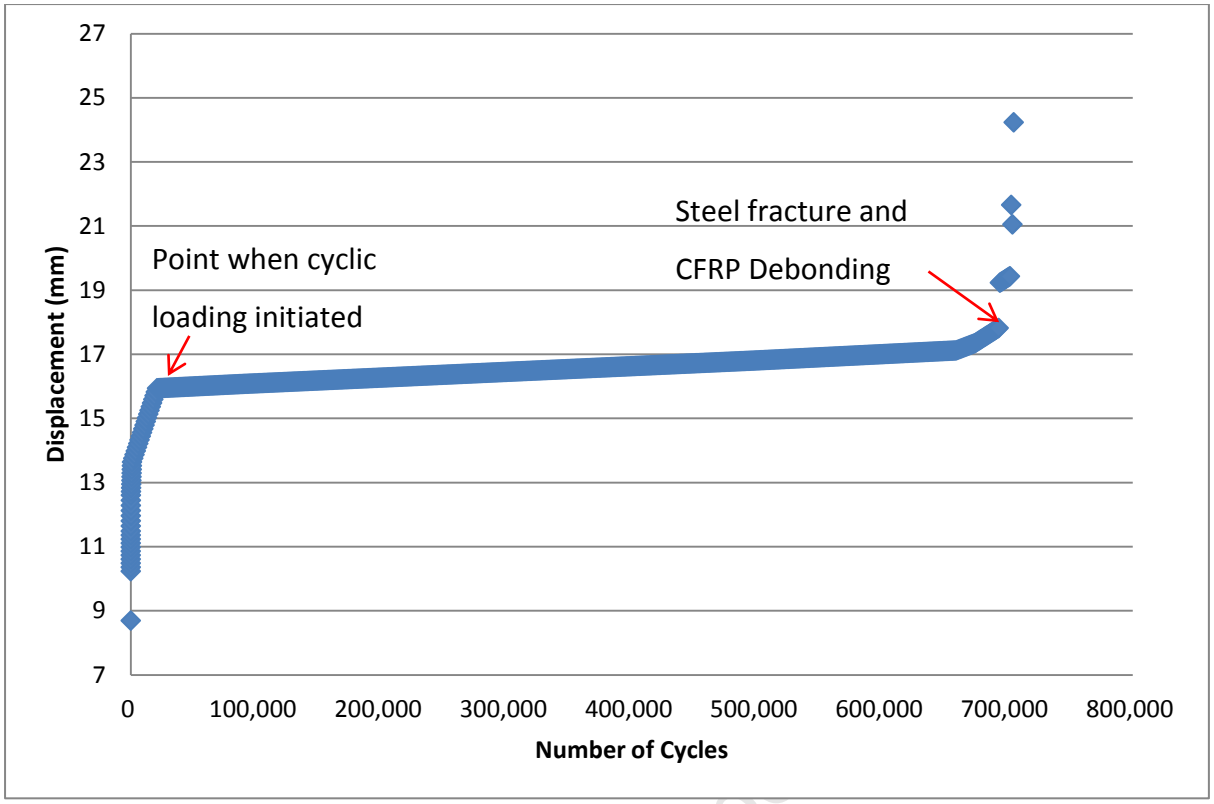

Figure 57: F-50-2 - Number of Cycles versus Displacement

4.4.2.3 Cyclic Load Test: F-50-3

F-50-3 refers to high amplitude range (3) of fatigue load testing of the 50MPa RC structure until ultimate failure was reached. Failure was identified as the point when the CFRP ruptured or debonded or the structure could no longer resist any further loading.

F-50-3 was tested under cyclic loading conditions at high amplitude of approximately 25.15kN, this was in the range equalling 67% of the ultimate static load capacity for the patch repaired and CFRP strengthened 50MPa RC beam, S-50.

Due to the high amplitude applied to F-50-3, the test specimen exhibited significant structural damage after only 100,000 cycles (See Figure 60). The early age crack patterns were similar to that of F-50-1 and F-50-2, although the degree was worse, which was expected.

The early age cracking on F-50-3 was more severe and uniform across the entire section of the beam. It was observed that the cracking in the patch repaired section did not arrest once it reached the original substrate, these cracks began to protruded into the substrate before 100 000 cycles. Early age cracking between the original substrate and patch repair

interface was also observed, but in this case the cracks followed along the boundary of the patch repair mortar and joined up with the other mid spanning cracks. In the cases of F-50-1 and F-50-2, the interfacial cracks simply cracked along the corner and propagated upwards towards the point of loading (See Figure 60).

After 200,000 cycles, the original cracks propagated further and started to converge towards the point of loading. No delamination of the CFRP laminate was observed but the crack widths had dramatically increased under the cyclic loading.

Over the next 100,000 cycles, the cracks increased considerably resulting in the CFRP laminates enduring the majority of the tensile stresses once the concrete had significantly cracked (See Figure 58).

After 330,000 cycles the RC beam has almost completely failed due to the excessive concrete cracking at the midspan. The CFRP laminate along the entire length of the beam suddenly delaminated resulting in the sudden ultimate fatigue failure after only 355,436 cycles.

Figure 58: F-50-3 Cracking, debonding and spalling

Figure 59: F-50-3 internal steel fracture

Crack Patterns	Description
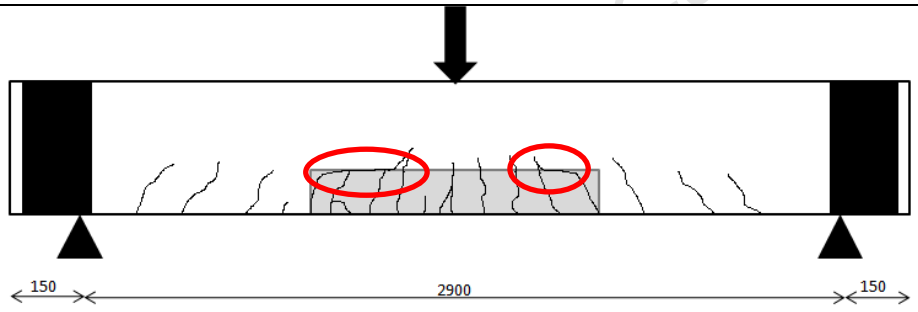	Crack patterns after 100 000 cycles. Common cracking occurs along entire patch repair section.
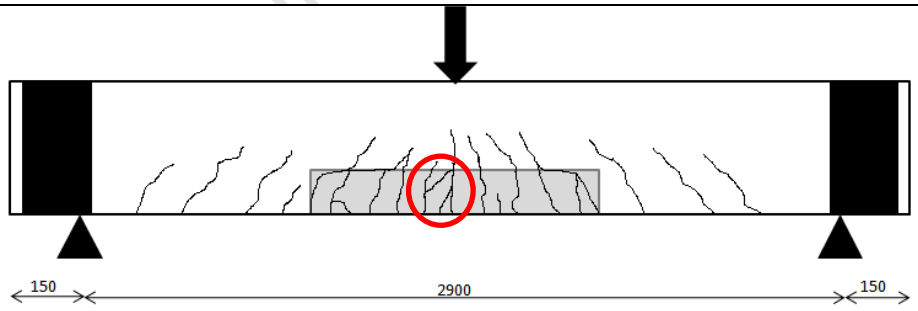	Crack pattern after 200 000 cycles. Cracks begin to converge.

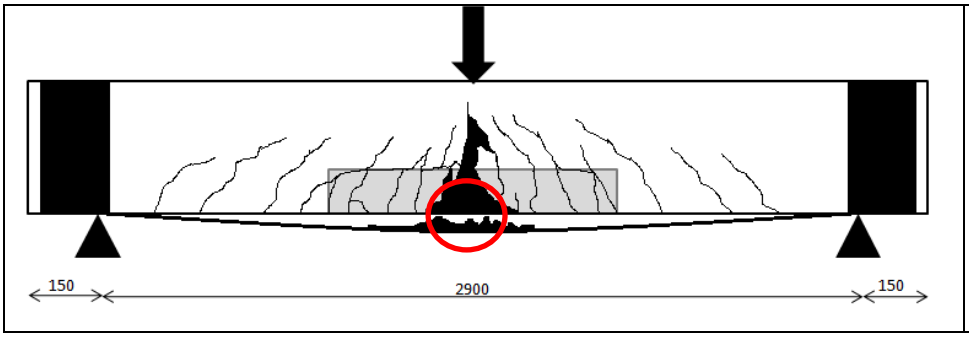

Crack pattern at failure, 355 000 cycles.
FRP debonded at failure.

Figure 60: F-50-3 Crack distribution

Figure 61 clearly illustrates the fatigue behaviour of F-50-3. The graph shows the relationship between the RC beam displacements versus the number of cycles under high cyclic loading. Once again the beam behaves similar to that of F-50-1 and F-50-2, whereby there was a consistent increase in displacement over time until the beam reached fatigue failure when the CFRP delaminated and the RC beam exceeded the maximum set displacement.

After later inspection, it was discovered that the steel reinforcement once again had fractured during the testing period. Analysis of the graph below indicated that the steel fractured at a similar time to when the CFRP debonded and the excessive mid-span cracking was observed. Therefore the ultimate fatigue failure was sudden and was a result of the three different modes of failure occurring within a short period of time (See Figure 61).

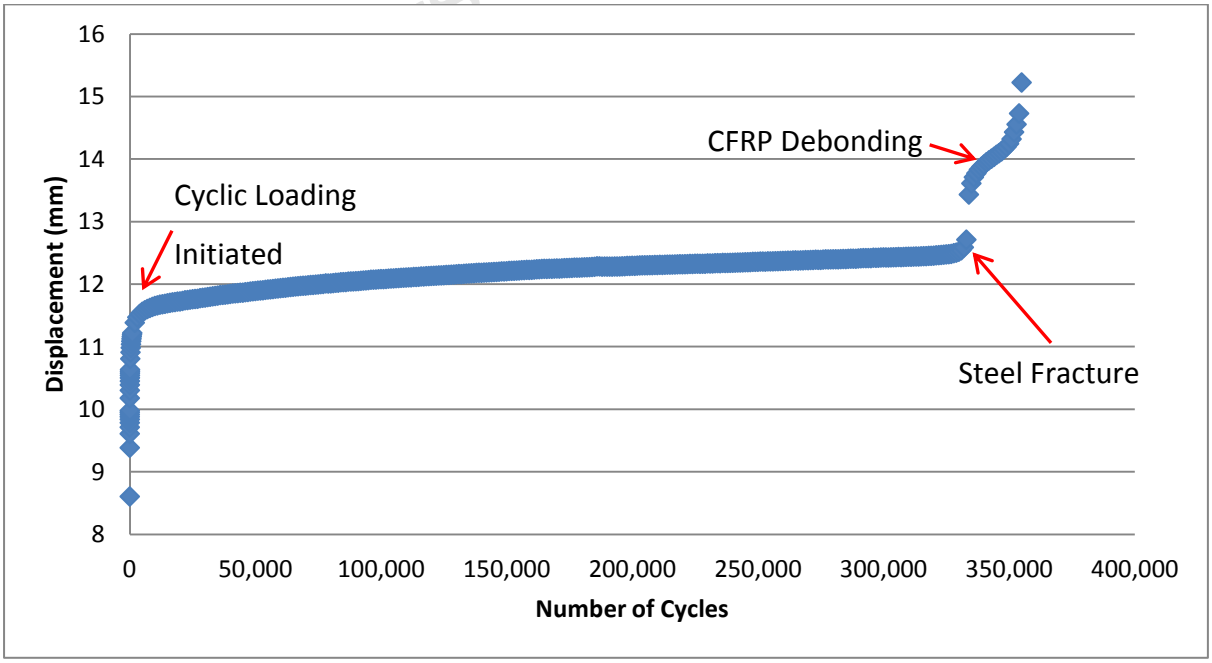

Figure 61: F-50-3 - Number of Cycles versus Displacement

4.4.2.4 Cyclic Load Test: F-40-2

F-40-2 refers to medium amplitude range (2) of fatigue load testing of the 40MPa RC structure until ultimate failure was reached. Failure was identified as the point when the CFRP ruptured or debonded or the structure could no longer resist any further loading.

F-40-2 was tested under cyclic loading conditions at medium amplitude of approximately 17.7kN, this was in the range equalling 55% of the ultimate static load capacity for the patch repaired and CFRP strengthened 40MPa RC beam, S-40.

Since F-40-2 was the only 40MPa cyclic loaded RC beam, a medium amplitude range was used to estimate the fatigue performance which would give an average value which could be compared to the 50MPa RC beam results.

The test specimen, F-40-2 displayed severe cracking after only 100 000 cycles. The excessive early cracking was caused from the combination of a lower strength concrete and the medium amplitude of cyclic loading.

Initial cracks occurred along the entire length of the patch repaired surface as well as at the substrate – patch repair interface. These cracks did not stagnate at the substrate boundary but rather protruded into the original substrate. Cracks were also observed outside of the patch repaired section, indicating that the loading is rather severe on the 40MPa concrete.

After 200,000 cycles, further cracks developed along the length of the patch repaired section and the initial cracks propagated further into the substrate. An interesting trend developed, where the interfacial cracks propagated at a faster rate towards the point of loading than the midpoint cracking (See Figure 62), thus suggesting a combined shear and bending failure scenario was developing. At the same time, the initial midpoint cracks had stagnated after initially protruding into the substrate after only 100 000 cycles. The cracks closest to the interfacial cracks began to converge forming a weakened area in the beam to the left of the repaired section.

As the beam neared fatigue failure, the interfacial cracks propagate towards the point of loading at a 45 degree angle, reinforcing the fact that the shear cracks were the main cause of failure. The initial early age cracks at the midpoint and right hand side of the beam did not propagated any further after 200 000 cycles, the only cracks to propagate were the

shear cracks. The shear cracks increased in width under loading and further converged, forming a web of cracks at a localised area between the original substrate and the cementitious patch repair mortar (Figure 63).

After 400,000 cycles, the beam failed in shear, but due to the CFRP bond still fully intact the beam was able to recover in strength and resist further cycles of loading. Finally, the CFRP completely debonded and the beam ultimately failed due to shear fatigue failure after 411,790 cycles.

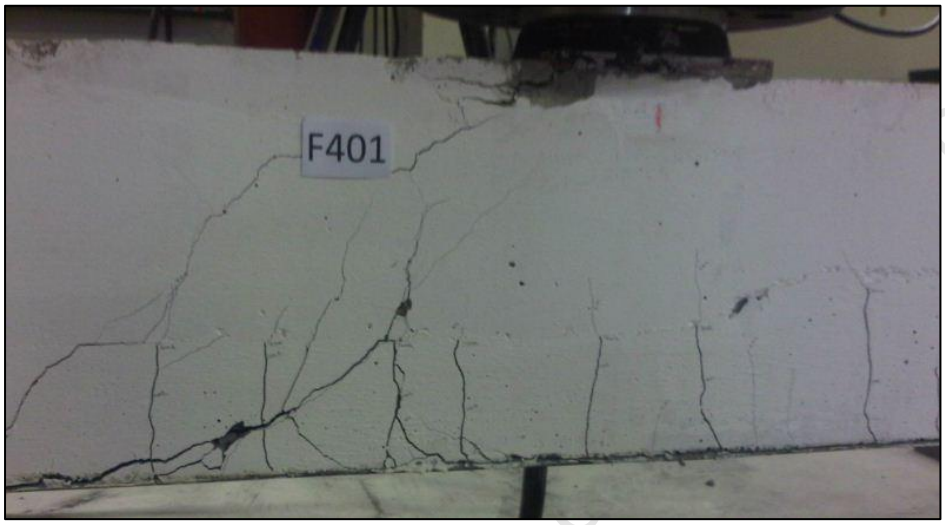

Figure 62: F-40-2 Combined shear-bending failure

Figure 63: F-40-2 Shear failure

Crack Patterns	Description
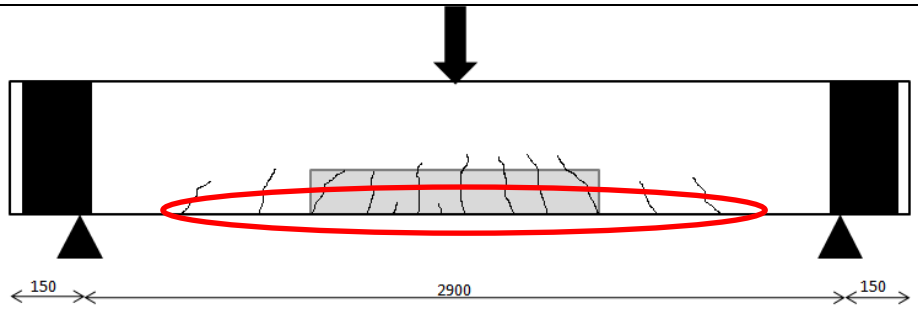	Crack patterns after 100 000 cycles. Common cracking occurs along entire patch repair section.
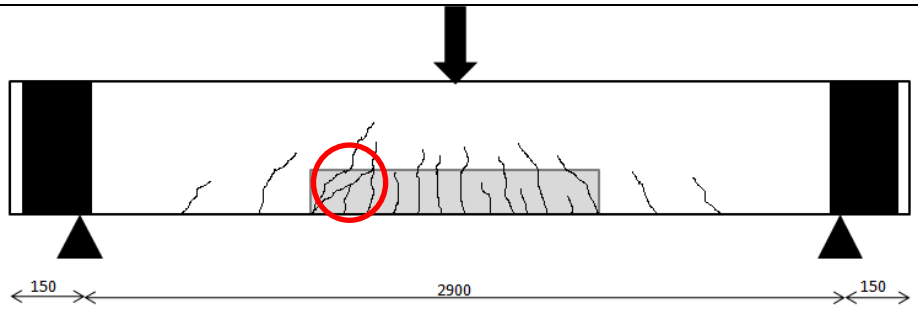	Crack pattern after 200 000 cycles. Cracks begin to converge.
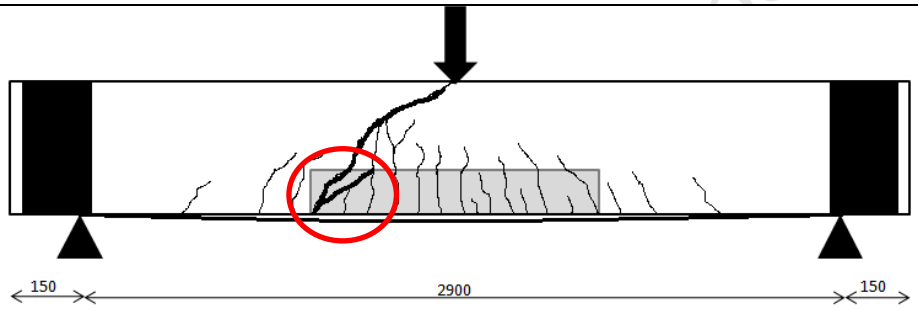	Crack pattern at failure, 411 000 cycles. FRP debonded at failure. Shear failure.

Figure 64: F-40-2 Crack Distribution

Figure 67 graphically represents the fatigue behaviour of F-40-2 under medium amplitude of cyclic loading. It was clear from the curve that F-40-2 sustained a large initial displacement under the medium loading, but since the concrete was weaker than the 50 MPa RC beams, this was to be expected.

Unlike, the fatigue behaviour graphs of the other beams, F-40-2 had a consistent increase in displacement between initiation of the cyclic loading and 250,000 cycles. After 250,000 cycles the displacement increased dramatically, this was due to the shear cracking which occurred long before the fatigue failure.

At approximately 400,000 cycles, there is yet another increase in displacement graph. This was a result of further, more severe, cracking. At can also be assumed that at this point, the

steel reinforcement fractured. The CFRP was still fully bonded and able to withstand most of the stresses until the point of failure.

At failure, the CFRP bond completely delaminated along the entire length of the RC beam, resulting in the ultimate shear failure. The failure mechanisms associated with the fatigue failure due to shear indicated a shift in the mode of failure from bending to shear due to the fact that the shear fatigue failure value was exceeded.

An internal inspection of the reinforcing steel revealed that the steel had completely fractured. On the graph, it can be observed that this occurred a short time before ultimate failure and can be observed on the graph (See Figure 67).

Figure 65: Internal steel fracturing (1)

Figure 66: Internal steel fracturing (2)

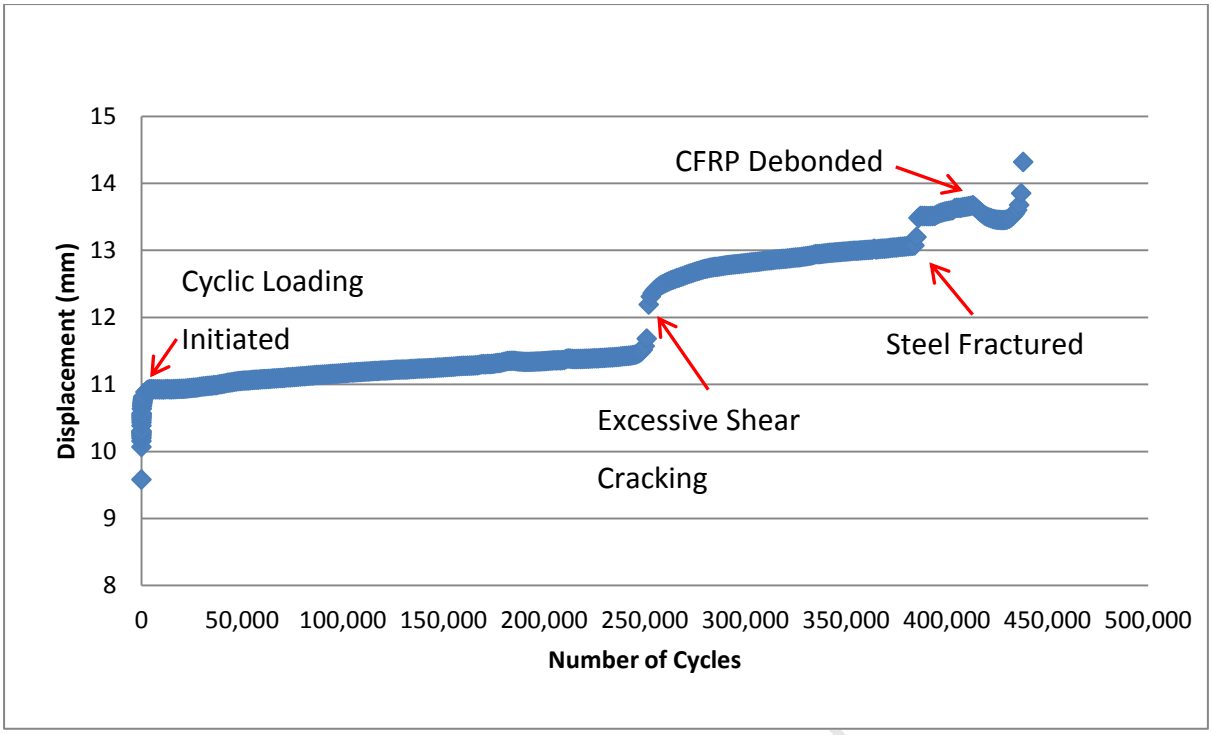

Figure 67: F-40-2 - Displacement versus Number of cycles

4.5 Summary

A significant observation that was made throughout all the cyclic load tests was the common early age crack patterns. All the beams had a very similar crack pattern after 100 000 cycles, the varying degrees of crack lengths were proportional to the amplitude that was applied, but the positions and trends of the cracks were very similar.

Early age cracking was a combination of the load applied and the brittle patch repair mortar shrinkage cracks that were exaggerated under the initial loading. Another reason for the early age cracking was due to the high strength of the cementitious patch repair mortar coupled with the strong CFRP laminate and epoxy bond used. This made for an extremely brittle composite, which was highly susceptible to early age cracking once the load was applied.

All four of the RC beams exhibited early interfacial cracking at the patch repair – substrate boundary as well as uniform cracking along the entire length of the patch repaired section. Early age cracking outside of the patch repaired section was only excessive on the RC beams that were loaded with medium or high amplitudes.

All the 50MPa RC beams exhibited similar failure mechanisms. Initial early age cracking would lead to further excessive propagating cracks which resulted in the fatigue failure of the concrete due to the mid-span cracks which propagated towards the point of loading. At that point, the CFRP took full effect and provided the additional strength required to recover the RC beams. The addition of CFRP allowed for an increased cyclic loading until finally, the CFRP debonds from the patch repair and substrate, which results in fatigue failure.

However, F-40-2 RC test specimen displayed similar early age cracking but it was apparent that the beam was exhibiting different failure mechanisms once the shear cracks developed early into the cyclic test. This meant the CFRP had to recover the RC beams strength from a significantly earlier age. It was also surprising to note, from Figure 68, that there is a distinct relationship between F-40-2 and F-50-3. F-40-2 had a lower compressive strength substrate concrete and was exposed to lower amplitude of loading, but completed more cycles than the stronger F-50-3 RC beam, which experienced a high amplitude of loading. The modes of failure were also distinctly different, F-50-1 failed in bending, while F-40-2 failed due to a combination of shear and bending fatigue.

The two test specimens which experienced the similar amount of cyclic loading, F-40-2 and F-50-2, displayed different failure mechanics. It was also clear that the weaker 40MPa test sample experienced a significantly lower number of cycles than the 50MPa sample until ultimate fatigue failure was reached. Therefore, illustrating that even though the patch repair mortar, interfacial bond strength and CFRP were identical, the ultimate limiting factor for the fatigue failure was the strength of the substrate concrete which degraded at an earlier rate.

F-50-1 is not shown on Figure 68 since the beam completed over 3,000,000 cycles and would not compare well with the other test specimens. It was observed that the F-40-2 trend line, where the CFRP recovered the strength of the RC beam, was possibly more apparent than the lines of F-50-2 and F-50-3 since the failure mechanisms were completely different.

Although, for both F-50-2 and F-50-3 you can see the point of increased deflection, at this point the concrete had failed and the progression of cyclic loads was due to the extreme tensile loads the CFRP was able to resist.

All the graph lines on Figure 68 exhibited a constant rate of increased deflection after reaching an equilibrium point after a relatively similar number of cycles, at this point the initial cracks had developed and the beam was oscillating at a constant frequency with the sinusoidal load wave applied.

It was also interesting to observe the fact that for all the test specimens, the steel reinforcement fractured. There was also no relation made between the locations of the fractured steel and the locations of the pitting corrosion in the steel. This would suggest that the treatment of the corroded steel prior to the patch repair was in fact sufficient and adequate. The pitted sections of the steel reinforcement did not contribute to the locations of ultimate fatigue failure.

Table 12: Summary of Load versus Number of cycles

Description	Load % of Static ULS	Cycles to failure
F-50-1	45	3,010,817
F-50-2	55	704,137
F-50-3	67	355,436
F-40-2	55	439,790

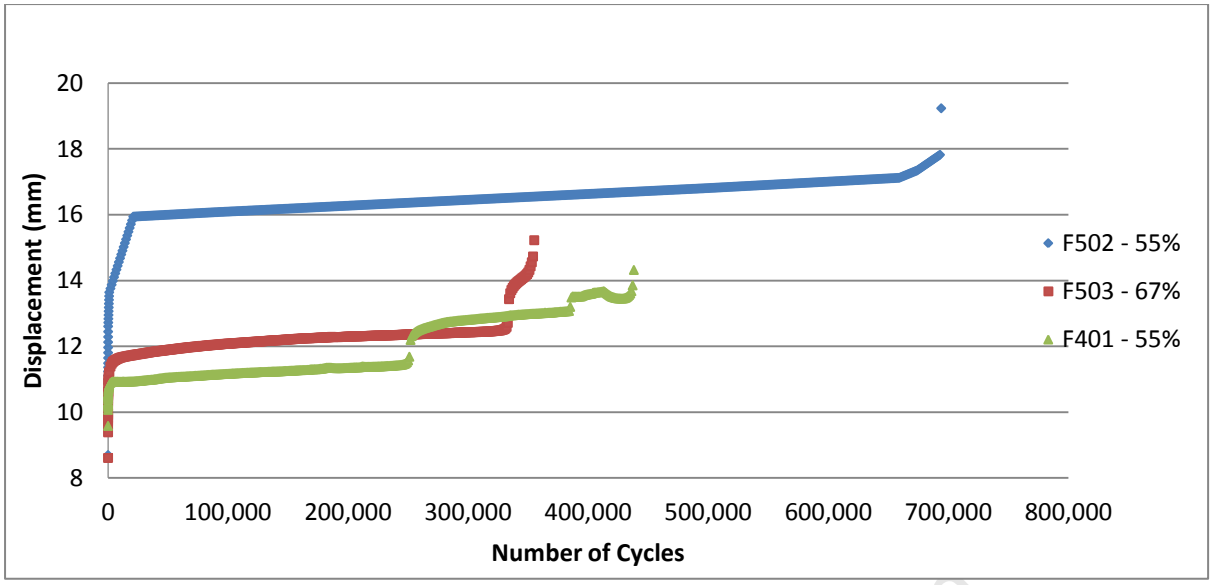

Figure 68: F-50-2, F-50-3, and F-40-2 - Displacement versus Number of Cycles comparison

A significant observation made, which can be seen in **Error! Reference source not found.**, was the number of cycles the 50 MPa RC beam completed at low amplitude before failure compared to that of the medium or high amplitude RC beams. F-50-1 completed almost three times as many cycles as F-50-2, which was only loaded 10% more, whilst F-50-2 completed double the amount of cycles as F-50-3, which was loaded only 12% more. The end results of the test methodology were used to derive the predicted failure curve illustrated in Figure 69.

This curve can be used as a guideline to predict the amount of cycles until failure for a patch repaired and external CFRP strengthened RC beam of similar dimensions for a specific percentage of cyclic loads applied. The cyclic load applied is dependent on the increased ultimate static load at failure for the patch repaired and externally strengthened CFRP reinforced concrete beam of similar dimensions and loading as used in this dissertation.

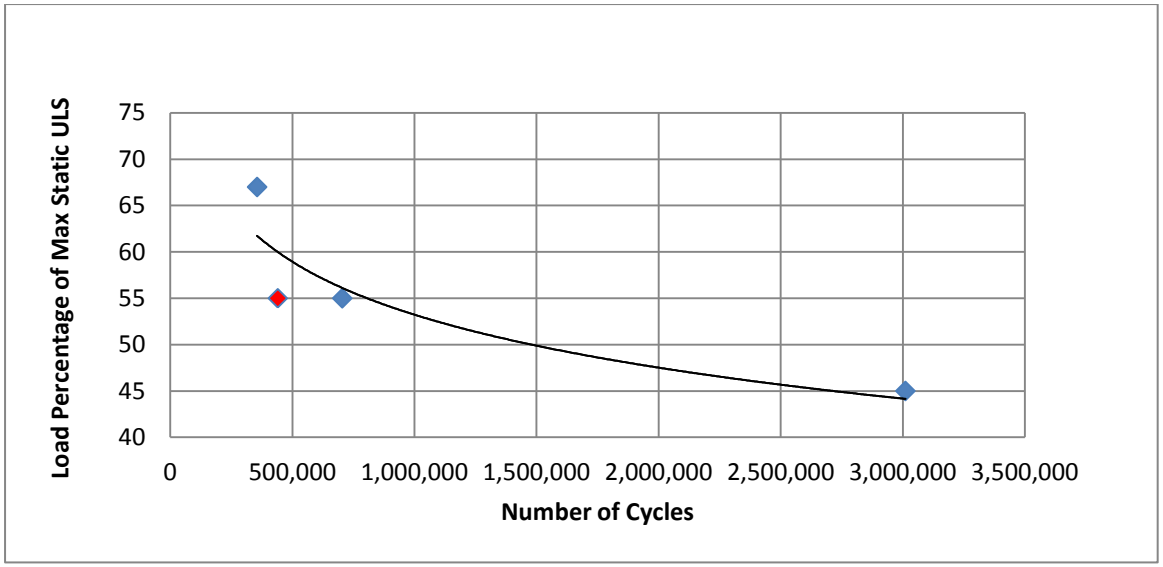

Figure 69: Predicted failure curve for F-50 and F-40 RC repaired and CFRP strengthened beams

5 Chapter 5: CONCLUSIONS

The aim of this dissertation has been to study the fatigue performance of corrosion damaged, reinforced concrete beams which had been repaired with a cementitious patch repair mortar and externally strengthened using carbon fibre reinforced polymers. The study was conducted using six RC beams of dimensions 3200mm x 153mm x 254mm, two of which were subjected to static loading and the remaining four were subjected to sinusoidal cyclic loading of varying amplitudes.

Prior to testing, all of the test specimens were initially subjected to the same degree of accelerated corrosion across a 1200mmx140mm mid-span section of the tensile face, once an estimated 10% mass loss of steel was reached, the damaged concrete was removed and the internal corroded steel was treated using a corrosion retarded chemical coating. A cementitious patch repair mortar was used to repair the section and finally carbon fibre reinforced polymer strips were externally bonded across the entire tensile face to strengthen the repaired RC beam.

The experimental design was successful in acquiring the relevant data to validate the objectives of the dissertation. The static tests performed determined the ultimate load bearing capacities of the repaired and CFRP strengthened beams. The ultimate static loads determined were then used as a function of the varying cyclic amplitudes to be applied to analyse the fatigue behaviour of the remaining four test specimens.

5.1 Accelerated Corrosion

The process of accelerated corrosion was to simulate internal structural damage to the beam by decreasing the diameter of the internal steel chemically. The reductions in the diameter of steel rebar results in a net loss of capacity or overall strength of the structure. The loss in strength was restored using CFRP. The initial induced corrosion formed corrosive cracks in the concrete and pitting of the steel. The damaged concrete was removed and repaired using a cementitious patch repair mortar.

The general conclusions regarding the influence of the accelerated corrosion on the composite structure is summarised below;

- The pitting corrosion of the steel reduced the overall capacity of the structure. The loss of capacity would have been proportional to the reduction of area of steel due to the corrosion, but with the addition of externally strengthening CFRP laminates, the loss of strength was restored..
- The loss of strength due to the steel pitting was negligible, since the externally applied CFRP increased the overall bending capacity of the structure enormously.
- The locations of the steel pitting contribute to the regions of steel fracture during fatigue failure since the locations of pitting create spots of high stress concentration which leads to crack initiation and possible fracture.

Steel pitting corrosion has major implications in the nature of failure modes for structures that have not been adequately repaired and later strengthened. The results of this dissertation reinforce the fact that if the damaged concrete is completely removed and the corroded steel reinforcement is sufficiently treated the fatigue performance can be restored. But, this is only the case if a combination of a cementitious patch repair of similar or greater strength is used with the aid of external CFRP strengthening.

A patch repair alone is not sufficient enough to ensure the sustainable repair of a corrosion damaged RC structure. Externally bonding CFRP in combination with a patch repair is recommended as the CFRP is able to provide the sufficient tensile or shear capacity lost due to the decrease in diameter of the corroded steel. Therefore the strength of the patch repaired and an externally strengthened composite far exceeds the original design strength of the RC structure.

5.2 Patch Repair

The following observations were made and conclusions were derived which were specific to the patch repaired section;

- The boundary between the patch repaired section and original substrate concrete proved to be the primary weak interface under cyclic loading. Under relatively low loads, it was observed that cracks developed along the interface, which under continued loading, later propagated towards the point of loading at the mid-span.

- The cementitious patch repair mortar also proved to be extremely brittle under loading and was susceptible to shrinkage cracks soon after curing. These early age cracks propagated further once the cyclic load was applied.
- The patch repair without the existence of any external strengthening is vulnerable to stress related cracks, which may lead to loss of durability.
- It is concluded that when a patch repair is utilized, the additional strength lost needs to be replaced with CFRP bonded externally along the tensile face; this will ensure the fatigue performance of the composite structure is restored.

The results of fatigue performance of the patch repair system were not compared with any previous studies done. This was due to the fact that to the author's knowledge, there has not been any previous studies which involved both the combination of a patch repair and external strengthening system.

Therefore, the observations made and results obtained during testing are unique to this specific sample configuration and can be used to describe the expected failure crack pattern and mechanisms.

5.3 Static Loading

Static load tests were conducted to determine the effect that the patch repair and external CFRP strengthening had on the maximum static load capacity for the RC beams. It was concluded that the combination of both materials effectively doubled the bending moment capacity of both test specimens, and even shifted the mode of failure for sample S-40 from bending to shear type failure mode.

Initial observations and conclusions were as follows;

- The static loads experienced were expected as there have been many previous experiments conducted which focused on the analysis of CFRP strengthened RC beams under static loads. Therefore it was no surprise that the original design strength was exceeded, but all past experiments of this nature did not incorporate a combination of a patch repair and CFRP strengthening scheme together.
- The load application method varied per beam. The rates of displacement and load control were according to previous works which also performed static load tests on

similar RC beams. The modes of failure could however not be compared, as the test samples configurations differed as well as the combination of composites.

- The static load tests achieved the desired objectives of identifying the maximum static loads at failure as well as identifying the mechanisms of failure.
- The static loads at failure were used to calculate the relative fatigue test amplitudes of the sinusoidal wave load corresponding to the low, medium and high stress range.

The results of the static tests were as follows;

- The original test beam prior to accelerated corrosion, patch repair and external CFRP strengthening had design strengths of approximately 41.3kN, according to the simplified stress block method.
- The static tests conducted after the accelerated corrosion, patch repair and CFRP strengthening, were 97kN for S-40 and 108kN for S-50 respectively.
- S-40 failed in bending as expected, but S-50 failed in shear. This was due to the fact that the additional CFRP exceeded the beams bending capacity above the original design shear capacity and therefore the eventual mode of failure in shear. This could be avoided by ensuring that if the bending capacity is increased, the shear capacity must also be carefully examined.
- The typical failure pattern of the static beams was very similar to that of the fatigue tests, therefore observations can help determine the stage of deterioration that a patch repaired and CFRP strengthened beam is currently at in practice.

5.4 Dynamic Loading

The long term performance and fatigue endurance of the patch repaired and CFRP strengthened beams was determined using sinusoidal cyclic load tests. The beams were each subjected to different amplitudes of loading until eventual fatigue failure was reached. Fatigue failure was defined at the point when the CFRP either delaminated from the original substrate or completely ruptured or the beam exceeded the maximum set displacement.

5.4.1 The objectives of the fatigue load tests

- Capturing the fatigue behavior of each test specimen.
- Representing the captured data graphically.
- Identifying the points of failure and the failure mechanisms.

- Perform a clinical analysis on the life span of the fatigue failure
- Identifying the key milestones throughout fatigue failure.

All of the above mentioned objectives were achieved.

5.4.2 General Fatigue Behaviour

- It was apparent from all the fatigue tests that the primary cause of failure is due to the fatigue concrete cracking at the mid-span before the CFRP delaminated.
- The CFRP laminates were able to perform well under cyclic loading even with substantial cracking of concrete.
- The mode of failure for all specimens tested was debonding.

5.4.3 Locations of Fatigue Failure

- The most significant point of initial cracking is at the interfacial bond between the patch repair mortar and original substrate; this interface was often susceptible to early age cracking which would propagate along the boundary and through the patch repaired section at the midspan.
- These initial cracks then converge with the expected load and much larger mid-span bending cracks in the patch repair mortar.
- At low stress ranges, after approximately 100,000 cycles the mid-span cracks would widen and cause primary fatigue failure of the concrete. This was observed once the cracks began to propagate and widen at an increased rate.
- Ultimate fatigue failure occurs when the bond between the CFRP and epoxy bond was broken or between the original substrate and epoxy bond. Thus, leading to delamination of the CFRP strips and ultimate fatigue failure.
- Predicting which bond will fail is a difficult task as it was not consistent throughout the test samples, it is assumed that the bond of failure is relative to the thickness of the epoxy applied and the quality of the surface of the substrate to which it is bonded to.
- The breakdown of the bonds described above would often occur at the locations where the greatest cracks along the tensile face were present.
- Previous studies have identified that a thicker epoxy bond results in a stronger and more reliable interfacial bond.

- Fracturing of the steel is a significant observation, and the point of fracture is clearly identified in the fatigue performance graphs. In practice, it is difficult to predict if the steel has infact fractured without on-going testing, the displacements would have to be regularly monitored.

5.4.4 Representation of Captured Data

The fatigue behavior of each test specimen was graphically represented in a displacement versus number of cycle's graph. The graph clearly indicated the number of cycles each test sample experienced before ultimate fatigue failure. The points of interest along the graph line are also identified and described. These points of interest include, when the cyclic loading was initiated, the locations where discontinuities in the rate of displacement were evident, and points of failure.

- The graphs clearly indicate the fatigue performance of each test sample.
- The fatigue performance per beam describes graphically the life span of the test sample from the initiation of the cyclic loads to the ultimate fatigue failure of the CFRP laminates.

The graphs indicate the time with respect to number of cycles of each mechanism of failure and as a result can be used as a great tool to predict the future fatigue performance of existing concrete structures with similar structural characteristics.

5.4.5 Results Conclusions

The following summary concludes the results of the experimental methodology;

- At low amplitudes of loading, a repaired and CFRP strengthened RC beam can resist an excessive amount of cyclic loads versus those with medium or high amplitudes.
- F-50-1 resisted over 3,000,000 cycles versus the 704,000 and 355,000 cycles of F-50-2 and F-50-3 respectfully.
- All the 50MPa test samples experienced very similar failure mechanisms with varying degrees of degradation based on the specific cyclic loads applied.
- F-40-2 was the only 40MPa beam that was cyclic loaded. It was loaded with medium amplitude of loading and completed over 430,000 cycles, but exhibited a different mode of failure.

- F-40-2 failed due to fatigue shear failure, which indicated a shift in the mode of failure and that the loading was possibly too high for the weaker concrete structure.
- A further important observation made after the testing was complete, is that all the test specimens' internal steel reinforcement had fractured prior to the completion of the tests. The point at which the steel fractured can be identified in the graphs.
- The fact that the steel fractured reinforces the fact that the use of CFRP laminates are more effective and reliable than simply strengthening with only steel plates.
- The locations of the steel fractures could not be related to the locations of the steel pitting.

5.4.6 Failure Prediction Curve

Finally, with the use all the data collected, a failure prediction curve was generated. The predication curve indicates the number of cycles a specific patch repaired and CFRP strengthened RC beam can resist until ultimate fatigue failure is reached for a specific amplitude of loading. The load is defined as a percentage of a corresponding ultimate static failure for the exact same beam.

This prediction curve presented is defined for the specific test configurations and beam compositions related to this dissertation. Further studies are needed to define this curve further, but it can be confidently concluded that the use of CFRP in combination with a cementitious patch repair effectively increases the fatigue life of the structure.

The outcome of this dissertation; reinforces the argument that composite systems are an effective method to increase the fatigue performance of a damaged structure. The failure mechanisms observed during the testing phase can be used as a guideline for future RC structural investigations and the prediction of future fatigue failures.

5.4.7 Summary

Much of the concluded work is based on the physical observations made while undergoing the testing procedure. Further observations are made based on the fatigue performance graphs. But due to the nature of the testing, very little of the results can be compared to previous research studies conducted as this is the first time that a study of this nature has been carried out.

Due to the originality of the experimental methodology, the following insights into the fatigue behaviour of patch repaired and CFRP strengthened structures have been learnt;

- Engineers will be able to identify the possible failure mechanics of similar structures before significant damage or failure occurs.
- The failure prediction curve allows designers to determine the expected additional life span for an existing repaired and strengthened structure as long as the structures geometry and configurations are similar.
- Emphasis has been shown on the importance of ensuring suitable quality epoxy bond is assured between the CFRP and concrete surface.
- The locations of primary concern are the interfacial bonds between the high strength patch repair mortar and the original substrate.

5.5 Recommendations for future study

On the basis of the findings and conclusions, the following recommendations for future research are proposed;

- An increased number of test specimens and varying amplitudes with the exact same testing methodology will help further derive the predicted failure curve.
- Study on the effect of fatigue corrosion cracking after the patch repair and CFRP strengthening has been complete. It is assumed that further accelerated corrosion will induce cracking of the patch repair mortar; a study to investigate the influence of these corrosion cracks in combination with the CFRP strengthening would prove vital to the fatigue behavior of the RC beams.
- An in depth FEM analysis of the entire composite under cyclic loading would give a better understanding of the fatigue failure mechanisms of each material within the composite.
- Using smaller test samples, achieving the same results, will allow for easier manageability and subsequently increase the number of available test samples, therefore increasing the amount of data collected.
- Using an increased number of LVDT's would result in the better understanding of the stiffness of the repaired and CFRP strengthened samples throughout the entire testing phase.

- Consider different CFRP arrangements and patch repair mortars which will vary the fatigue performance of the test samples, compare the results with the current completed dissertation.
- The use of a lower strength concrete and patch repair mortar will dramatically reduce the time of testing and give a better understanding of the significance of the bonded CFRP once the concrete has failed in fatigue.
- A study to compare the use of external CFRP strengthening versus the use of steel plates as an external strengthening scheme.

5.6 Limitations to current study

The following limitations to the research conducted were identified below;

- The number of test specimens could have been increased but this was unable due to a lack of time to test in the laboratory and space to store the samples during the accelerated corrosion, patch repair and CFRP strengthening phases.
- The varying concrete strengths added another unnecessary parameter to the already complex composite, for future studies it is recommended to use the exact same strength of concrete for all test specimens in order to eliminate any further parameters.
- Strain gauges would have assisted in the analysis of each composite while under cyclic loading.
- Much of the previous work concluded at the University of Waterloo did not use a combination of a patch repair and CFRP strengthening scheme and therefore the results could not be compared.

References

- "ACI 440. Guide for the design and construction of externally bonded FRP systems for strengthening concrete structures." *ACI 440.2R-02* (American Concrete Institute), 2002.

- Badawi, K. Soudki. "Control of Corrosion-Induced Damage in Reinforced Concrete Beams using CFRP Laminates." *Journal of Composites for Conctruction*, 2005: 195-201.

- Balanguru, P. *FRP Composites for Reinforced and Prestressed Concrete Structures.* New York: Taylor & Francis, 2009.

- Beushausen, M. Alexander. *Fultons Concrete Technology.* Midrand: Cement & Concrete Institute, 2009.

- Beushausen, M. Alexander. "Fultons Concrete Technology." Midrand: Cement & Concrete Institute, 2009.

- Bohni, H. *Corrosion in Reinforced concrete structrues.* Abington Cambridge: Woodhead Publishing Limited, 2005.

- Chen, Teng. "Shear Capacity of Fibre-Reinforced Polymer Strengthened Reinforced Concrete Beams: FRP Rupture." *Journal of Structural Engineering*, 2003: 615-625.

- E. David, C. Djelal, F. Buyle-Bodin. "Repair and Strengthening of Reinforced Concrete Beams using Composite Materials." *2nd Int. PhD Symposium in Civil Engineering*, 1998.

- El Maaddawy, Soudki. *Carbon-Fibre-Reinforced polymer Repair to extend Service Life of Corroded Reinforced Concrete Beams.* 2005.

- El Maaddawy, Soudki K, Topper T. "Long Term Performance of Corrosion Damaged Concrete Beams." *ACI Structural Journal*, 2005.

- Gussenhoven, Brena. "Fatigue Behaviour of Reinforced Concrete Beams Strengthened with Different FRP Laminate Configurations." *Journal of Composites for Construction*, 2005: 613-630.

- Gussenhoven, S.F. Brena. "Fatigue Behaviour of Reinforced Concrete Beams Strengthened with Different FRP Laminate Configurations." *Journal of Composites for Construction*, 2005: 613-630.
- Hollaway, L.C. "A review of the present and future utilisation of FRP composites in the civil infrastructure with reference to their important in-service properties." *Construction and Building Materials*, 2010: 2419-2445.
- J.F Chen, J.G Teng. "Shear Capacity of Fibre-Reinforced Polymer Strengthened Reinforced Concrete Beams: FRP Rupture." *Journal of Structural Engineering*, 2003: 615-625.
- Keller, Thomas. *Use of Fibre Reinforced Polymers in Bridge Construction.* Zurich: IABSE, 2003.
- Khaled A, Soudki, Sherwood T, Masoud S. *FRP repair of corrosion-damaged reinforced concrete beams.* Waterloo, Canada: University of Waterloo, 2005.
- M. Badawi, K. Soudki. "CFRP Repair of RC Beams with Shear-Span and Full-Span Corrosions." *Journal of Composites for Construction*, 2010: 323-335.
- Malumbela G, Moyo P, Alexander M. "Behaviour of RC beams corroded under sustained load." *Construction and Building Materials*, 2009.
- Malumbela, G. *Measurable parameters for performance of corroded and repaired RC beams under load.* Cape Town: University of Cape Town, 2010.
- Masoud, K. Soudki and T. Topper. "Postrepair Fatigue Performance of FRP-Repaired corroded RC beams: Experimental and Analytical Investigation." *Journal of Composites for Construction*, 2005: 441-449.
- McSweeney, Lopez. "FRP-Concrete Bond Behaviour: A Parametric Study Through Pull-Off Testing." *American Society for Civil Engineers*, 2005.
- O, Buyukozturk. "Failure behaviour of FRP bonded concrete affected by interface fracture." *National Science Foundation*, 2005.

- Parish, G. "CFRP Repair of concrete beams aged by accelerated corrosion." *Journal of Aerospace Engineering*, 2011: 227.
- SG, Masoud. *Behaviour of corroded reinforced concrete beams repaired with FRP sheets under monotonic and fatigue loads.* Waterloo, Canada: University of Waterloo, 2002.
- Shahawy, Beitelman. "Static and Fatigue Performance of RC Beams Strengthened with CFRP Laminate." *Journal of Structural Engineering*, 1999: 613 - 621.
- Smith S, Teng TG. "FRP-strengthened RC beams: Review of debonding strength models." *Engineering Structures*, 2002: 385-395.
- Soudki K, Sherwood T G. "Behaviour of reinforced concrete beams strengthened with carbon fibre reinforced polymer laminates subjected to corrosion damage." *Canadian Journal of Civil Engineering*, 2000: 1005-1010.
- Taljsten, Bjorn. *FRP Strengthening of Existing Structures.* Lulea: Lulea University of Technology, 2006.
- Tigeli, M. *Effect of Structural Repair and Strengthening and Ultimate Capacity of Corrosion-Damaged RC Beams.* Cape Town: University of Cape Town, 2010.
- Vaysburd, M.A. "Holistic system approach to design and implimentation of concrete repair." *Cement & Concrete Composites*, 2006: 671-678.

Appendices

1. Ultimate Moment of Resistance Calculations

Determining the Ultimate Moment of Resistance and Cracking moment of the RC Beam

<u>Determining the Ultimate Moment of Resistance</u>

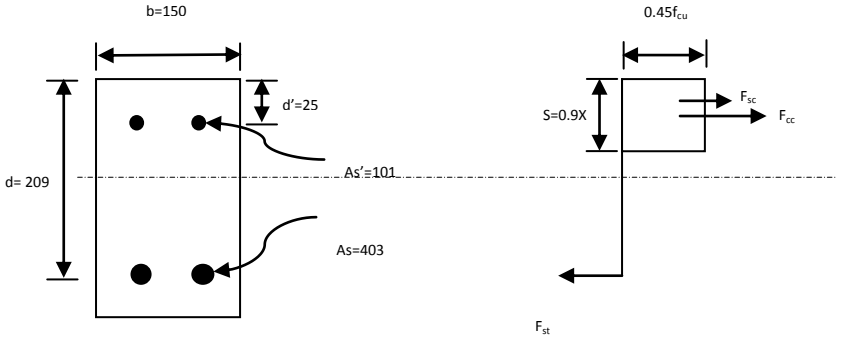

SECTIO STRESS BLOCK

i.) Using the Simplified Stress Block:

Check:

Taking moments about the tension steel:

ii) Using the Design Charts

Therefore for safety use **M_{ult} = 26.2 kNm**

Determining the Cracking Moment

Cracking moment of the beam (N.mm); tensile strength of concrete (MPa); gross second moment of area of a beam (mm^4); gross depth of the neutral axis of a beam measures from its tensile face (mm).

Calculating F_{cr}

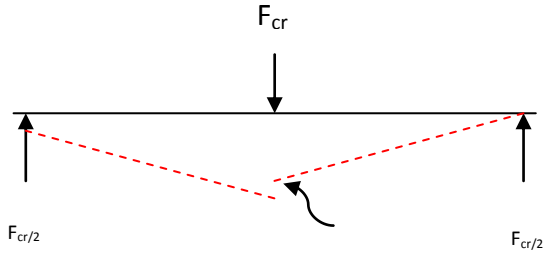

F_{ULS} prior to Repair and Strengthening

3-point load:

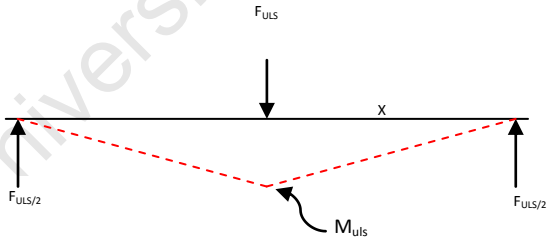

2. Amplitude Calculations

Static load results:

S40 – Ultimate load at failure ≃96kN

S50 – Ultimate load at failure ≃107kN

Fatigue load amplitudes:

F501: Minimum load = 0.1x107 = 10.7kN

Maximum load = 0.45x0.85x107 = 40.9 ≃ 41kN

Amplitude = 15.15kN

F502: Minimum load = 0.1x107 = 10.7kN

Maximum load = 0.55x0.85x107 = 51.2 ≃ 52kN

Amplitude = 20.65kN

F503: Minimum load = 0.1x107 = 10.7kN

Maximum load = 0.67x0.85x107 = 60.9 ≃ 61kN

Amplitude = 25.15kN

F401: Minimum load = 0.1x96 = 9.6kN

Maximum load = 0.55x0.85x96 = 44.8 ≃ 45kN

Amplitude = 17.7kN

Frequency:

All cyclic load tests were performed at a constant frequency of 2Hz.

Test Stages:

Stage 1, Load applied from 0kN – 10% Static ULS, at a monotonic rate of 2kN/min.

Stage 2, Cyclic load in a sinusoidal wave from according to the above amplitudes.

3. Accelerated Corrosion Calculations

Calculating the amount of current required to achieve an estimated amount of steel lost during the accelerated corrosion process:

Mass of steel consumed (g); Atomic weight of steel (56g); Current (A); time (s); Ionic charge (2); Faradays constant (96 500 A/s).

From the specimen, there are 2 x 16mm bars in the tension zone to be corroded; the length of the corrosion is 750mm. The mass of the steel bars to be corroded is calculated as follows:

Density of steel,

Mass of two steel bars of length 750mm:

Based on the required mass loss of 10%, the current required to achieve the corrosion level can be assumed

Beam No.	Mass Loss (%)	Mass loss (g)	Current (mA)	Duration (Days)
1 (Control)	10	237	480	20
2	10	237	480	20
3	10	237	480	20
4	10	237	480	20
5	10	237	480	20
6	10	237	480	20

Ex for all six beams: